

Molecular Mechanisms of Synaptic Vesicle Degradation

Patricia Sheehan

Submitted in partial fulfillment of the
requirements for the degree of
Doctor of Philosophy
under the Executive Committee
of the Graduate School of Arts and Sciences

COLUMBIA UNIVERSITY

2016

© 2016
Patricia Sheehan
All rights reserved

ABSTRACT

Molecular Mechanism of Synaptic Vesicle Degradation

Patricia Sheehan

Neurons rely on precise spatial and temporal control of neurotransmitter release to ensure proper communication. Neurotransmission occurs when synaptic vesicles in the presynaptic compartment fuse with the plasma membrane and release their contents into the synaptic cleft, where neurotransmitters bind to receptors on the postsynaptic neuron. Synaptic vesicle pools must maintain a functional repertoire of proteins in order to efficiently release neurotransmitter. Indeed, the accumulation of old or damaged proteins on synaptic vesicle membranes is linked to synaptic dysfunction and neurodegeneration. Despite the importance of synaptic vesicle protein turnover for neuronal health, the molecular mechanisms underlying this process are unknown. In this thesis, we present work that uncovers key components that regulate synaptic vesicle degradation. Specifically, we identify a pathway that mediates the activity-dependent turnover of a subset of synaptic vesicle membrane proteins in mammalian neurons. This pathway requires the synaptic vesicle-associated GTPase Rab35, the ESCRT machinery, and synaptic vesicle protein ubiquitination. We further demonstrate that neuronal activity stimulates synaptic vesicle protein turnover by inducing Rab35 activation and binding to the ESCRT-0 component Hrs, which we have identified as a novel Rab35 effector. These actions recruit the downstream ESCRT machinery to synaptic vesicle pools, thereby initiating synaptic vesicle protein degradation via the ESCRT pathway. Interestingly, we find that not all synaptic vesicle proteins are degraded by this mechanism, suggesting that synaptic vesicles are not degraded as units, but rather that SV proteins are degraded individually or in subsets. Moreover, we find that lysine-63

ubiquitination of VAMP2 is required for its degradation, and we identify an E3 ubiquitin ligase, RNF167, that is responsible for this activity. Our findings show that RNF167 and the Rab35/ESCRT pathway facilitate the removal of specific proteins from synaptic vesicle pools, thereby maintaining presynaptic protein homeostasis. Overall, our studies provide novel mechanistic insight into the coupling of neuronal activity with synaptic vesicle protein degradation, and implicate ubiquitination as a major regulator in maintaining functional synaptic vesicle pools. These findings will facilitate future studies determining the effects of perturbations to synaptic homeostasis in neuronal dysfunction and degeneration.

Table of Contents

List of Figures	v
List of Tables	vi
Acknowledgements	vii
Chapter 1: General Introduction	1
Neuronal Communication	1
Synaptic Vesicle Cycle	1
Exocytosis	2
Endocytosis	3
Endosomal Sorting of Synaptic Vesicles	4
Synaptic Protein Turnover.....	6
Ubiquitination	7
Ubiquitin-Proteasome System	8
Roles of UPS at the Synapse.....	9
Ubiquitin-Mediated Endosomal Sorting.....	10
Axonal Transport of MVBs	11
Rab GTPases	12
Endocytic SV-associated Rab GTPases.....	13
Protein Homeostasis in Neuronal Health.....	15
Chapter 2: Materials and Methods	17
Cell Culture	17
Cultured rat neurons.....	17
Microfluidic culturing.....	17
Molecular Techniques	17
Constructs, shRNAs.....	17
qPCR.....	18
Lentivirus production, transduction, and DNA transfection.....	19
Pharmacological treatments	19
Electrophysiology	20
Imaging Techniques.....	20
Immunofluorescence microscopy	20
Confocal microscopy	21
SNAP-labeling	21
Super-Ecliptic pHluorin Imaging.....	21
Live Imaging.....	22

Electron Microscopy	23
Biochemical techniques	23
Co-immunoprecipitation and pull-down assays.....	23
Ubiquitination assay for VAMP2	24
GST Pull-down	24
Immunoblotting.....	25
Analysis	25
Fold-change calculation	25
Image Analyses.....	26
Evaluation of neuronal health.....	27
Statistical analyses	27
Chapter 3: A subset of SV proteins undergo activity-dependent degradation by the ESCRT pathway.....	31
Rationale	31
Results	32
SV integral membrane proteins turn over at different rates.....	32
Neuronal activity stimulates the degradation of specific SV membrane proteins	34
The ESCRT pathway is required for activity-dependent SV protein degradation.....	36
ESCRT proteins undergo activity-dependent recruitment to SV pools	38
Discussion	44
Chapter 4: Rab35 regulates activity-dependent degradation of SV2 and VAMP2 through its effector, Hrs	47
Rationale	47
Results	47
Rab35 interacts with Hrs and stimulates SV protein degradation	47
Rab35 is necessary for activity-dependent SV protein degradation upstream of the ESCRT pathway.....	54
Hrs is an effector of Rab35	59
Neuronal activity stimulates Rab35 activation	63
Discussion	64
Chapter 5: Ubiquitination serves as a signal for VAMP2 degradation.....	69
Rationale	69
Results	69
Ubiquitination of VAMP2 is required for its basal and activity-dependent degradation.....	69

K63-linked poly-ubiquitination of VAMP2 is required for its degradation	71
Ubiquitination of VAMP2 is required for its degradation by Rab35.....	73
RNF167 ubiquitinates VAMP2	74
RNF167 is necessary for the degradation of VAMP2	75
Discussion	75
Chapter 6: General Discussion and Future Directions	79
References.....	85

List of Figures

Chapter 1

Figure 1.1: The synaptic vesicle cycle	2
Figure 1.2: Ubiquitination.....	8
Figure 1.3: Recognition of ubiquitination by the ESCRT pathway	10
Figure 1.4: Rab GTPase cycle.....	12

Chapter 3

Figure 3.1: SV proteins exhibit different fractional amounts of degradation after protein synthesis inhibition	33
Figure 3.2: Neuronal activity drives the degradation of a subset of SV-associated proteins	35
Figure 3.3: The ESCRT pathway is required for basal and activity-dependent SV protein degradation	37
Figure 3.4: Neuronal activity recruits ESCRT proteins to synaptic vesicle pools	39
Figure 3.5: Neuronal activity changes Hrs trafficking dynamics.....	42
Figure 3.6: Ultrastructural analysis of presynaptic boutons	43

Chapter 4

Figure 4.1: A subset of endocytic Rabs interact with Hrs and/or drive SV protein degradation	48
Figure 4.2: A subset of endocytic Rabs drive SV protein degradation	51
Figure 4.3: Rab35 drives SV protein degradation at synapses.....	53
Figure 4.4: Rab35 is necessary for SV membrane protein degradation.....	55
Figure 4.5: Knockdown of Rab35 inhibits activity-dependent SV protein degradation..	57
Figure 4.6: The ESCRT pathway functions downstream of Rab35 to mediate SV protein degradation	58
Figure 4.7: ESCRT-0 component Hrs is an effector of Rab35	60
Figure 4.8: Rab35 recruits ESCRT proteins to synaptic vesicle pools.....	62
Figure 4.9: Neuronal activity activates Rab35 and stimulates Rab35-Hrs binding	66

Chapter 5

Figure 5.1: KR VAMP2 localizes to synapses and exhibits normal recycling kinetics but reduced ubiquitination	70
Figure 5.2: Ubiquitination is required for basal and activity-driven degradation of VAMP2.....	72
Figure 5.3: Ubiquitination of VAMP2 is required for its Rab35-mediated degradation. 74	
Figure 5.4: RNF167 ubiquitinates VAMP2 and is necessary for its degradation.....	76

List of Tables

Chapter 2

Table 2.1: List of DNA constructs	28
Table 2.2: List of antibodies	30

Chapter 3

Table 3.1: Fractional protein degradation in a 24-hour period, based on neuronal activity levels.....	36
---	----

Acknowledgements

I never could have completed my Ph.D. without the constant support and guidance of so many. First of all, I cannot thank Clarissa enough for her mentorship, motivation, and immense knowledge. She always made herself available to offer invaluable help and advice on anything from experiments to writing and career choices. Other than Clarissa, I would like to thank the members of my thesis committee: Dr. Gil Di Paolo, Dr. Ulrich Hengst, Dr. David Sulzer, and Dr. Ai Yamamoto. Their valuable insights over the years have shaped my scientific development by challenging me to view my research from various perspectives. Additionally, I have to thank the members of the Waites lab who have kept me sane by providing endless support and entertainment. Finally, I need to thank my family and friends for all the happy hours, lunch breaks, phone calls, and general love and inspiration they have provided through this process.

Chapter 1 - Introduction

Neuronal Communication

Neurons have a highly unique morphology that underlies their functionality. They consist of a cell soma, dendrites, and axons. The soma is largely responsible for protein synthesis while the dendrites and axons extend away from the soma and form connections with other neurons. These connections, called synapses, are specialized compartments of neurons that mediate neuronal communication. Most classically these are formed between an axonal presynaptic bouton and a dendritic postsynaptic spine. On the presynaptic side, neuronal synapses translate electric impulses (action potentials) into the regulated release of neurotransmitter from synaptic vesicles (SVs) in order to communicate with connecting neurons. These neurotransmitters bind to receptors on the postsynaptic neuron, opening ion channels and functioning to create an electrical change in postsynaptic membrane potential. If this change in membrane potential reaches a threshold, the postsynaptic neuron will fire an action potential and propagate the signal to its connecting neurons.

Synaptic Vesicle Cycle

The presynaptic bouton is an area of particularly high protein and membrane flux. SVs release neurotransmitter by fusing with the neuronal membrane (exocytosis). SV fusion is followed by membrane recycling (endocytosis), allowing for SV re-formation and additional rounds of neurotransmitter release (Figure 1.1). SV exocytosis and endocytosis depend upon precise protein-protein interactions that are carefully regulated in time and space (Li and Chin, 2003; Sudhof, 2004).

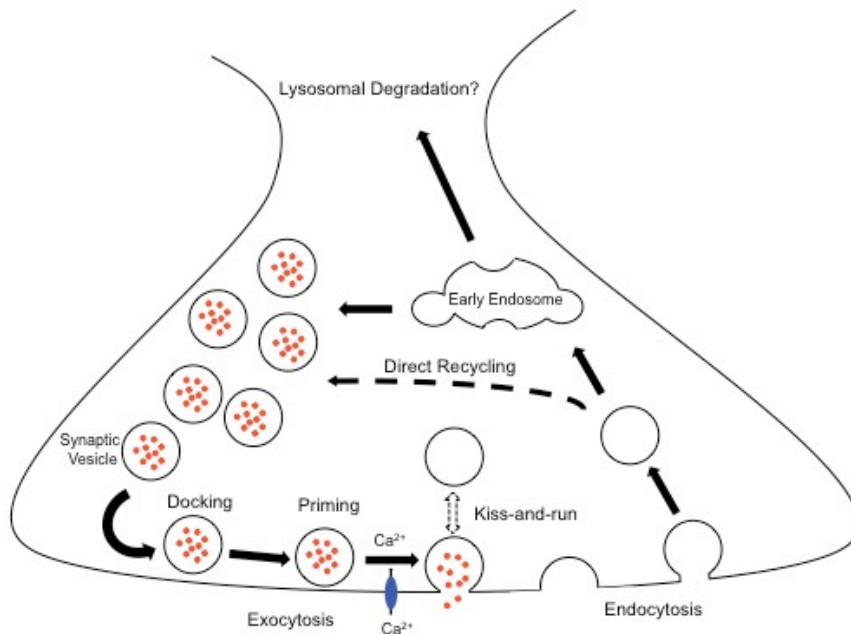


Figure 1.1 - The synaptic vesicle cycle

Synaptic vesicles (SVs) filled with neurotransmitter are translocated to the presynaptic active zone where they undergo docking and priming. Following an action potential, calcium enters the presynaptic bouton, causing vesicles to fuse with the plasma membrane and release neurotransmitter. SV proteins are then endocytosed and either recycled for use in another round of exocytosis, or sorted for degradation.

Exocytosis

The exocytosis of SVs is a multi-step process that involves the docking, priming, and fusion of SVs with the plasma membrane. In order to be released, SVs filled with neurotransmitter are translocated to the presynaptic active zone where they are docked, in a manner that is not well understood but is thought to involve Rab3, Munc-18 and a variety of active zone proteins (Dulubova et al., 1999; Geppert et al., 1994; Hata et al., 1993). Docking ensures spatial regulation of neurotransmitter release by preparing SVs for neurotransmitter release at the active zone. Then, the priming machinery, including Munc-13, RIM, and RIM binding proteins, functions to promote the partial formation of the soluble NSF attachment protein receptor (SNARE) complex (Brose et al., 1995; Wang et al., 1997; Wang et al., 2000). This SNARE complex includes the vesicular-SNARE VAMP2 and target-SNAREs syntaxin-1 and SNAP-25

(Sollner et al., 1993). This priming step prepares the SNARE complex in a manner that ensures quick temporal reaction upon an action potential reaching the synapse. The SNARE mediated fusion between an SV and the plasma membrane is driven by calcium influx into the presynaptic terminal. Calcium binds to the SV integral membrane protein, Synaptotagmin-1, which promotes the full zippering of the SNARE complex (Katz and Miledi, 1967; Shao et al., 1998). This zippering releases energy which causes SV fusion with the plasma membrane allowing neurotransmitter to be released into the synaptic cleft (see (Sudhof, 2004)).

Endocytosis

Following exocytosis, it is conventionally believed that SVs fully collapse into the plasma membrane. SV proteins and lipids then intermix with plasma membrane components and undergo endocytosis to retrieve vesicle constituents. Various forms of endocytosis have been observed including clathrin mediated endocytosis (CME), bulk endocytosis, ultra-fast endocytosis and “kiss-and-run” endocytosis. CME is the most-studied form of endocytosis and occurs in all cell types. Indeed, budding clathrin-coated pits can be observed by electron microscopy at the plasma membrane as well as at endosomal cisternae (Heuser and Reese, 1973; Miller and Heuser, 1984). However, it has been shown that under high frequency stimulation another form of endocytosis, deemed bulk endocytosis, can be observed. This is seen as large membrane enfoldings and the formation of endosome-like compartments near the presynaptic active zone (Clayton and Cousin, 2008; Miller and Heuser, 1984; Rizzoli and Betz, 2005). It is believed that this form of endocytosis allows for quick reversal of membrane expansion under high frequency stimulation whereby CME would be rate limiting under these conditions. From these bulk endosomal-like structures, SVs can bud off and reform to repopulate the vesicle pool. Most recently, another form of endocytosis has been observed in which 100 ms after stimulation,

endocytosing vesicles are observed just outside of the active zone (Watanabe et al., 2014). This process has been named ultra-fast endocytosis and is believed to represent a mechanism whereby plasma membrane expansion by exocytosis is immediately compensated for by endocytosis.

Additionally, some evidence supports another model of endocytosis whereby SVs do not fully collapse into the plasma membrane but instead form a small transient fusion pore through which neurotransmitter is released (Fesce et al., 1994). This differs from ultra-fast endocytosis in that it allows for the retention of SV identity and the direct reformation of SVs. Overall, there are many models by which SV endocytosis can occur suggesting that different stimuli/activity paradigms invoke different mechanisms to compensate for changes in SV exocytosis.

Endosomal Sorting of Synaptic Vesicles

For many decades, controversy has surrounded the post-endocytic cycling and reformation of SVs. In the early 1970s, two independent studies applied extracellular tracers to neurons of the frog neuromuscular junction in order to examine the cycling of SVs. The conflicting findings of these studies initiated the controversy surrounding the role of endosomes in SV recycling.

Heuser and Reese applied high frequency stimulation (10 Hz for 1-15 minutes) to nerve terminals and found that the number of SVs per terminal was reduced. This reduction occurred together with the formation of large cisternal membranes. Both phenotypes were reversed upon rest, suggesting that these cisternae were the precursors to SV replenishment (Heuser and Reese, 1973). A later study found that clathrin coated vesicles could be observed budding from these cisternae, suggesting that endosomes play an intermediary role in reforming SVs after endocytosis (Miller and Heuser, 1984). However, another study performed by Ceccarelli et al. offered opposing results. While tracer was observed being taken up by synaptic vesicles upon stimulation, no reduction in number of SVs and no formation of cisternal structures were

observed, suggesting no role for endosomal intermediates in SV recycling (Ceccarelli et al., 1973). The important difference between these two studies comes down to the stimulation paradigm. While Heuser and Reese used high frequency stimulation, Ceccarelli et al. used low frequency stimulation (2 Hz for up to 4 hours). The findings from these studies therefore suggested that different stimulation paradigms could invoke different forms of endocytosis, which varied with regards to their reliance on an endosomal intermediate.

Another prominent argument against endosomal sorting in the SV cycle came from a study using FM1-43 dye uptake, where it was noted that the amount of FM uptake per vesicle was equal to the amount released per vesicle upon exocytosis (Murthy and Stevens, 1998). This suggested that no diffusion of dye occurred via the fusion of SVs to an endosomal intermediate. However, this study did not address the possibility that other, non-recycling pools of vesicles may exchange their membrane with an endosome, nor did it address the idea that SVs may undergo homotypic fusion to form synaptic endosomes. This type of fusion is common in non-neuronal cells, where incoming vesicles fuse to form endosomes (Scita and Di Fiore, 2010) and importantly, such fusion would not lead to a dilution of dye. It has been shown *in vitro* and possibly *in vivo* (Rizzoli et al., 2006; Shimizu et al., 2003) that SVs can undergo homotypic fusion, suggesting that SVs can form endosomes. Furthermore, the Ceccarelli study did not investigate the cycling of SVs under high activity demands, and therefore did not address the idea that synaptic endosomes only form under such stimulation. Indeed, the existence of synaptic endosomes has been shown *in vivo* by immuno-EM at the Calyx of Held synapse and the neuromuscular junction (Uytterhoeven et al., 2011; Wucherpfennig et al., 2003). However, these endosomes have been shown to be fairly rare and extremely dynamic. Indeed, within mouse hippocampal neurons, the large endocytic vesicles formed by ultrafast endocytosis resolve back

into SVs within six seconds of stimulation (Watanabe et al., 2014). Though the study by Ciccarelli et al. disregarded many potential interpretations, its findings managed to further fuel the controversy surrounding the endosomal sorting of SVs.

More recent investigations into the composition of SVs have revealed the presence of a large number of endosomal proteins on SVs such as diverse endosomal Rab GTPases, endosomal SNAREs, endosome-derived coat proteins (Takamori et al., 2006). The presence of these proteins on SVs suggests that endosomes do have a role in the SV cycle. Furthermore, perturbations in a variety of these proteins lead to changes in neurotransmission and the structure and composition of SVs, some of which will be discussed in more detail. Overall these findings suggest that endosomal sorting is an important regulatory step in maintaining the fidelity of neurotransmission. Although it is now accepted that an endosomal intermediate can play a role in the cycling of SVs under certain conditions, the signals and pathways responsible for regulating the trafficking and sorting of SV proteins through the endosomal pathway remain poorly understood.

Synaptic Protein Turnover

While SV endosomal sorting and reformation is becoming better characterized, little remains known about the pathways responsible for SV protein degradation. Furthermore, another fundamental but unexplored question is how SVs are targeted for degradation. Ubiquitination serves as the signal for degradation of soluble proteins by the proteasome, and is also used by lysosomal degradation pathways for membrane-bound cargo recognition (Clague and Urbe, 2010). Intriguingly, a recent study reported that SV membrane proteins are among the most highly ubiquitinated neuronal proteins (Na et al., 2012), suggesting that this modification may play an important role in their degradation. However, ubiquitination also regulates many non-

degradative protein trafficking events (*i.e.* endocytosis, protein-protein interactions), and its role in SV protein trafficking/degradation is completely unexplored.

Ubiquitination

Ubiquitin is a small protein that is covalently attached to other proteins as a post-translation modification to signal for their intracellular transport and degradation. Ubiquitin is conjugated to lysine residues on target proteins by a series of enzymes deemed E1, E2, and E3 enzymes. E1s are ubiquitin-activating enzymes that transfer ubiquitin to ubiquitin-conjugating enzymes, E2s, which then bind the target protein and a ubiquitin-ligase, E3. E3s then covalently attach ubiquitin to the target protein by transferring ubiquitin from the E2 to lysine residues on the target substrate (Figure 1.2) (Haas et al., 1982; Hershko et al., 1983). Different E3 enzymes are responsible for different ubiquitin chain linkages. Both the length of the ubiquitin chain and the lysine residue on which the ubiquitin molecule or chain is attached signal for different trafficking events ranging from intracellular signaling to degradation (Chau et al., 1989; Hicke and Dunn, 2003). A variety of proteins responsible for the regulation of protein degradation and trafficking contain domains capable of recognizing ubiquitination. These include ubiquitin-interacting motifs (UIM), ubiquitin E2-variant (UEV), ubiquitin-associated (UBA), ubiquitin-like (UBL), and CUE domains. Finally, ubiquitin must be removed from target proteins in order to maintain a pool of free ubiquitin and allow target substrates entrance into degradative structures. This task is carried out by deubiquitinating enzymes (DUBs) that cleave ubiquitin at the G76 isopeptide bond (see (Helton and Ehlers, 2008)). There are two degradative pathways that recognize ubiquitinated proteins: the ubiquitin-proteasome system (UPS) and the Endosomal Sorting Complex Required for Transport (ESCRT) pathway.

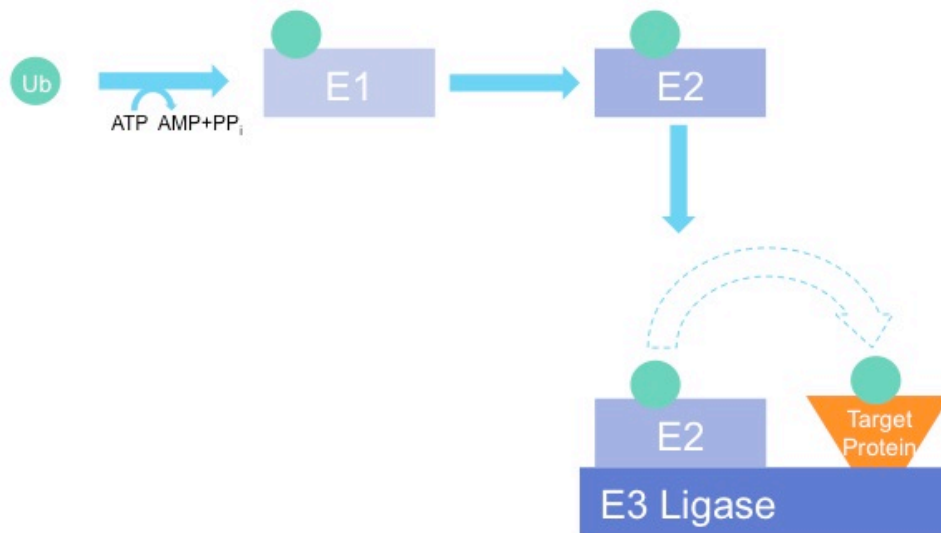


Figure 1.2 – Ubiquitination

Ubiquitination is a post-translation modification that occurs via the covalent attachment of ubiquitin to target proteins. Ubiquitin is activated by an E1 enzyme and then conjugated to an E2 enzyme. An E3 ligase then simultaneously binds the E2 enzyme and the target protein, and functions to transfer ubiquitin from the E2 to the target protein.

Ubiquitin-Proteasome System

The proteasome is an incredibly abundant structure comprising more than 1% of the total cellular protein. Furthermore, they can be found in all neuronal compartments including the presynaptic terminal. The eukaryotic proteasome is comprised of two multimeric complexes, the catalytic 20S core particle and two 19S regulatory complexes. Four heptameric rings that contain various proteolytic sites form a cylinder that is the 20S core particle. Each 19S regulatory complex is made up of eight subunits and a ring of 6 AAA family ATPases that gate the lumen of the 20S core and regulate the energy-dependent unfolding of proteins necessary for entrance into the core (see (Tanaka, 2009)). Multiple components of the 19S regulatory complex are capable of ubiquitin recognition on target proteins (Lam et al., 2002). Specifically, lysine 48-linked poly-ubiquitination is known to serve as a signal for protein degradation by the proteasome. Typically,

at least four lysine-48 linked ubiquitin molecules are necessary to bind the proteasome (Kish-Trier and Hill, 2013).

Roles of UPS at the Synapse

The UPS plays an intimate role in both synapse formation and in the regulation of synaptic function. Dysregulation in the ubiquitination and degradation of a variety of proteins can lead to defects in synapse formation and elimination as well as axonal growth, steering and pruning. In mature neurons, the UPS continues to play an important role in regulating neurotransmitter release, the composition of the postsynaptic density (PSD), and synaptic plasticity. Intriguingly, many of these processes are tightly linked to neuronal activity (Alvarez-Castelao and Schuman, 2015) suggesting a coupling between neuronal activity and UPS function.

Indeed, ubiquitination and degradation of certain postsynaptic proteins can occur in an activity-dependent manner (Ehlers, 2003; Lussier et al., 2011; Schwarz et al., 2010; Scudder et al., 2014). Specifically, the abundance of various PSD proteins changes in response to changes in neuronal activity levels in a proteasome-dependent manner (Ehlers, 2003). Furthermore, the global ubiquitination state of the PSD increases with increasing neuronal activity and decreases with neuronal silencing, suggesting that ubiquitination of these proteins is tightly linked to neuronal activity (Ehlers, 2003). While few studies have examined the relationship between activity and presynaptic protein turnover, it has been reported that silencing neurons leads to the down regulation of presynaptic scaffolding protein levels (e.g. Piccolo/Bassoon, Munc13, RIM) that is partially restored by blocking the proteasome. Interestingly, this silencing also leads to an accumulation of SV proteins (i.e. SV2B, synaptotagmin-1, vGlut1), suggesting that presynaptic proteins levels are differentially regulated by changes in neuronal activity (Lazarevic et al., 2011).

Ubiquitin-Mediated Endosomal Sorting

Ubiquitination also serves as a signal for sorting through the endocytic pathway. Endocytosed proteins can be sent to endosomes where they are then sorted for recycling back to the plasma membrane, retrograde transport to the secretory pathway, or degradation by the lysosome. Multi-monoubiquitination and Lysine-63 (K63)-linked polyubiquitination target proteins for degradation through interactions with the ESCRT pathway. The ESCRT pathway is comprised of a series of protein complexes (ESCRT-0, -I, -II, -III) that are sequentially recruited to the endosomal membrane. It is believed that the ESCRT-0 protein, Hrs, is first recruited to the endosomal membrane through its FYVE domain, a lipid-binding domain that preferentially interacts with phosphoinositol 3-phosphate (PI3P) the phosphoinositide enriched on early endosomes. Proteins of the ESCRT-0, -I and -II complexes contain various ubiquitin recognition motifs and function to sort and retain ubiquitinated proteins in microdomains on the endosomal membrane (Figure 1.3). The ESCRT-III complex functions to form intraluminal vesicles (ILVs) by inducing membrane deformation and recruiting accessory proteins for the budding and abscission of ILVs from the endosomal membrane. Once an endosome contains two or more ILVs, it is deemed a multivesicular body (MVB). The cargo contained within the ILVs is destined for lysosomal degradation (see (Raiborg and Stenmark, 2009)).

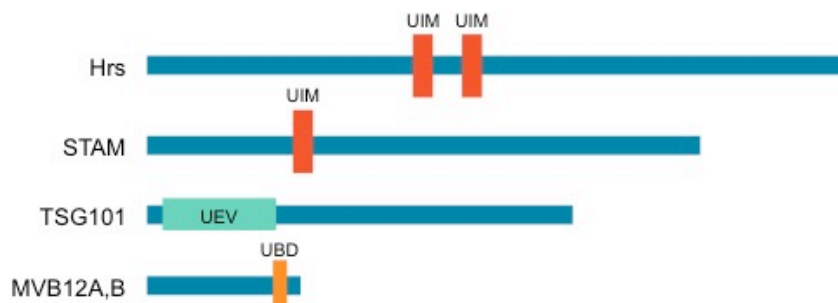


Figure 1.3 - Recognition of ubiquitination by the ESCRT pathway

The various ubiquitin recognition motifs in ESCRT-0 (Hrs, STAM) and ESCRT-I (TSG101, MVB12A,B) components.

Axonal transport of MVBs

Lysosomes are rarely detected in axons and presynaptic boutons. Although LysoTracker and LAMP1 positive structures can be localized to axons, it is becoming increasingly evident that these structures are not fully mature functional lysosomes. Indeed, a recent study has determined that there are distinct populations of lysosomes in neurons and that those located in axons are strikingly deficient in lysosomal proteases (Gowrishankar et al., 2015). This finding corroborates those of others who have shown that endocytic and autophagosomal vesicles mature via increasing acidification concomitantly with their retrograde transport (Hollenbeck, 1993; Maday et al., 2012; Overly and Hollenbeck, 1996).

Although MVBs are major intermediates in the endo-lysosomal pathway, little is known regarding the dynamics of MVB formation and transport within axons. A plethora of work has shown that various cargos, including cannabinoids, tracers, and SV markers, can be found within MVBs in axons (Lees et al., 1981; Vitalis et al., 2008), suggesting that MVBs are responsible for the retrograde transport of these cargo. Interestingly, other cargo that is seen to accumulate in somatic MVBs, such as trophic factors, are not detected in axonal MVBs, suggesting that other endocytic vesicles are responsible for this transport (Altick et al., 2009). Together, these studies suggest that the endocytic vesicles for retrograde transport are cargo-specific.

Interestingly, MVBs can be detected in presynaptic boutons by electron microscopy (EM) (Ceccarelli et al., 1973; LaVail and LaVail, 1975; Teichberg et al., 1975) and often appear following neuronal stimulation (Teichberg et al., 1975), suggesting that their formation may be activity-dependent. However, so far the studies addressing synaptic and axonal MVBs employ static imaging techniques, namely EM, and fail to give a dynamic picture of MVB formation and

transport. Additionally, the proteins responsible for regulating cargo sorting and vesicular trafficking through the endolysosomal pathway are largely uncharacterized in neurons.

Rab GTPases

The Rab family of small GTPases are important regulators of membrane trafficking in all eukaryotic cells. Rab GTPases act as “molecular switches” that cycle between ‘active’ (GTP-bound) and ‘inactive’ (GDP-bound) states. Although Rab GTPases have intrinsic GTPase activity, the hydrolysis of GTP to GDP is further aided by GTPase activating proteins (GAPs), which facilitate the inactivation of Rabs. On the other hand, the activation of Rabs is catalyzed by guanine nucleotide exchange factors (GEFs), which release GDP and allow Rabs to bind cytosolic GTP. GTP-bound Rabs in turn recruit effectors that specifically recognize activated Rabs, and catalyze downstream events such as membrane fusion (i.e. SNARE proteins) and vesicle trafficking (i.e. motor proteins, Figure 1.4) (see (Stenmark, 2009)). Thus, regulation of Rab activation/inactivation by GEFs and GAPs allows for spatiotemporal coordination of critical membrane trafficking events.

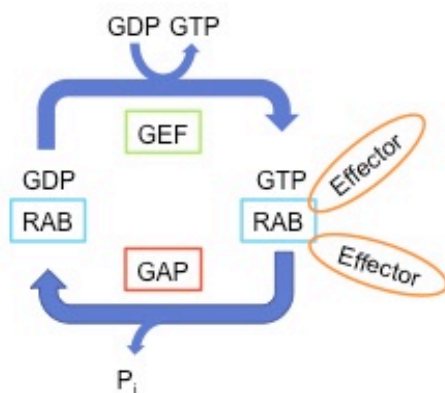


Figure 1.4 - Rab GTPase cycle

Rab GEFs function to activate Rab proteins by catalyzing the exchange of GDP for GTP. Active Rabs then recruit effectors to mediate downstream trafficking events. Rab GAPs function to inactivate Rab proteins by hydrolyzing GTP to GDP.

As key regulators of vesicle trafficking, Rab GTPases are hypothesized to regulate multiple steps of the SV life cycle, from biogenesis to recycling and degradation. Among the >60 Rabs in mammalian brain, at least 30 are reported to associate with SV pools (Pavlos and Jahn, 2011; Takamori et al., 2006). However, only a few of these (*e.g.* Rab3, Rab27) have well-established roles in the SV cycle (Mahoney et al., 2006; Pavlos et al., 2010; Schluter et al., 2004; Schluter et al., 1999; Yu et al., 2008). While Rab3 has a well-characterized role in exocytosis (see (Regazzi, 2007)) in non-neuronal cells and is found on synaptic vesicles, its genetic loss-of-function was found to have minimal effects on synaptic transmission (Geppert et al., 1994). However, it was later found that Rab3 GEFs also act on Rab27, suggesting Rab27 can compensate for Rab3 in SV exocytosis. Indeed, the loss of both Rab3 and Rab27 leads to a dramatic decrease in SV exocytosis (Mahoney et al., 2006). These findings suggest that the Rab GTPases have critical regulatory roles in the SV cycle.

Endocytic SV-associated Rab GTPases

Lending credence to the proposed role of endosomal sorting in the SV cycle, many of the SV-associated Rabs identified have known endocytic functions in non-neuronal cells (Hoopmann et al., 2010; Rizzoli et al., 2006; Takamori et al., 2006; Uytterhoeven et al., 2011; Wucherpfennig et al., 2003), though many questions remain regarding their roles in neurons. For example, it is not known how and where specific Rab GTPases act at the synapse to mediate SV protein sorting, although recent evidence implicates presynaptic endosomes as important sites of Rab-mediated SV protein sorting (Hoopmann et al., 2010; Rizzoli et al., 2006; Shimizu et al., 2003; Takamori et al., 2006; Uytterhoeven et al., 2011; Wucherpfennig et al., 2003). As mentioned previously, the early endosome-associated Rab5 is present on recycling SVs (Hoopmann et al., 2010; Pavlos et al., 2010; Shimizu et al., 2003; Takamori et al., 2006; Wucherpfennig et al., 2003) and Rab5

loss-of-function has been shown to impair SV recycling and neurotransmitter release in *Drosophila* (Shimizu et al., 2003; Wucherpennig et al., 2003).

Another study in *Drosophila* has demonstrated that endosomal sorting and replenishment of SV proteins is necessary to maintain a releasable pool of SVs, and that this process requires Rab35 (Uytterhoeven et al., 2011). The ESCRT system and the pre-lysosomal homotypic fusion and vacuole protein sorting (HOPS) complex were also identified through genetic interactions as components of this pathway (Fernandes et al., 2014; Uytterhoeven et al., 2011). Specifically, these studies have demonstrated that loss-of-function of Skywalker/TBC1D24, a Rab GAP, leads to Rab35 over-activation and the excessive endosomal sorting and replenishment of SV proteins in *Drosophila*. Additionally, alterations in Rab7 and Rab11 activation have been reported to affect neurotransmission at the neuromuscular junction (Uytterhoeven et al., 2011), suggesting that the trafficking routes of SVs are complex and highly dependent upon the Rab GTPases.

Interestingly, some of these SV-associated Rabs (*i.e.* 5, 11, 26) are implicated in macroautophagy (Ao et al., 2014; Binotti et al., 2015), another lysosomal degradative pathway that may also be important for SV protein turnover. Macroautophagy begins with the *de novo* synthesis of a pre-autophagosomal structure (PAS). This membrane expands to engulf cytoplasmic contents, which can include protein aggregates and whole organelles. Eventually, the membrane closes and forms a double membrane structure referred to as an autophagosome (see (Feng et al., 2014)). Autophagosomes can then fuse with compartments of the endocytic pathway (*i.e.* early endosomes, MVBs) to form an intermediate structure called an amphisome, which will then fuse with lysosomes, or autophagosomes can directly fuse with lysosomes (see (Fader and Colombo, 2009)). While autophagy functions at a basal level to degrade cellular

contents, it can also be highly upregulated in response to stress such as nutrient deprivation (see (Russell et al., 2014)).

Indeed, macroautophagy has been shown to mediate the degradation of SVs under certain conditions (Hernandez et al., 2012). In neurons, stimulating autophagy with rapamycin was shown to reduce SV pool size and evoked neurotransmission in dopaminergic neurons (Hernandez et al., 2012). Moreover, another SV-associated Rab (Rab26) appears to link SV clusters to the macroautophagy machinery by recruiting Atg16L1, a component of pre-autophagosomes (Binotti et al., 2015). In addition, a forward genetic screen in *Drosophila* recently identified presynaptic voltage-gated calcium channels as key regulators of autophagosome-lysosome fusion, indicating that components of the presynaptic SV release machinery also function in autophagic degradation (Tian et al., 2015). These studies provide evidence that macroautophagy can regulate SV pool size, but it is unclear whether this pathway is essential for the basal turnover/degradation of SV proteins. Thus, the pathway(s) for SV protein degradation, and the roles of SV-associated Rabs in regulating this process, remain unresolved.

Protein Homeostasis in Neuronal Health

A clear connection between a variety of neurodegenerative diseases and synaptic protein homeostasis has led to a great interest in understanding the basic mechanisms involved in this process. While all cells must degrade damaged or dysfunctional proteins, the structure and function of neurons and their synapses necessitates specialized mechanisms to maintain healthy proteins throughout the lifetime of an organism. Whereas other cell types can undergo complete turnover, the embedded nature of neurons within a network and the specialization of synapses to encode specific information precludes this possibility. Although there is the potential for entire

synapses to turnover, this has only been observed in the barrel cortex and at neuromuscular junctions (Grillo et al., 2013; Shi et al., 2012; Zuo et al., 2005).

The presynaptic compartment in particular is an area of high membrane dynamics. In order for neurons to maintain efficient neurotransmission, SVs must undergo repeated cycles of exocytosis, endocytosis, and vesicle reformation. These processes depend upon SV-associated proteins whose proper conformation and function are of paramount importance to neuronal health (Bezprozvanny and Hiesinger, 2013; Wang et al., 2013). Indeed, the buildup of damaged or misfolded SV proteins can lead to synaptic dysfunction and neurodegeneration (Garden and La Spada, 2008; Scott et al., 2010; Uytterhoeven et al., 2011). However, despite the importance of SV protein turnover for neuronal health, the molecular mechanisms underlying this process are largely unknown.

Chapter 2 - Materials and Methods

Cell Culture

Cultured rat neurons

Timed-pregnant Sprague Dawley rats were housed, handled, and euthanized using methods consistent with recommendations from the *Guide for the Care and Use of Laboratory Animals* prepared by the National Research Council, and with the Columbia University Medical Center Institutional Animal Care and Use Committee. Hippocampal neurons were prepared from rat brains (E18) using a modified Banker culture protocol (Banker and Goslin, 1998; Waites et al., 2009). Briefly, neurons were dissociated in TrypLE Express (Fisher/Life Technologies) for 20 minutes, washed with Hank's Balanced Salt Solution (Sigma) and plated in Neurobasal medium with B27 supplement and Glutamax (all Life Technologies) at a density of 250,000 neurons per well (12 well plates) or coverslip (22x22 mm square).

Microfluidic culturing

Primary hippocampal neurons were plated in two adjacent channels of a three-channel microfluidic chamber at a density of 60,000 neurons in the larger channel and 40,000 neurons in the smaller channel. Half the media of all channels was changed every 48 hours. On 7 days in vitro (DIV), fluidic isolation was performed to preferentially transduce neurons in the larger channel with mCh-Hrs virus. A volume difference of 60 μ l was maintained between the transduced and untransduced channels (Park et al., 2006). Prior to imaging, fluorescence was examined in all channels to ensure fluidic isolation was successful.

Molecular techniques

Constructs, shRNAs

Sources of the constructs used are listed in Table 2.1. For shRNAs, target sequences for rat Rab35, Hrs, and TSG101 were modified from published work or designed using siDirect (sidirect2.rnai.jp). Target sequences are as follows: Rab35: 5'-GGGCAGATGGGGATCCAGC-3' (nucleotides 418-436)(Allaire et al., 2010) Hrs: 5'-GAACTACTGGGAGAAGAAA-3' (nucleotides 996-1014), TSG101: 5'-GGATGAAGGAGGAAATGGA-3' (nucleotides 725-743), RNF167: 5'-CCAAAGAGCAACTGAAACA-3' (nucleotides 626-644). shRNAs were sub-cloned into pZOff 2.0 and subsequently into the modified FUGW H1 vector as described previously (Leal-Ortiz et al., 2008). To evaluate shRNA knockdown efficiency, neurons were transduced with lentivirus on 3-7 DIV, collected on 12-16 DIV, and processed for immunoblotting as described below. Protein intensity was measured and compared to that in neurons expressing a scrambled hairpin (scRNA). Transduction was timed to achieve the highest knockdown efficacy without noticeable toxicity (assessed by bright field microscopy). To create shRab35-resistant Rab35, the following mutations (shown in italics) were made to rat Rab35 5'-GGCCA*AA*TGGGCATTCAAC-3' (nucleotides 418-436). Neurons were transduced with either scRNA or shRab35 on 3 DIV then on 9 DIV with sh-resistant Rab35.

qPCR

RNA was isolated from 14 DIV primary hippocampal neurons using Qiagen RNeasy Micro kit. Reverse transcription was then performed using SuperScript VILO master mix (Invitrogen) followed by qPCR using TaqMan primers to RNF167, GAPDH, and actin. Each reaction was performed in triplicate and quantified using the $\Delta\Delta C_t$ method (Livak and Schmittgen, 2001). RNF167 RNA levels were normalized to actin RNA and to GAPDH RNA levels. The average

normalized RNF167 RNA value was calculated and compared between soluble-GFP expressing control neurons and shRNF167 expressing neuron.

Lentivirus production, transduction, and DNA transfection

Lentivirus was produced as previously described (Leal-Ortiz et al., 2008; Lois et al., 2002) except that Calfectin (SignaGen Laboratories) was used for transfection of HEK293T cells. HEK medium was replaced with Neurobasal medium 18-24 hours after transfection, and this medium (viral supernatant) was harvested 24 hours later. Neurons were transduced with 50-200 μ l lentiviral supernatant/well (6 or 12 well plates) between 3-10 DIV depending on the experiment (see Results), and processed for immunoblotting or immunocytochemistry between 14-15 DIV. For biochemical experiments, high viral titer producing >80% infectivity was ensured by transducing test wells of neurons with varying amounts of virus, and calculating of the number of infected cells divided by the number of DAPI-positive nuclei (DAPI VectaShield, Vector Laboratories) per field of view using fluorescence microscopy.

Neurons were transfected using Lipofectamine 2000 (Life Technologies) on 7-10 DIV. For each 22x22 mm coverslip, 2.5 μ l Lipofectamine was incubated with 62.5 μ l Neurobasal for 5 minutes, combined with 1-2.5 μ g DNA diluted in 62.5 μ l Neurobasal for 20 minutes, then added to neurons for 45 minutes at 37°C. Neurons were transfected in Neurobasal medium containing 50 μ M AP5 and 10 μ M CNQX, and returned to their original dishes and medium following transfection. Neurons were fixed for immunofluorescence microscopy on 12-16 DIV.

Pharmacological treatments

Pharmacological agents were used in the following concentrations and time courses:

cycloheximide (Calbiochem, 0.2 μ g/ μ l, 24hrs), bicuculline (Sigma, 40 μ M, 12-24hrs), 4-aminopyridine (Tocris, 50 μ M, 12-24hrs), AP5 (Tocris, 50 μ M, 24 hrs), CNQX (Tocris, 10 μ M,

24hrs), tetrodotoxin (Tocris, 0.5 μ M, 24hrs), GDP (Sigma, 5 mM), GTP γ S (Sigma, 5 mM), PR-619 (LifeSensors, 50 μ M, 6hrs).

Electrophysiology

Changes in neuronal activity in the presence of bicuculline/4-aminopyridine or CNQX/APV/TTX were measured using whole-cell voltage clamp electrophysiology. Dissociated hippocampal neurons were recorded on 15 DIV at room temperature using a Multiclamp 700B amplifier (Molecular Devices) and a 1550A Digidata digitizer (Molecular Devices) interfaced to a computer equipped with Clampex 10 software (Molecular Devices). Neurons were continuously perfused with extracellular solution (140 mM NaCl, 2.4 mM KCl, 10 mM HEPES, 10 mM glucose, 4 mM CaCl₂, 4 mM MgCl₂; pH 7.35, 300 mOsm) via a gravity-based perfusion system. Patch pipettes pulled from borosilicate glass (World Precision Instruments) had resistances of 4-5 M Ω when filled with intracellular solution (135 mM K-gluconate, 10 mM HEPES, 1 mM EGTA, 4.6 mM MgCl₂, 4 mM Na-ATP, 15 mM creatine phosphate; pH 7.35, 320 mOsm). The series resistance was <15 M Ω and experienced minimal change (<15 %) from the start of the recording to the end of the recording. The membrane potential was clamped at -70 mV. Following baseline activity recordings for 4 minutes, either 40 μ M bicuculline/50 μ M 4-aminopyridine or 10 μ M CNQX/50 μ M APV/0.5 μ M TTX was perfused onto the neurons and recording continued for a further 6 minutes. Traces were analyzed using MiniAnalysis software. Activity was measured as the frequency of spontaneous events during the first 4 minutes (baseline) and the last 4 minutes (with drug) of the trace.

Imaging techniques

Immunofluorescence microscopy

Primary antibodies are listed in Table 2.2. Alexa 488- or Alexa 647-conjugated secondary antibodies (Life Technologies) were used at 1:800 or 1:400, respectively. Neurons were immunostained as described previously (Leal-Ortiz et al., 2008). Briefly, coverslips were fixed with Lorene's fix (60 mM PIPES, 25 mM HEPES, 10 mM EGTA, 2 mM MgCl₂, 0.12 M Sucrose, 4% formaldehyde) for 15 minutes, primary and secondary antibody incubations were performed in blocking buffer (2% glycine, 2% BSA, 0.2% gelatin, 50 mM NH₄Cl in 1X PBS) for 1-2 hours at room temperature or overnight at 4°C, and all washes were done with PBS. Coverslips were mounted with DAPI VectaShield (Vector Laboratories) and sealed with clear nail polish. Images were acquired with a 40X objective (Neofluar, NA 1.3) or a 63X objective (Neofluar, NA 1.4) on an epifluorescence microscope (Axio Observer Z1, Zeiss) with Colibri LED light source, EMCCD camera (Hamamatsu) and Zen 2012 (blue edition) software.

Confocal microscopy

Super-resolution imaging was performed with a Zeiss LSM 800 confocal microscope equipped with Airyscan module, using a 63x objective (Plan-Apochromat, NA 1.4). Images were obtained and processed using Zen Blue 2.1 software.

SNAP-labeling

SNAP-Cell Oregon Green (New England BioLabs) was diluted in Neurobasal media to a final concentration of 10 μM. 13 DIV neurons were incubated for 30 minutes at 37°C, washed 3 times with Neurobasal media, incubated for 30 minutes at 37°C in fresh media, washed once more, and returned to the original media (adapted from (Bodor et al., 2012)). 15 hrs and 2 days after SNAP labeling, neurons were fixed, immunostained using anti-Flag antibody, and imaged as described above.

Super-Ecliptic pHluorin imaging

Neurons were lentivirally transduced with super-ecliptic pHluorin (SEP)-tagged WT or K/R mutant VAMP2 or synaptophysin on 2-3 DIV, and imaging experiments performed between 13-16 DIV. SEP fluorescence is quenched inside acidic SVs, increased upon exposure to the neutral extracellular pH during stimulation, and re-quenched after endocytosis, thus enabling us to visualize the kinetics of SV exo/endocytosis via changes in SEP fluorescence, as in (Burrone et al., 2006; Voglmaier et al., 2006). Images were acquired every 5 seconds for 5 cycles prior to stimulation, 6 cycles during 10Hz, 30 sec stimulation, and 49 cycles following stimulation. At the end of each experiment, NH_4Cl Tyrodes was added to de-acidify neurons, allowing us to visualize total SEP fluorescence and to measure the size of the recycling pool of SVs (maximum SEP fluorescence during stimulation) as a fraction of total SV pool (SEP fluorescence after NH_4Cl Tyrodes treatment). To plot SV exo/endocytosis curves, fluorescence changes of individual SEP puncta over time were measured with an ImageJ plugin (Time Series Analyzer v2, author Balaji), and normalized to initial fluorescence intensity. For each coverslip, an average curve was calculated from individual punctum intensity values. These curves were combined to plot average curves for each condition.

Live Imaging

Neurons were plated in microfluidic chambers on glass bottom dishes. On 7 DIV, neurons were lentivirally transduced with mCh-Hrs virus. On 10 DIV, time series images taken every 5 seconds for 50 frames were acquired with a 40X objective (Zeiss Neofluar, NA 1.3) on an epifluorescence microscope (Axio Observer Z1, Zeiss) with Colibri LED light source, EMCCD camera (Hamamatsu) and Zen 2012 (blue edition) software. Neurons were treated with bicuculline and 4-AP to increase neuronal activity for 1 hour. Puncta direction and velocity were analyzed using the Manual Tracking plugin (Frabrice Cordeli) in ImageJ. Average velocity was

calculated for all puncta in a given axon. Puncta were classified as primarily moving if any movement was observed in >45% of frames. The directionality of moving puncta was further classified as primarily anterograde or primarily retrograde if a puncta moved in a given direction for >45% of frames or bidirectional if neither direction was favored in >45% of frames.

Electron Microscopy

On 14 DIV, neurons plated on Lab-Tek chamber slides (Nunc) were treated with bicuculline and 4-AP for 12 hours. Following this treatment, cells were then fixed with glutaraldehyde and then dehydrated, embedded, sectioned, stained and subjected to electron microscopy at Columbia University's Pathology Imaging Core.

Biochemical techniques

Co-immunoprecipitation and pull-down assays

For co-immunoprecipitation studies, HEK293T cells were transfected using Calfectin according to manufacturer's protocol (SignaGen Laboratories). Cell lysates were collected 48 hours after transfection in lysis buffer (50 mM Tris-Base, 150 mM NaCl, 1% Triton X-100, 0.5% deoxycholic acid) with protease inhibitor cocktail (Roche) and clarified by centrifugation at high speed (20000 rcf). For neuronal co-immunoprecipitation and pull-down studies, neurons were transduced between 7-10 DIV and collected in lysis buffer on 14-15 DIV. Neuronal lysates were centrifuged at low speed (1000 rcf) to pellet nuclei. Resulting supernatant from HEK293T cells or neurons was incubated with Dynabeads (Life Technologies) coupled to anti-Flag (monoclonal; Sigma), anti-mCherry (polyclonal; Biovision), anti-HA (monoclonal; Santa Cruz), anti-VAMP2 (monoclonal; Synaptic Systems), or anti-GTP-Rab35 (NewEast Biosciences) antibodies. For all studies, lysates were incubated at 4°C under constant rotation for 1-2 hours. Beads were washed 2-3 times with PBS containing 0.05% Triton (PBST) then once with PBS.

Bound proteins were eluted using sample buffer (Bio-Rad) and subject to SDS-PAGE immunoblotting as described below. For active GTP-Rab35 immunoprecipitation experiments, 2.5 mM MgCl₂ was added to all buffers.

For co-immunoprecipitation studies assessing the nucleotide dependence of the Rab35-Hrs interaction, lysates from HEK293T cells co-transfected with Flag-Hrs and HA-Rab35 were collected and clarified as above. The resulting supernatant was divided equally and treated with either 5 mM GDP or 5 mM GTP γ S. Lysates were incubated at 37°C with agitation for 30 minutes to facilitate nucleotide exchange. Lysates were briefly chilled on ice, treated with 60 mM MgCl₂ to lock Rab35 in either the GDP or GTP bound state, and then subjected to immunoprecipitation with anti-Flag coated Dynabeads. Bound proteins were washed as described with wash buffer containing 2.5 mM MgCl₂, then eluted in sample buffer.

Ubiquitination assay for VAMP2

HA-ubiquitin was co-transfected with either untagged WT VAMP2 or untagged KR VAMP2 in HEK293T cells. For RNF167 ubiquitination assays, HA-ubiquitin was co-transfected with untagged WT VAMP2 and either soluble mCh or mCh-RNF167. Prior to collection, cells were incubated with 50 μ M PR-619 (LifeSensors), a deubiquitination inhibitor, for 6 hours. Cell lysates were collected and clarified as described in above. Resulting supernatant from HEK293T cells was incubated with Dynabeads (Life Technologies) coupled to anti-VAMP2 (monoclonal; Synaptic Systems) antibodies. Lysates were incubated for 12 hours at 4°C under constant rotation. Beads were washed 3 times with PBS. Bound proteins were eluted using sample buffer (Bio-Rad) and subject to SDS-PAGE immunoblotting as described.

GST Pull-down

GST and GST-Rab35 protein purification and pull-down were performed as described previously (Brymora et al., 2004) with minor changes. Specifically, protein expression was induced with 0.4 mM IPTG overnight at 25°C, bacterial cell pellets were resuspended in a solution containing 50 mM Tris, 150 mM NaCl, 2.5 mM MgCl₂ with protease inhibitors at pH 7.4, and cells were subsequently lysed in the same buffer with 0.5% Triton X added. GST, GST-Rab35-GDP or GST-Rab35-GTP γ s were coupled to agarose beads, then incubated with HEK293T lysate expressing Flag-Hrs for 2 hours at 4°C under constant rotation. Beads were then washed 3 times in 50 mM Tris, 150 mM NaCl, 2.5 mM MgCl₂, 0.5% Triton X with protease inhibitors and once in the same buffer without Triton. Proteins were eluted directly in 2X SDS sample buffer (Bio-Rad) and processed for immunoblotting as described below. For all co-immunoprecipitation and pull-down assays, 1-5% of lysate applied to the beads was run as ‘input’.

Immunoblotting

For all other immunoblotting experiments, neurons were collected directly in 2X SDS sample buffer (Bio-Rad). Samples were subjected to SDS-PAGE, transferred to nitrocellulose membranes, probed with primary antibody (Table 2.2) in 5% BSA/PBS+0.05% Tween-20 overnight at 4°C, followed by DyLight 680 or 800 anti-rabbit, anti-mouse, or anti-goat secondary antibodies (Thermo Scientific) for 1 hour. Membranes were imaged using an Odyssey Infrared Imager (Model 9120, LI-COR Biosciences). Protein intensity was measured using the ‘Gels’ function in ImageJ.

Analysis

Fold-change calculation

For cycloheximide-chase experiments, the normalized intensity of protein remaining after 24 hours of treatment was reported as a fraction of the normalized intensity of that protein in lysates

from the same condition with DMSO treatment. Protein levels were first normalized to the intensity of tubulin. Next, the fractional amount of degradation that occurred for each protein over the 24-hour period was calculated by dividing its intensity with cycloheximide treatment (chx) to its intensity with DMSO control treatment (c)(Table 3.1). These fractional amounts of degradation were further normalized to “fold change in degradation vs. control” by dividing the perturbation condition (i.e. blockers, Bic/4AP, shRNA) by the control condition (i.e. DMSO, scRNA).

Image Analyses

Colocalization analyses of Hrs and CHMP2B with VAMP2 were performed manually in ImageJ using the Time Series Analyzer V2 plugin (Balaji) to create ROIs (8x8, oval) over Hrs or CHMP2B puncta. ROIs with VAMP2 immunostaining above a threshold value (determined empirically, typically <5% in Threshold window) were counted and expressed as a fraction of the total. Puncta intensity analyses were performed in ImageJ by creating a selection in the Rab channel and applying it to the VAMP2 channel. Mean intensity values of VAMP2 puncta (‘gray values’) were then measured using the ‘Analyze Particles’ function. The experimental condition was reported as a fraction of the control condition by dividing intensity values from three experimental images by the average of three images from the control condition. In experiments coexpressing shHrs or scrambled shRNAs with mCh-Rab35, VAMP2 intensity was measured in OpenView (written by Noam Ziv, Technion Institute, Haifa, Israel) as described previously (Waites et al., 2011). Briefly, VAMP2 puncta were selected from processes expressing both EGFP and mCh-Rab protein, mean intensity values were measured, and average intensity calculated and reported as in the ImageJ analyses. Puncta per unit length (measured in arbitrary units) was calculated in ImageJ using the ‘freehand line’ tool to trace and measure Tau positive

axons containing Hrs puncta. To measure BG-Oregon Green colocalization with Flag, the ImageJ colocalization plug-in (Pierre Bourdoncle) was used. BG-Oregon Green and Flag puncta above a threshold value were determined empirically, total vs. colocalized puncta counts were measured using the ‘Analyze Particles’ function, and the fraction of colocalized puncta over total Flag puncta calculated. OpenView was used to measure BG-Oregon Green intensity as described above.

Evaluation of neuronal health

14 DIV hippocampal neurons on coverslips were treated with 0.2 $\mu\text{g}/\mu\text{l}$ cycloheximide for 24-36 hours, fixed in Lorene’s Fix, and processed for immunostaining against Tau (polyclonal; Synaptic Systems) and MAP2 (monoclonal; Sigma), mounted with DAPI Vectashield (Vector Laboratories), and images acquired as described (Immunofluorescence Microscopy section). The following features were scored per field of view: condensed nuclei (DAPI staining in MAP2 positive neurons), enlarged cell bodies (DAPI/MAP2 area), blebbing dendrites (based on MAP2 staining), and axonal beading (punctate Tau staining). In control conditions, <15% of neurons exhibited one or more of these features.

Statistical analyses

Graphing and statistics were performed using Prism (GraphPad). Unpaired, two-tailed t-tests were used to calculate p-values for all bar graph analyses.

Table 2.1 - List of DNA constructs

name of protein	species	accession #	source	Vector and cloning information
Rab35	rat	NM_001013046.1	Genewiz, Inc. gene synthesis	Subcloned into pEGFP/mCh-C2 and pKH3 vectors at EcoRI site, moved into FUGWm with MfeI/NheI and EcoRI/XbaI (FUGWm), PCR into pGEX-4T2 at SalI/NotI sites
Rab3	human		Gift from C. Garner	Received in pEGFP vector subcloned mCh at AgeI/BsrGI sites, moved into FUGWm using MfeI/NheI and EcoRI/XbaI (FUGWm)
Rab5	human		Gift from G. DiPaolo	Received in pEGFP, subcloned mCh at AgeI/BsrGI sites, moved into FUGW using MfeI/NheI, PCR into pKH3 at BamHI/ClaI sites
Rab10	rat	NM_017359.2	Genewiz, Inc. gene synthesis	Subcloned into pEGFP/mCh-C2 and pKH3 vector at EcoRI site, moved into FUGWm with MfeI/NheI and EcoRI/XbaI (FUGWm)
Rab14	rat	NM_053589.1	Genewiz, Inc. gene synthesis	Subcloned into pEGFP/mCh-C2 and pKH3 vector at EcoRI site, moved into FUGWm with MfeI/NheI and EcoRI/XbaI (FUGWm)
Rab21	rat	NM_001004238.1	Genewiz, Inc. gene synthesis	Subcloned into pKH3 vector at EcoRI site
Hrs	human		Addgene #29685	Received in RFP vector, moved into FUGWm using MfeI/NheI, PCR into pCS2-FLAG at XhoI/XbaI sites
TSG101	human		Addgene #38318	Received in mCh vector, used as is
STAM	human		Addgene #21499	Subcloned into pmCh N1 at XhoI/HindIII sites
CHMP2B	human		Gift from C. Garner	Received in pmCh-C2 vector, used as is
Connecdenn1/ DENND1A	rat	NM_001191747.1	Genewiz, Inc. gene	Subcloned into pEGFP-C1 at EcoRI site

			synthesis	
VAMP2	rat	NM_012663.2	Genewiz, Inc. gene synthesis	Subcloned into pEGFP/SEP-N1 vectors at EcoRI site, moved into FUGWm with MfeI/NheI and EcoRI/XbaI (FUGWm)
KR VAMP2	rat	NM_012663.2	Genewiz, Inc. gene synthesis	Subcloned into pEGFP/SEP-N1 vectors at EcoRI site, moved into FUGWm with MfeI/NheI and EcoRI/XbaI (FUGWm)
HA-Ubiquitin	human		Addgene #18712	Used as is

Table 2.2 - List of antibodies

Antibody	Source	Species	Catalog number
VAMP2	Synaptic Systems	rabbit	104202
VAMP2	Synaptic Systems	mouse	104211
SV2	Developmental Studies Hybridoma Bank	mouse	
Tubulin	Abcam	rabbit	ab4074
Tubulin	Sigma	mouse	t9026
mCherry	Biovision	rabbit	5993
Hrs	Santa Cruz	rabbit	m-79 sc30221
Rab35	Gift from Peter McPherson	rabbit	
Synaptotagmin 1	Synaptic Systems	rabbit	105012
Snap-25	Synaptic Systems	mouse	111011
Rim1 α	Synaptic Systems	rabbit	140003
Munc-13	Synaptic Systems	rabbit	126102
Synaptophysin	Santa Cruz	rabbit	h-93 sc9116
HA	Santa Cruz	rabbit	y-11 sc805
HA	Santa Cruz	mouse	f-7 sc7392
Flag	Sigma	mouse	clone m2 f3165
TSG101	Santa Cruz	mouse	c-2 sc7964
Tau	Santa Cruz	rabbit	v-20 sc1996
MAP2	Sigma	mouse	ap-20 m1406
Synapsin 1	Synaptic Systems	mouse	106001
Rab3	Synaptic Systems	mouse	107111
Rab5	Santa Cruz	mouse	D-11 sc-46692
Rab10	Santa Cruz	goat	C-18 sc-6564
Rab14	Santa Cruz	rabbit	H-55 sc-98610
Active Rab35	NewEast Biosciences	mouse	26922
Rab35	Proteintech	rabbit	11329-2-AP
GST	Abcam	rabbit	ab9085
Homer 1	Synaptic Systems	rabbit	160003

Chapter 3: A subset of SV proteins undergo activity-dependent degradation by the ESCRT pathway

Rationale

The release of chemical neurotransmitter from synaptic vesicles (SVs) is essential for synaptic communication. In order for neurons to maintain rapid, efficient neurotransmission, SVs must undergo repeated cycles of fusion with the plasma membrane (exocytosis), followed by membrane retrieval (endocytosis) and vesicle reformation. These processes are mediated by a group of SV-associated proteins whose proper conformation and function are critical for synaptic health (see (Bezprozvanny and Hiesinger, 2013; Wang et al., 2013)). Indeed, without proper maintenance of SV pools, synapses become dysfunctional over time, leading to the loss of neuronal communication and ultimately to neurodegeneration (Garden and La Spada, 2008; Scott et al., 2010; Uytterhoeven et al., 2011). However, while the molecules that mediate SV exocytosis and endocytosis have been well characterized, very little is known about the molecular pathways responsible for SV protein turnover and degradation.

In addition to its role in cellular homeostasis, protein degradation is also essential for synaptic plasticity and synapse formation/elimination, processes tightly linked to neuronal activity (see (Alvarez-Castelao and Schuman, 2015)). While the ability of neuronal activity to regulate postsynaptic protein degradation has been demonstrated (Ehlers, 2003; Lussier et al., 2011; Schwarz et al., 2010; Scudder et al., 2014), few studies have examined the relationship between activity and presynaptic protein turnover. It has been reported that silencing neurons leads to the accumulation of presynaptic proteins (Lazarevic et al., 2011), suggesting that their turnover is slowed in the absence of activity; however, the direct effects of neuronal activity on SV protein degradation have not been investigated. In this chapter, we discover that the

degradation of a subset of SV proteins is regulated by neuronal activity. Further, we find that neuronal activity functions to recruit proteins of the ESCRT pathway to synapses to initiate endolysosomal degradation.

Results

SV integral membrane proteins turn over at different rates

We first developed an assay to monitor the degradation of SV integral membrane proteins. A previous study used the protein synthesis inhibitor cycloheximide to monitor protein degradation in neurons (Sharma et al., 2011), and we tested this approach in hippocampal neurons cultured for 14 days in vitro (DIV), using DMSO (vehicle control) or cycloheximide (chx) to block protein synthesis for 24 or 36 hours. We performed immunostaining against Tau (axonal protein) and MAP2 (dendritic protein), and counterstained with the nuclear label DAPI to evaluate whether this long-term chx treatment caused neuronal toxicity, reflected by enlarged cell bodies, dendritic blebbing, axonal beading, and nuclear chromatin condensation (Figure 3.1A,B). We found that 36 hours of chx treatment led to one or more of these phenotypes in >60% of the fields of view scored, but that 24 hours of chx did not cause any detectable changes in neuronal health versus DMSO treatment alone (Figure 3.1A,B). Given this 24-hour chx treatment window, we next assessed whether it was possible to detect SV protein degradation during this time period. Lysates from neurons treated for 24 hours with DMSO or chx were collected and subjected to immunoblotting with antibodies against SV integral membrane proteins (VGLUT1, synaptophysin (Syp), SV2, synaptotagmin1 (Syt1), VAMP2) and the plasma membrane-associated SNARE protein SNAP-25. Resulting immunoblots were imaged using the Odyssey Imaging System (LI-COR), which acquires images in the linear range without saturation or over-exposure of protein bands, enabling very accurate quantification of protein levels. For each

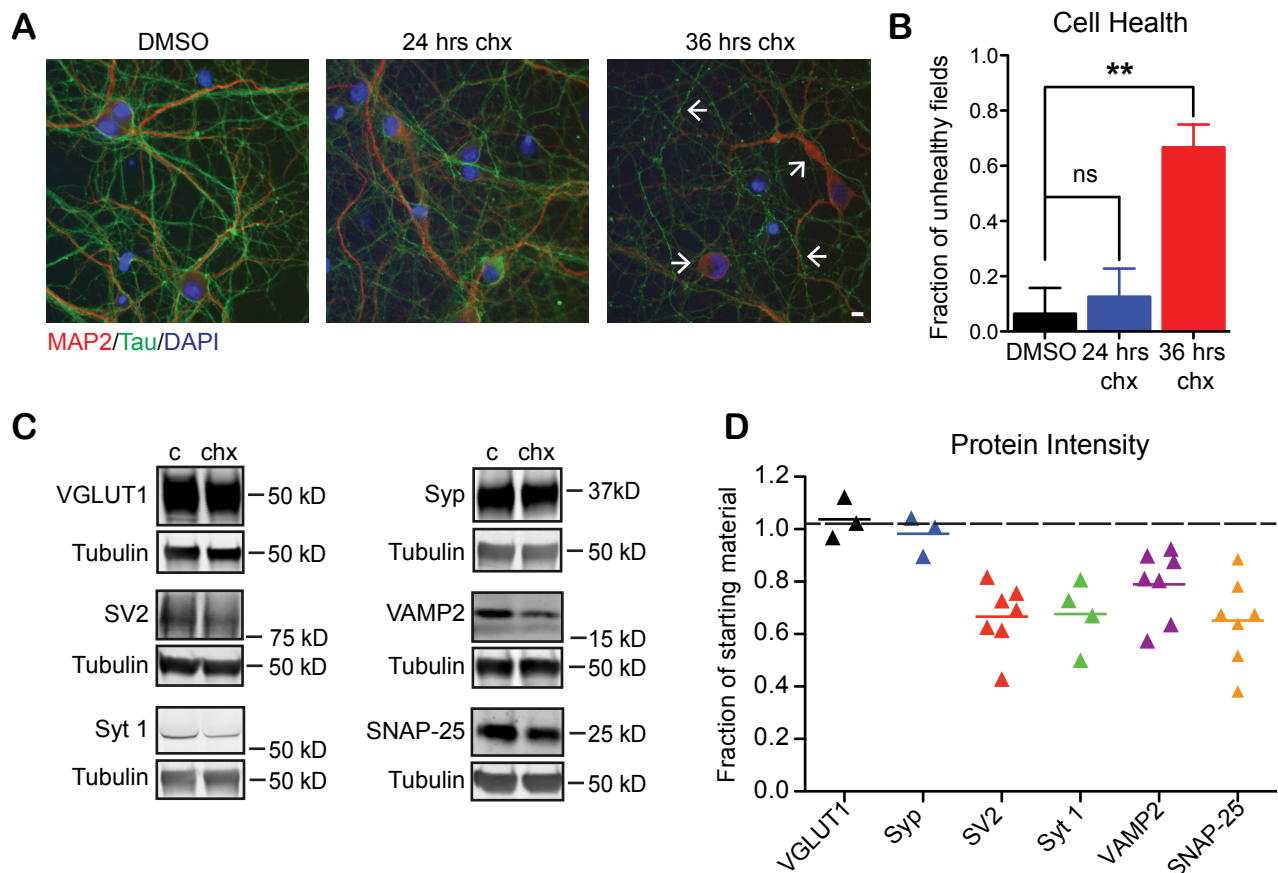


Figure 3.1: SV proteins exhibit different fractional amounts of degradation after protein synthesis inhibition. A) Representative images from 14 DIV neurons treated with DMSO or chx for 24 or 36 hours, immunostained with Tau antibodies to label axons (green), MAP2 antibodies to label dendrites (red), and mounted with DAPI to label nuclei (blue). Arrows in 36 hr panel denote the characteristics of cell health that were scored for B, including enlarged cell bodies, blebbing dendrites, and axonal beading. Note that Tau immunostaining becomes weaker following chx treatment due to protein synthesis inhibition. White scale bar=10 μ m. B) Quantification of cell health based on nuclear and process morphology (see Methods for details; n=5-7 fields of view/condition, *p<0.05, two-tailed t-test). C) Representative immunoblots of SV membrane proteins (VGLUT1, Synaptophysin (Syp), SV2, Synaptotagmin 1 (Syt 1), VAMP2) and the plasma membrane-associated SNAP-25, from lysates of 14 DIV neurons treated for 24 hours with either DMSO (c) or cycloheximide (chx). D) Quantification of protein intensity after 24 hrs chx treatment, normalized to tubulin and reported as a fraction of the DMSO control intensity (starting material). Averages are denoted by colored lines; each triangle represents one experiment. Black dotted line denotes no change in fractional degradation.

protein, the fractional amount of degradation that occurred over 24 hours was expressed as a ratio of its intensity with chx treatment to its intensity with DMSO control treatment (c) (Figure 3.1C,D), and normalized to tubulin. Since tubulin is a very stable protein, its levels were nearly always unchanged over the 24-hour time course. However, we found that the levels of SV2, Syt1, VAMP2 and SNAP-25 all decreased by approximately 20-35% within this time frame, while VGLUT1 and Syp levels were not significantly altered (Figure 3.1C,D). These findings indicate

that SV membrane proteins do not all turn over at the same rate, and therefore that SVs may not be degraded as discrete units.

Neuronal activity stimulates the degradation of specific SV membrane proteins

For those SV proteins whose levels were reduced following 24-hour chx treatment, we next evaluated whether their degradation was influenced by neuronal activity. Neurons were again treated for 24 hours with DMSO or cycloheximide, this time in the presence of commonly used pharmacological agents that either block neuronal activity (the Na⁺ channel blocker tetrodotoxin (TTX), the NMDA receptor blocker APV, and the AMPA receptor blocker CNQX), or increase activity (the GABA receptor antagonist bicuculline and the voltage-gated K⁺ channel blocker 4-aminopyridine; Bic/4AP)(Ehlers, 2003; Tauskela et al., 2008; Wijayatunge et al., 2014). The efficacy of these agents was verified in 14 DIV neurons by recording and quantifying the frequency of spontaneous excitatory postsynaptic currents before and after drug application. We found that TTX, APV, and CNQX (blockers) significantly decreased this number, while Bic/4AP significantly increased it (Figure 3.2A,B). The amounts of protein degradation were expressed as “fold change in degradation vs. control” by dividing the activity conditions (blockers, Bic/4AP) by the DMSO control condition (see Chapter 2 for details). Faster protein degradation was expressed as an increase in fold change (>1), and slower degradation by a decrease in fold change (<1; Figure 3.2C-E). While the amounts of protein degradation were not significantly different between the DMSO control and blocker conditions (Figure 3.2C,E, Table 3.1), we found that Bic/4AP treatment significantly sped SV2 and VAMP2 degradation during the 24-hour time course (by ~2-fold), but did not alter Syt1 or SNAP-25 degradation (Figure 3.2D,E). These interesting findings indicate that a subset of SV membrane proteins (VAMP2, SV2) is degraded in an activity-dependent manner. Such use-dependent turnover could be essential for

removing SV proteins that become damaged/misfolded through repeated cycles of SV exo/endocytosis, yet the underlying molecular mechanisms are unknown.

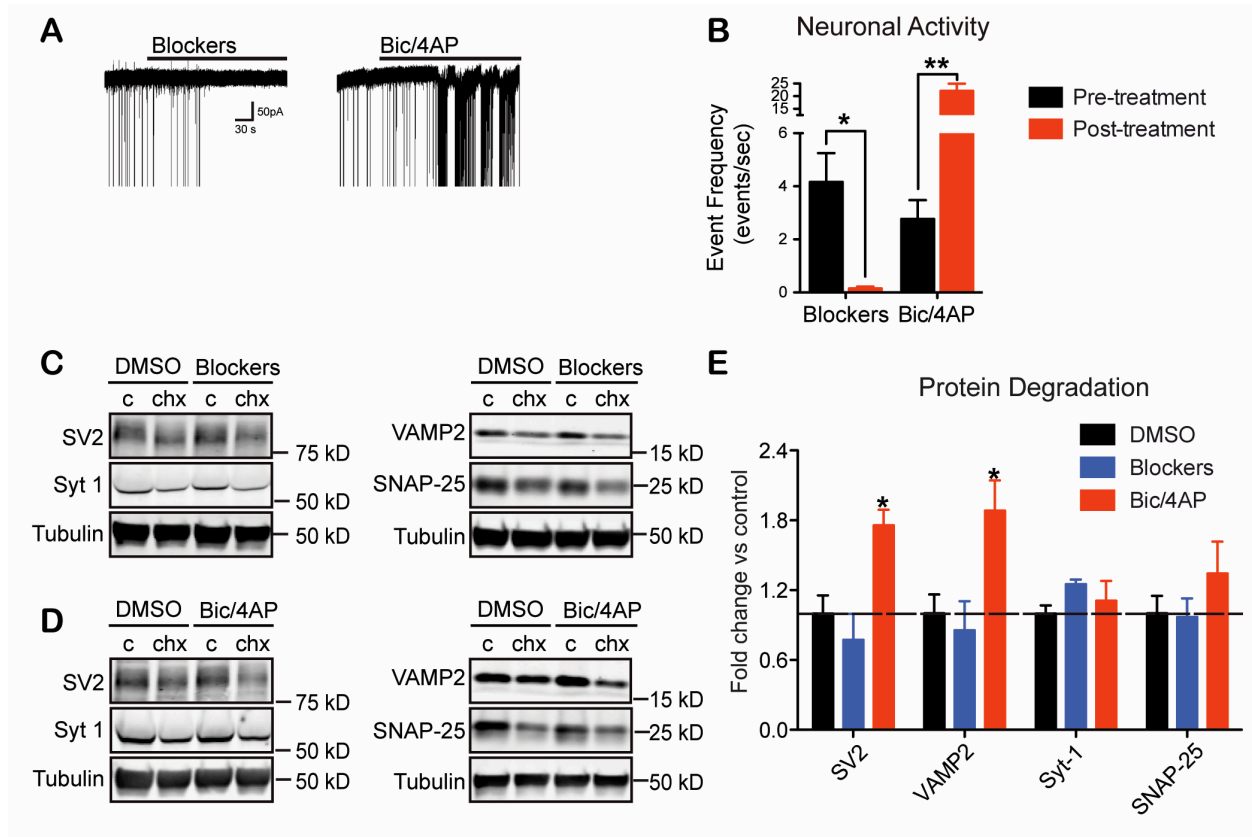


Figure 3.2 - Neuronal activity drives the degradation of a subset of SV-associated proteins. A) Representative traces of 14 DIV neurons before and after application (indicated by black line) of 50 μM AP5/10 μM CNQX/0.5 μM tetrodotoxin (blockers) to inhibit activity, or 40 μM bicuculline/50 μM 4-AP (bic/4AP) to stimulate activity. B) Quantification of spontaneous excitatory postsynaptic current frequency pre- and post-treatment with blockers or bic/4AP. C) Representative immunoblots from 14 DIV neurons treated for 24 hours with DMSO (c) or chx in the presence of additional DMSO or blockers. Blots probed for SV2 and Syt1, or VAMP2 and SNAP-25, are shown with corresponding tubulin loading controls. D) Representative immunoblots from 14 DIV neurons treated for 24 hours with DMSO (c) or chx in the presence of additional DMSO or bic/4AP to stimulate neuronal activity, and probed for the same proteins as in C. E) Quantification of protein degradation in each condition, expressed as the fold change versus DMSO control. Treatments that speed protein degradation are represented by an increase in fold change (>1). Black dotted line denotes fractional degradation in the presence of DMSO control (black bar). For this and all subsequent bar graphs, mean ± SEM is shown, and student's two-tailed t-tests are used to calculate significance of each experimental condition vs. control (n ≥ 3, **=p < 0.01).

Table 3.1 - Fractional protein degradation in a 24-hour period, based on neuronal activity levels.

Protein	DMSO	APV/CNQX/TTX	Bic/4AP
VGLUT1	1.04 ± 0.08	N/A	N/A
Synaptophysin	0.98 ± 0.08	N/A	N/A
SV2	0.811 ± 0.029	0.854 ± 0.042	0.669 ± 0.026**
VAMP2	0.813 ± 0.031	0.840 ± 0.047	0.647 ± 0.048**
Synaptotagmin-1	0.691 ± 0.021	0.614 ± 0.012	0.657 ± 0.052
SNAP-25	0.723 ± 0.042	0.732 ± 0.044	0.628 ± 0.076

The fractional amount of degradation that occurred over 24 hours was expressed as a ratio of protein intensity with cycloheximide treatment to its intensity with DMSO control treatment. Numbers represent the average plus or minus the standard error of the mean. Student's two-tailed t-tests were used to calculate significance of each experimental condition vs. DMSO control. Significantly different values are indicated (**=p<0.01).

The ESCRT pathway is required for activity-dependent SV protein degradation

To identify the cellular pathway responsible for activity-dependent degradation of SV2 and VAMP2, we initially focused on the ESCRT pathway. The ESCRT pathway comprises a series of protein complexes (ESCRT-0, -I, -II, -III, and Vps4) that catalyze the formation of MVBs and the sorting of cargo into MVBs for delivery to lysosomes (Raiborg and Stenmark, 2009). To confirm that this pathway has a role in SV protein degradation, as previously reported (Fernandes et al., 2014; Uytterhoeven et al., 2011), we examined the fold change in SV2 and VAMP2 degradation in the presence of an shRNA against the ESCRT-0 component Hrs (shHrs). Hrs, the initial component of the ESCRT-0 complex that binds and recruits ubiquitinated protein substrates, appears to be required for the initiation of MVB formation (see (Schmidt and Teis, 2012)). When expressed between 7-14 DIV, we found that shHrs led to a 67.8±/0.10% knockdown of Hrs protein (Figure 3.3A) without any observable toxicity. Further, shHrs significantly attenuated SV2 and VAMP2 degradation compared to scRNA control (Figure 3.3B,C), indicating that basal degradation of these proteins occurs through the ESCRT pathway.

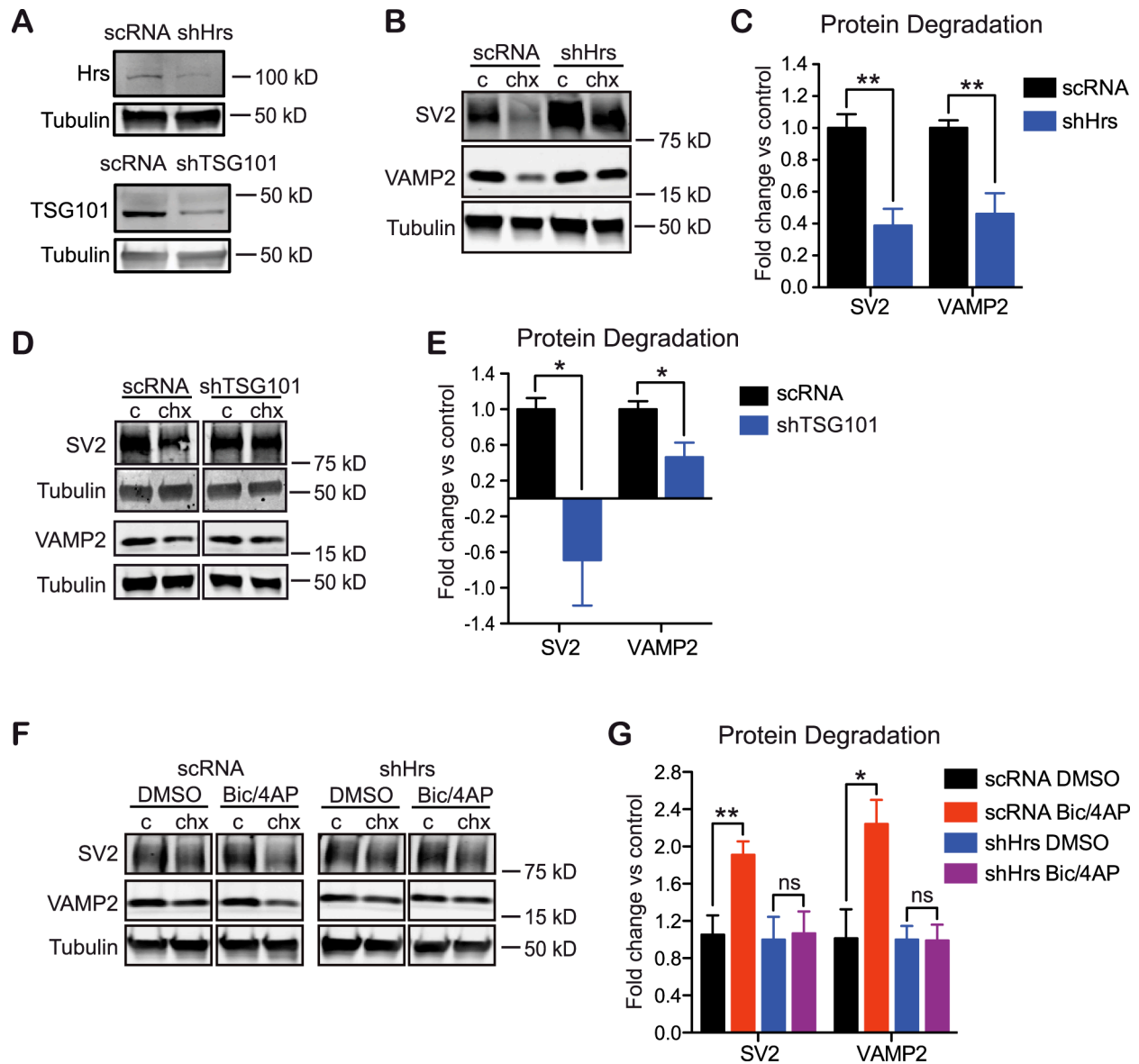


Figure 3.3 - The ESCRT pathway is required for basal and activity-dependent SV protein degradation.

A) Representative immunoblots of Hrs, TSG101, and corresponding tubulin loading controls from 14 DIV neurons transduced with scRNA, shHrs, or shTSG101. Knockdown efficacy is 67.8±0.1% of scRNA control for shHrs, and 58.2±0.04% of control for shTSG101. B) Immunoblots from 14 DIV neurons transduced with scRNA or shHrs, treated for 24 hours with DMSO (c) or chx, and probed for SV2, VAMP2 and tubulin. C) Quantification of the fold change in degradation of SV2 and VAMP2 compared to scRNA control (n=4; **=p<0.01). D) Immunoblots from 14 DIV neurons transduced with scRNA or shTSG101, treated for 24 hours with DMSO (c) or chx, and probed for SV2, VAMP2 and tubulin. E) Quantification of fold change in degradation of SV2 and VAMP2 compared to scRNA control (n=4; *p<0.05). F) Immunoblots from 14 DIV neurons transduced with scRNA or shHrs and treated for 24 hours with DMSO (c) or chx in the presence of additional DMSO or bic/4AP, and probed for SV2, VAMP2 and tubulin. G) Quantification of fold change in degradation of SV2 and VAMP2 in the presence of scRNA or shHrs, +/- activity. DMSO control is set to 1 for each condition (scRNA black bars, shHrs blue bars), and bic/4AP treatment is expressed as fold change vs. DMSO control for that condition (n=6; *p<0.05).

To bolster this finding, we repeated this experiment with an shRNA against TSG101, a component of the ESCRT-I complex that acts downstream of Hrs. Like shHrs, shTSG101 led to a relatively efficient 58.2±0.04% knockdown of TSG101 (Figure 3.3A) and attenuated SV2 and VAMP2 degradation (Figure 3.3D,E), indicating that the ESCRT pathway, and not just Hrs or the ESCRT-0 complex, facilitates the degradation of SV proteins. To assess whether this pathway also mediates the activity-dependent turnover of SV2 and VAMP2, neurons expressing scRNA or shHrs were treated with Bic/4AP or DMSO vehicle control, and changes in protein degradation measured after 24-hour chx treatment. We found that Bic/4AP treatment again increased the degradation of SV2 and VAMP2 by nearly two-fold in scRNA-expressing neurons (Figure 3.3F,G). In contrast, shHrs-expressing neurons exhibited no Bic/4AP-mediated increases in SV2 or VAMP2 degradation (Figure 3.3F,G). These findings indicate that the ESCRT pathway is essential for basal and activity-dependent turnover of these SV proteins.

ESCRT proteins undergo activity-dependent recruitment to SV pools

Although the ESCRT pathway has previously been linked to SV protein turnover (Fernandes et al., 2014; Uytterhoeven et al., 2011), the localization of ESCRT proteins in axons, and their behavior in response to neuronal activity, has not been investigated. Based on our findings, we hypothesized that ESCRT proteins would localize to axons and associate with SV pools, and that neuronal activity would increase this association. To test this concept, we transduced neurons with mCh-tagged Hrs (ESCRT-0 complex) or CHMP2B (ESCRT-III complex; MVB marker) on 9 DIV, and treated neurons with either DMSO or Bic/4AP for 12 hours on 14 DIV. Neurons were then fixed and immunostained for VAMP2 to label SV pools. The percent colocalization of mCh-Hrs or CHMP2B-mCh puncta with VAMP2, and the number of puncta per unit length of axon, were quantified and compared in the presence or absence of Bic/4AP. While

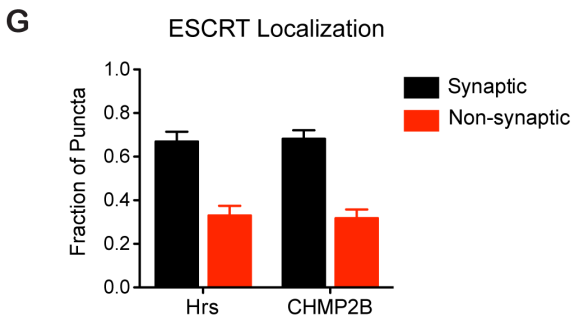
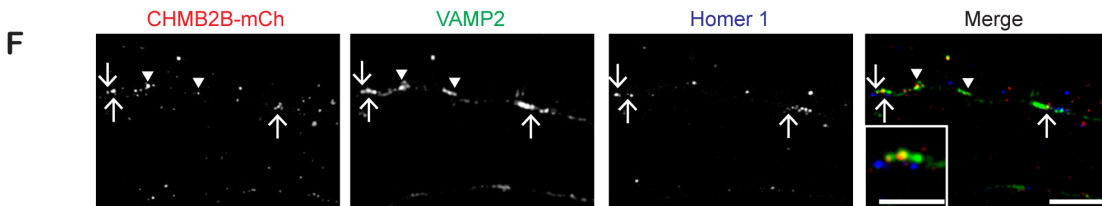
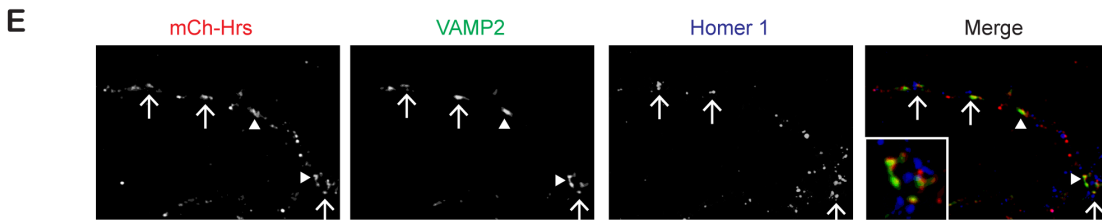
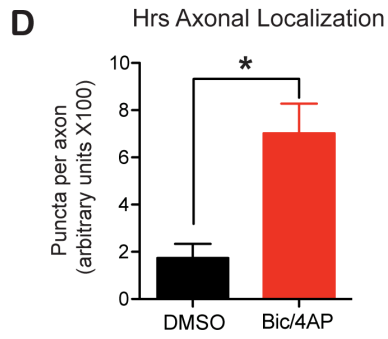
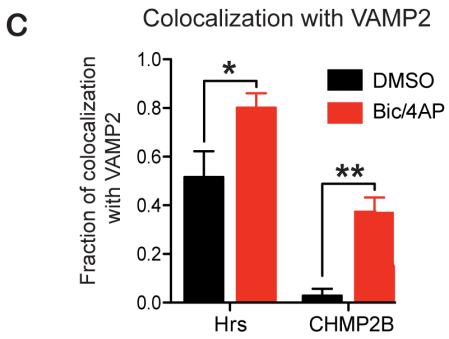
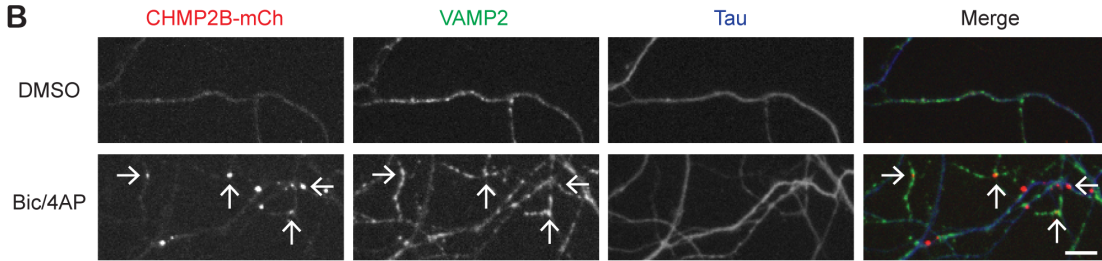
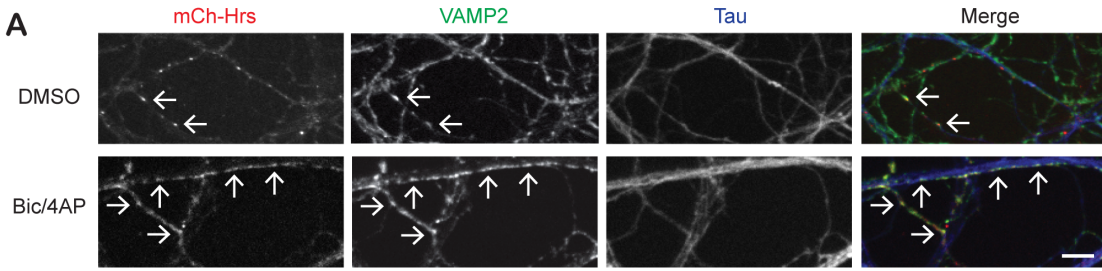


Figure 3.4 - Neuronal activity recruits ESCRT proteins to synaptic vesicle pools.

A) Images of neurons transduced with mCh-Hrs, treated with DMSO or bic/4AP for 12 hours, then fixed and immunostained against VAMP2 (green) and Tau (blue). Arrows represent VAMP2 puncta that colocalize with mCh-Hrs in axons. Scale bar=10 μ m. B) Images of neurons transduced with CHMP2B-mCh, treated with DMSO or bic/4AP for 12 hours, then fixed and immunostained against VAMP2 (green) and Tau (blue). Arrows represent VAMP2 puncta that colocalize with CHMP2B-mCh in axons. Scale bar=10mm. C) Quantification of the fraction of Hrs or CHMP2B puncta colocalized with VAMP2 (For Hrs: n=4 DMSO, n=8 bic/4AP from 3 replicate weeks, ~30 puncta/image; * p <0.05. For CHMP2B: n=5 for DMSO, n=8 for bic/4AP from 2 replicate weeks, ~10 puncta/image; ** p <0.01). D) Quantification of the number of Hrs puncta per unit length of axon (arbitrary units; n=4 DMSO, n=5 bic/4AP, * p <0.05, ~30 puncta/image, similar results obtained for 3 independent experiments). E) Super-resolution images of neurons transduced with mCh-Hrs, treated as in A and immunostained against VAMP2 and Homer1. Arrowhead indicates non-synaptic mCh-Hrs puncta, and arrows indicate synaptic puncta based on colocalization with Homer1. Inset shows higher magnification view of a synaptic site. F) Super-resolution images of neurons transduced with CHMP2B-mCh, treated as in A and immunostained against VAMP2 and Homer1. Arrowheads indicate non-synaptic CHMP2B-mCh puncta and arrows indicate synaptic puncta. Inset shows higher magnification view of a synaptic site. Scale bar=5 μ m, 2.5 μ m for inset. G) Quantification of the synaptic and non-synaptic fractions of Hrs and CHMP2B puncta in axons following neuronal activity (~200 puncta for Hrs, ~120 puncta for CHMP2B).

approximately 40% of mCh-Hrs puncta colocalized with VAMP2 at baseline, treatment with Bic/4AP increased this value to nearly 75% (Figure 3.4AC). At the same time, increased neuronal activity led to nearly four times as many mCh-Hrs puncta/unit length axon compared to control neurons (Figure 3.4A,D). We also observed a striking change in the localization of CHMP2B-mCh following Bic/4AP treatment. In control neurons, CHMP2B-mCh puncta rarely appeared in axons. However, following Bic/4AP treatment, multiple CHMP2B-mCh puncta were present in axons, and ~35% of these colocalized with VAMP2 (Figure 3.4B,C). Together, these data show that neuronal activity dramatically increases the entry of ESCRT proteins into axons and their association with SV pools.

To determine whether these SV pools were synaptic, and to examine the precise localization of the ESCRT proteins relative to SV pools, we performed high-resolution imaging of neurons transduced with mCh-Hrs or CHMP2B-mCh, treated with Bic/4AP, and immunostained with VAMP2 and the postsynaptic protein Homer1. Hrs and CHMP2B puncta associated with both synaptic and non-synaptic VAMP2 clusters, with nearly twice as many

puncta at synaptic clusters based on their colocalization with Homer1 (67% synaptic vs. 33% non-synaptic for Hrs, 68% synaptic vs. 32% non-synaptic for CHMP2B; Figure 3.4E-G).

Moreover, Hrs and CHMP2B puncta typically exhibited partial but not complete overlap with VAMP2 clusters (Figure 3.4E,F), suggesting that they could represent distinct vesicle populations or associate with subsets of SVs.

To further characterize the effect of neuronal activity on the localization of the ESCRT pathway, we performed live imaging of mCh-Hrs following activity treatment in microfluidic chambers. The use of these chambers allowed us to preferentially examine Hrs movement within axons and eased the ability to discern the directionality of these movements. We recorded time lapse movies of mCh-Hrs movement every 5 seconds for 50 frames. First, we generated kymographs in which a stationary particle appears as a straight line while anterograde or retrograde movements appear as diagonal lines to the left or right, respectively (Figure 3.5A). In DMSO treated neurons, Hrs puncta were primarily stationary with very few anterograde or retrograde events, whereas in Bic/4AP treated neurons, the majority of particles show movement in one or both directions (Figure 3.5A). Quantification of these events revealed that approximately 20% of Hrs puncta in DMSO treated neurons could be classified as ‘moving’, defined as showing any movement in >45% of the frames. As early as 1 hour after Bic/4AP treatment, a significant increase was observed, wherein nearly 70% of puncta were moving (Figure 3.5B). We next examined the directionality of the moving puncta, classifying their movement as primarily anterograde or retrograde, based on movement in the given direction for >45% of the frames, or as bidirectional. We found a trend towards increased retrograde movement ($p=0.07$), and a similar trend for increased bidirectional movement ($p=0.055$), though these values did not reach significance (Figure 3.5C). Additionally, the average velocity of all

Hrs puncta increased nearly 4 fold following treatment with Bic/4AP (Figure 3.5D). These results show that neuronal activity serves as cue to initiate Hrs transport within axons. Further work examining the dynamics of Hrs movement over an expanded timeframe of activity treatment, along with an examination of the co-trafficking of SV proteins over this timeframe, will be necessary to elucidate the activity-dependent changes in ESCRT-mediated SV trafficking.

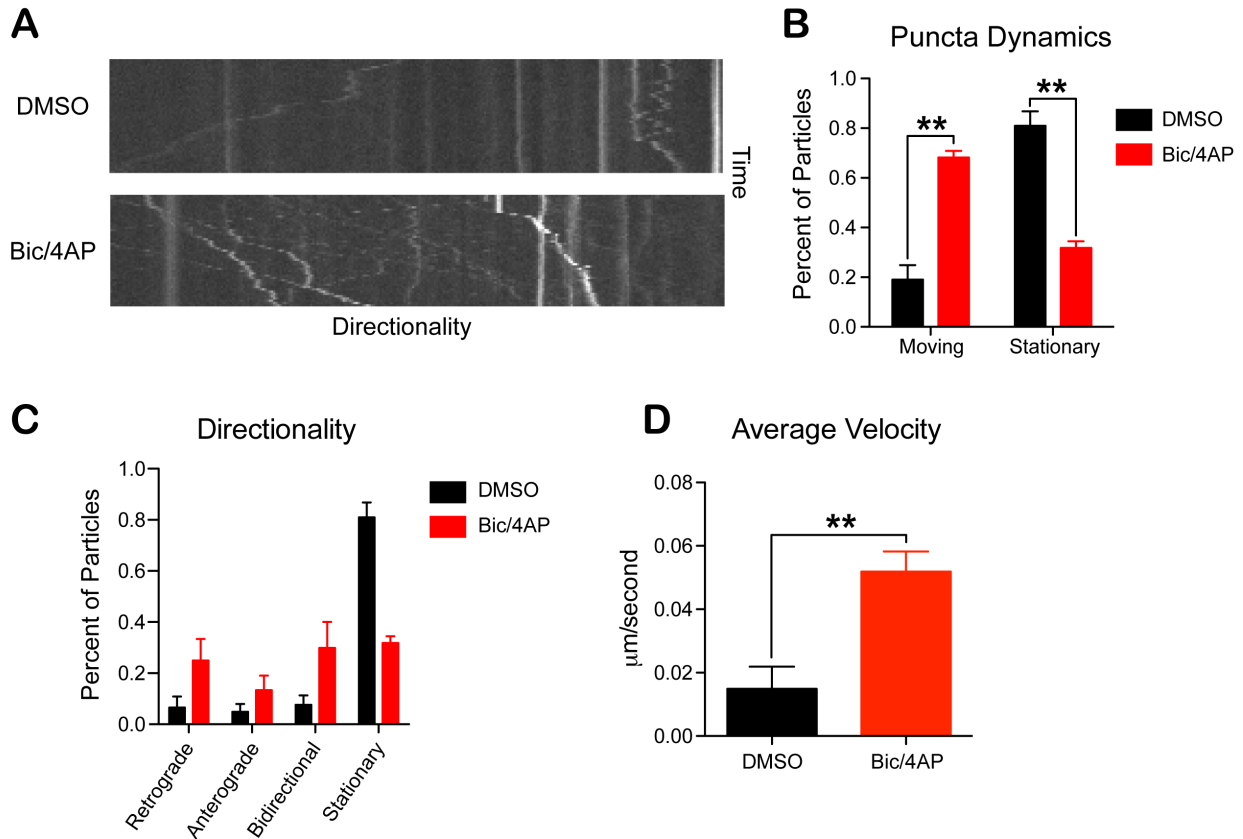


Figure 3.5 - Neuronal activity changes Hrs trafficking dynamics.

A) Representative kymographs of mCh-Hrs puncta from 10 DIV neurons treated with DMSO or Bic/4AP for 1 hour prior to imaging. Images were acquired every 5 seconds over an approximately four-minute time course. B) Quantification of stationary vs. moving mCh-Hrs puncta based on their behavior in >45% of the frames in each condition. Significantly more puncta were moving in neurons treated with Bic/4AP vs. DMSO control (**= $p < 0.01$, $n = 5-6$ neurons, 50 frames each). C) Quantification of the directionality of moving mCh-Hrs puncta. A trend towards increased retrograde ($p = 0.07$) and bidirectional ($p = 0.055$) movement was observed in neurons treated with Bic/4AP ($n = 5-6$ neurons). Quantification of the average velocity of mCh-Hrs puncta in each condition. mCh-Hrs puncta in neurons treated with Bic/4AP moved three-fold faster on average (**= $p < 0.01$, $n = 5-6$ neurons).

We next attempted to directly address the question of whether neuronal activity drives MVB formation at synapses by performing electron microscopy. Neurons were treated for 12 hours with Bic/4AP or DMSO, then fixed, sectioned, stained and subjected to electron microscopy. Though MVBs have been identified in axons and presynaptic compartments, these MVBs have very diverse morphologies (Altick et al., 2009; Kadota et al., 1994; Von Bartheld and Altick, 2011) and have primarily been characterized in motor neurons and neuromuscular junctions, not small central synapses. Thus, while we see a number of MVB-like structures that may represent distinct types of MVBs, or MVBs at different stages of formation (Figure 3.6A,B), we cannot definitively categorize them as MVBs. Further characterization of these structures in conjunction with MVB marker labeling or 3D reconstruction will be necessary to determine whether neuronal activity drives their formation.

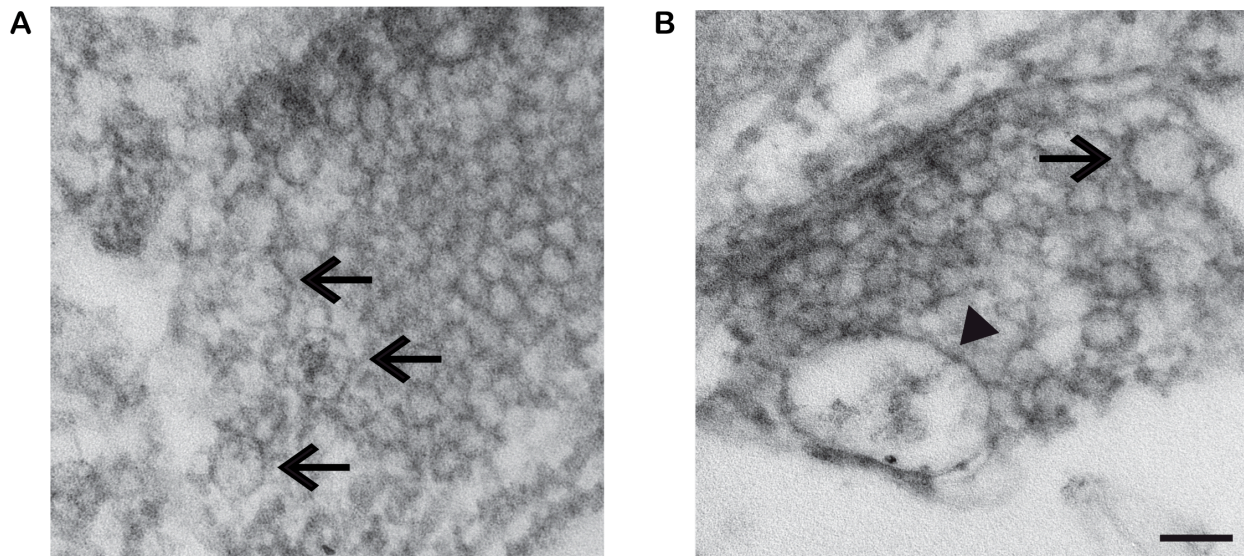


Figure 3.6 - Ultrastructural analysis of presynaptic boutons

A-B) EM micrographs of presynaptic boutons from 14 DIV neurons treated with Bic/4AP for 12 hours. Multiple endosomal structures can be seen, potentially representing sorting/recycling endosomes or MVBs at various stages of maturation (arrows; A). B) A large (200 nm) vesicular structure potentially representing an MVB (arrowhead; B). Scale bar=100nm.

Discussion

In this chapter, we find that a subset of SV proteins, SV2 and VAMP2, undergo activity-dependent degradation. Furthermore, we show that the degradation of these proteins relies on the ESCRT pathway, suggesting that they are sorted from an early endosomal structure, packaged into MVBs, and transported to the lysosome for degradation. Finally, we find that neuronal activity functions to recruit proteins of the ESCRT pathway into axons and specifically to pools of synaptic vesicles, suggesting that the initiation of degradation occurs locally at these sites.

Mechanisms of SV protein turnover

Mechanisms of SV protein degradation are poorly understood, and our study is among the first to investigate them. For instance, the fundamental question of whether SV membrane proteins turn over individually or as a group has not been resolved. In our cycloheximide assays, we observed that some membrane proteins (*i.e.* VGLUT1, synaptophysin) were long-lived, showing no significant change within the 24-hour time course, while others (*i.e.* SV2, synaptotagmin1) underwent a ~35% reduction compared to starting material. Another recent study that utilized SILAC and proteomics to measure synaptic protein turnover also found variation in the basal half-lives of different SV proteins, and calculated these half-lives to be on the order of 1-4 days, or ~2-40 molecules per hour per synapse (Cohen et al., 2013). Together, these findings indicate that SV protein turnover occurs through the regulated degradation of specific proteins as opposed to the degradation of entire SVs. They also demonstrate that SV protein degradation is an active, ongoing process, in contrast to earlier reports that estimated SV protein turnover to be extremely slow, with half-lives on the order of 20 days (Morris et al., 1971).

We also observed variability in the dependence of SV-associated protein degradation on neuronal activity, with SV2 and VAMP degradation increased by activity and Synaptotagmin1

and SNAP-25 degradation unchanged. Why this variability occurs remains an open question. One possibility is that cellular surveillance mechanisms (*i.e.* molecular chaperones, ubiquitinating enzymes) are coupled to activity in order to efficiently remove reactive or structurally complex proteins that are susceptible to damage from continuous SV recycling. VAMP2 and SV2 may have structural motifs that are particularly vulnerable to misfolding or oxidation. Alternatively, the specific functions of these proteins (*i.e.* VAMP2 as the primary v-SNARE in the brain, SV2 as a chaperone for Synaptotagmin1 (Zhang et al., 2015) may require particularly vigilant control mechanisms that are tightly linked to neuronal activity. Interestingly, several groups have shown that specific postsynaptic proteins are ubiquitinated and degraded in an activity-dependent manner while others are not (Ehlers, 2003; Lussier et al., 2011; Schwarz et al., 2010). Moreover, the ubiquitinating enzymes responsible for the ubiquitination/degradation of postsynaptic glutamate receptors are regulated by neuronal activity (Scudder et al., 2014), and such a mechanism could also link activity with SV2 or VAMP2 ubiquitination and degradation. An intriguing possibility is that they accumulate ubiquitin moieties through cycles of exo- and endocytosis, and that these cumulative linkages target heavily-used SV proteins for degradation. However, the identities of the ubiquitinating enzymes responsible for this activity, the signals that regulate these enzymes, and the specific SV proteins that are ubiquitinated in response to activity remain largely unknown and will be investigated in Chapter 5.

ESCRT pathway in SV protein homeostasis

Our studies show that the ESCRT pathway is responsible for the basal and activity-dependent turnover of SV2 and VAMP2. This finding lends further support to the growing evidence of the importance of endosomes in the SV life cycle. Our study implicating the ESCRT pathway as an essential component of SV protein degradation points to a role of endosomes in the removal of

dysfunctional or damaged proteins. Indeed, studies in *Drosophila* have also identified components of the ESCRT pathway as essential in preserving a healthy and functional readily releasable pool of SVs (Fernandes et al., 2014; Uytterhoeven et al., 2011). Together with our studies, these findings suggest that maintaining SV protein homeostasis is crucial to retaining proper neuronal communication and thus neuronal health, an idea we will further explore in Chapter 5.

One of the most interesting aspects of our findings is that neuronal activity functions as a cue to initiate ESCRT dependent degradation of SV2 and VAMP2 at synapses. Although we cannot conclude that MVBs form at the synapse, our data do suggest that ESCRT components are recruited to synapses in response to increases in neuronal activity. While these studies do not preclude the involvement of macroautophagy in presynaptic protein degradation, they do offer an intriguing possibility that different degradative pathways may be activated in response to specific signals. Perhaps neuronal activity activates certain proteins or signaling cascades that specifically interact with ESCRT proteins and lead to their synaptic recruitment. This idea will be further investigated in Chapter 4.

Chapter 4: Rab35 regulates activity-dependent degradation of SV2 and VAMP2 through its effector, Hrs

Rationale

In the previous chapter, we discovered that specific SV proteins are degraded in a use-dependent manner that relies on the ESCRT pathway. Further, we found that proteins of the ESCRT pathway are recruited into axons and to synaptic vesicle pools by neuronal activity. In this chapter, we investigate how this striking axonal recruitment of ESCRT proteins occurs. Based on their key roles in trafficking proteins into the endocytic pathway (Stenmark, 2009), we hypothesized that Rab GTPases might play a role in this process. More than half of the 60 mammalian Rabs can be co-purified with SV pools (Pavlos and Jahn, 2011; Takamori et al., 2006), and several of these (Rabs 5, 10, 14, 21, 35) associate with early and recycling endosomes in neurons and other cell types (Babbey et al., 2006; Fischer von Mollard et al., 1994; Junutula et al., 2004; Pavlos and Jahn, 2011; Sato et al., 2008; Uytterhoeven et al., 2011). Given their putative and reported roles in the endocytic pathway, we hypothesized that one or more of these would mediate SV protein degradation. Moreover, Hrs also localizes to early endosomes (Komada and Soriano, 1999; Sato et al., 2008) and is the initial component of the ESCRT pathway, leading us to further hypothesize that it could interact with one or more of the endocytic Rabs to mediate SV protein degradation.

Results

Rab35 interacts with Hrs and stimulates SV protein degradation

To test for Hrs/Rab interactions, we performed co-immunoprecipitation assays in HEK293T cells expressing Flag-Hrs and HA-tagged Rabs 5, 10, 14, 21, or 35. Interestingly, we found that Rabs 10, 14, and 35 were efficiently co-immunoprecipitated by Flag-Hrs, while Rabs 5 and 21 were

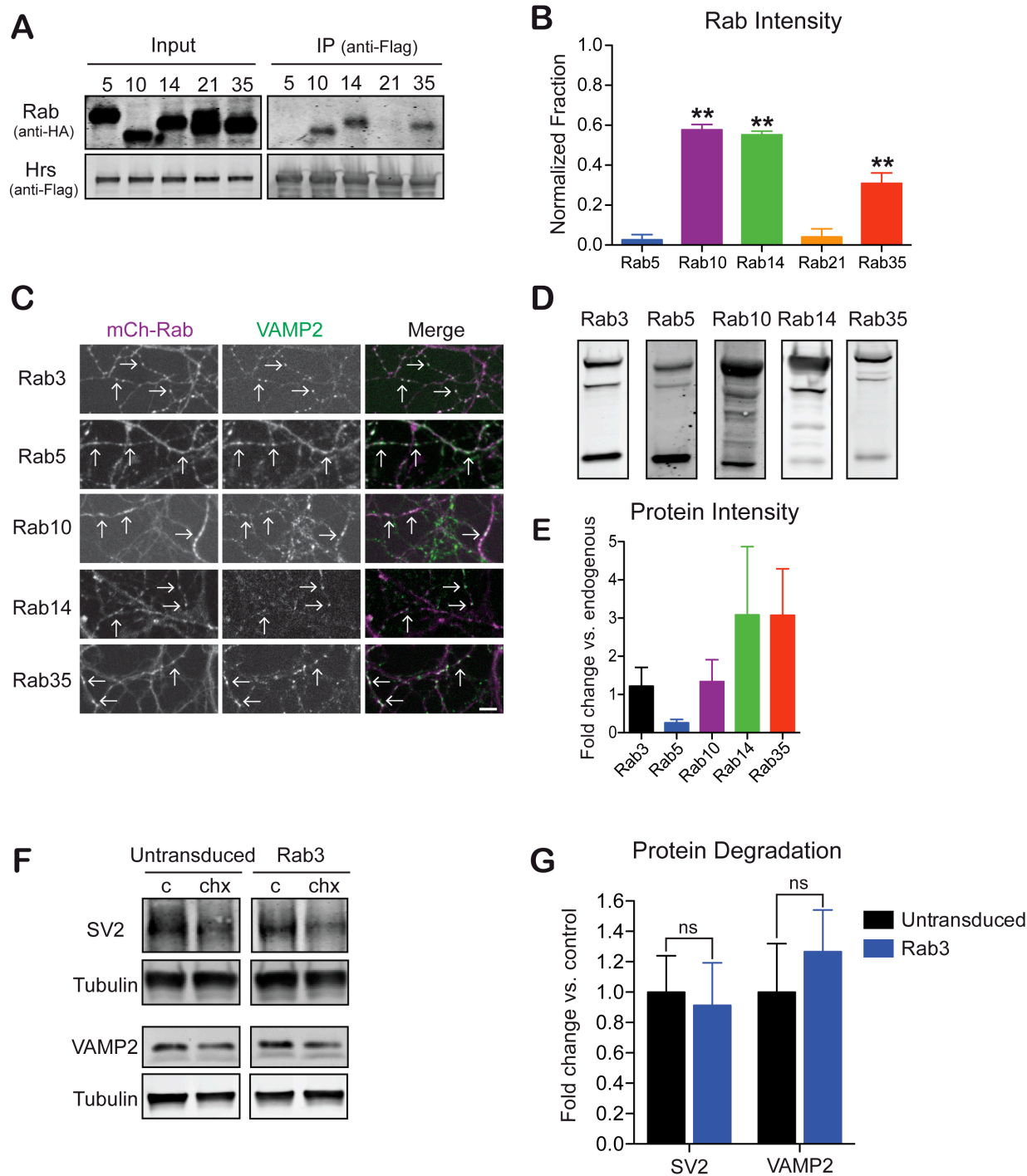


Figure 4.1 - A subset of endocytic Rabs interact with Hrs and/or drive SV protein degradation.

A) Immunoblot of HEK cell lysates expressing HA-Rab5, 10, 14, 21 or 35 and Flag-Hrs, subject to IP with Flag antibody and probed with HA or Flag antibodies. B) Quantification of HA-Rab intensity in the eluate, normalized to input intensity and Flag-Hrs intensity in the eluate (n=3, **p<0.01). C) Representative images from 14 DIV neurons transduced with mCh-tagged Rab3, Rab5, Rab10, Rab14, or Rab35 and immunostained with VAMP2 antibodies. Arrows represent VAMP2 puncta (green) in axons expressing mCh-Rab (purple). Scale bar=10 μ m. D) Immunoblots from 14 DIV neurons transduced with mCh-tagged Rab3, Rab5, Rab10, Rab14, or Rab35, and probed for the respective Rab. E) Quantification of mCh-tagged Rab intensity, expressed as fold change vs. endogenous Rab level (n=3). F) Immunoblots from 14 DIV neurons untransduced or transduced with mCh-Rab3, treated for 24 hrs with either DMSO (c) or chx, and probed for SV2 or VAMP2 and tubulin. G) Quantification of SV2 or VAMP2 intensity from each condition, normalized as in Figure 3.1, showing that Rab3 overexpression does not speed SV2 protein degradation (n=3).

not (Figure 4.1A,B). These findings demonstrate that a subset of endocytic Rabs interact with Hrs, and may participate in SV protein degradation.

We next tested whether overexpression of any of these endocytic Rabs could stimulate SV2 and VAMP2 degradation in hippocampal neurons. Multiple groups have reported that overexpression of wild-type small GTPases induces phenotypes that reflect their activation (Brondyk et al., 1993; Li and Stahl, 1993; McCaffrey et al., 2001; Ravikumar et al., 2008). Furthermore, it was recently demonstrated that the conventional ‘constitutively-active’ mutants are not active for all Rabs, including Rab35 (Langemeyer et al., 2014). We therefore used wild-type rather than constitutively-active Rabs for our studies, anticipating that their relatively modest overexpression by lentivirus would lead to phenotypes reflecting their activated states, while at the same time minimizing the toxicity often associated with Rab overexpression (Star et al., 2005). Indeed, when neurons were transduced with mCherry-tagged Rabs (5, 10, 14, or 35) for four days prior to cycloheximide-chase experiments, we found that they localized to axons and presynaptic boutons, and were overexpressed to similar degrees (Figure 4.1C-E) with no observable toxicity. Lysates from Rab-expressing neurons were collected and immunoblotted for SV2 and VAMP2, and the fold change in protein degradation calculated for each Rab. Rab3, an SV-associated Rab with a well-characterized role in SV exocytosis (Pavlos and Jahn, 2011; Yu et al., 2008), served as our control in these studies as its overexpression did not alter SV protein degradation compared to untransduced neurons (Figure 4.1F,G). Similarly, we found that Rabs 10 and 14 did not alter SV2 or VAMP2 degradation over the 24-hour period (Figure 4.2A,B). In contrast, overexpression of Rabs 5 and 35 increased the amount of SV2 and VAMP2 degradation by greater than two-fold (Figure 4.2A,B). Both of these Rabs were previously reported to have roles in SV recycling (Shimizu et al., 2003; Uytterhoeven et al., 2011; Wucherpfennig et al.,

2003) and Rab35 was recently implicated in the turnover/replenishment of SV proteins at the *Drosophila* neuromuscular junction (Fernandes et al., 2014; Uytterhoeven et al., 2011). However, as Rab35 interacts with Hrs and Rab5 does not (Figure 4.1A,B), we investigated the specificity of these Rabs for SV integral membrane protein degradation. We found that Rab5 overexpression sped the degradation of several presynaptic proteins, including SNAP-25 (a plasma membrane-associated protein) and Munc13 (an active zone protein), while Rab35 only sped the degradation of SV2 and VAMP2 (Figure 4.2C,D). These findings suggest that the Rab35/Hrs interaction is important for defining the specificity of the degradative pathway for SV integral membrane proteins.

Since the degradation of SV proteins and membranes has been reported to occur via lysosomes (Fernandes et al., 2014; Haberman et al., 2012; Tian et al., 2015), we assessed whether Rab35-mediated protein degradation required this organelle. Rab35-expressing neurons were treated with proteasome or lysosome inhibitors (200 nM epoxomicin or 100 mM chloroquine/leupeptin, respectively) for the last 18 hours of their 24-hour incubation with cycloheximide. As anticipated, we found that Rab35-mediated degradation of SV2 and VAMP2 was completely unaffected by epoxomicin, but significantly attenuated by chloroquine/leupeptin (Figure 4.2E-F), demonstrating that Rab35 acts in a lysosome-dependent degradative pathway.

We next wanted to determine whether Rab35-mediated SV protein degradation targeted the synaptic/axonal pool of proteins. To do this, we measured the levels of presynaptic/axonal VAMP2 by quantitative immunofluorescence microscopy. We compared the steady-state levels and the levels of VAMP2 remaining after 24 hours of chx treatment in axons from 14 DIV neurons expressing mCh-Rab35 versus mCh-Rab3 control. Average fluorescence intensities of VAMP2 puncta in axons expressing Rab3 or Rab35 were quantified and presented as a fraction

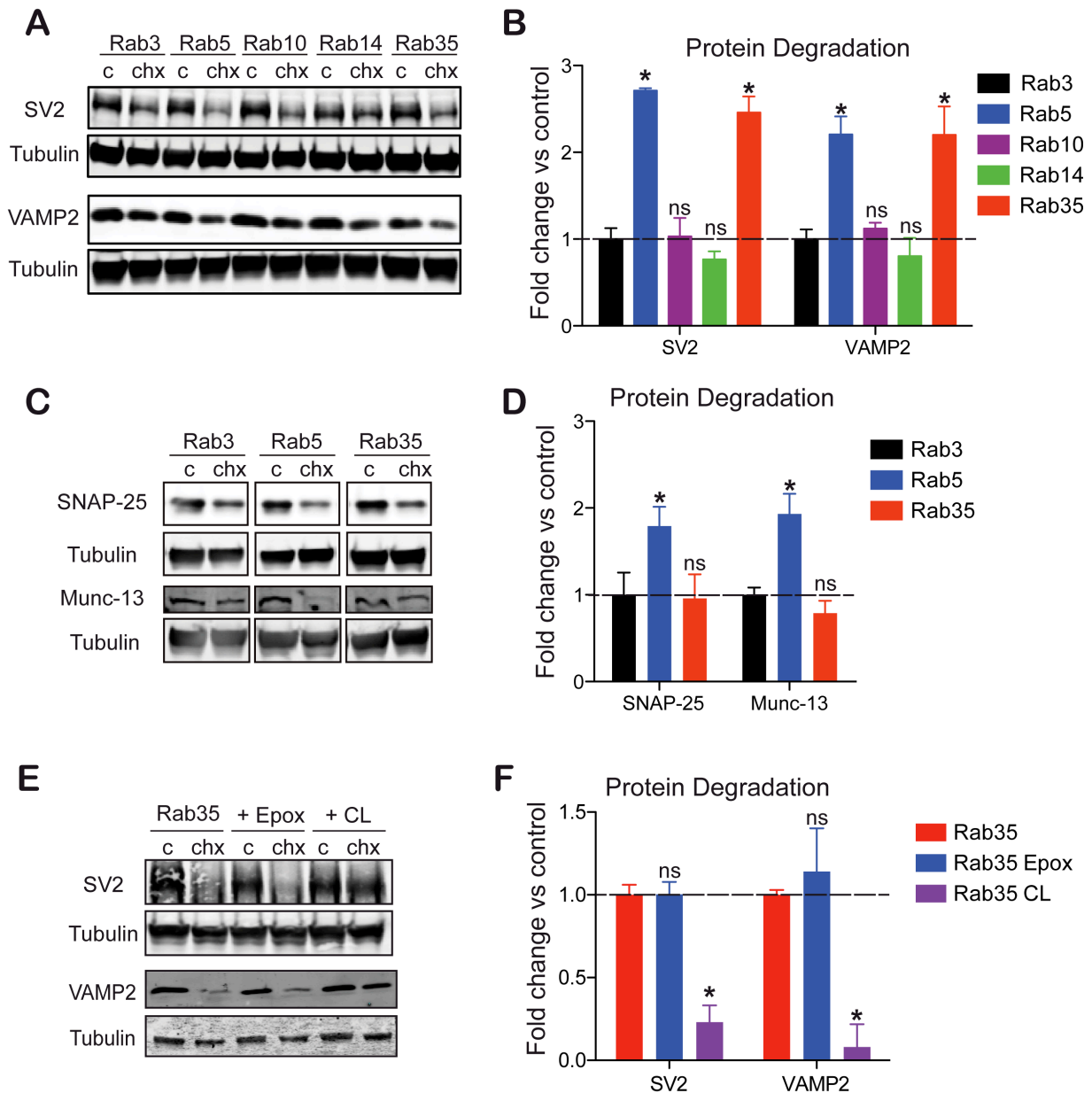


Figure 4.2 - A subset of endocytic Rabs drive SV protein degradation.

A) Immunoblots from 14 DIV neurons transduced with mCh-tagged Rab3, Rab5, Rab10, Rab14, or Rab35, treated for 24 hrs with either DMSO (c) or chx, and probed for SV2, VAMP2 and tubulin. B) Quantification of the fold change in degradation of SV2 and VAMP2 for each Rab vs. Rab3 control (n=3-4 independent experiments, *= $p < 0.05$). C) Immunoblots from 14 DIV neurons transduced with mCh-Rab3, -Rab5, or -Rab35, treated for 24 hours with DMSO (c) or chx and probed for SNAP-25, Munc-13, and tubulin. D) Quantification of the fold change in degradation of SNAP-25 and Munc-13 intensity for each Rab vs. Rab3 control (n=3; *= $p < 0.05$). E) Immunoblots from 14 DIV neurons transduced with mCh-Rab35, treated for 24 hours with DMSO (c) or chx, and further incubated with DMSO vehicle (Rab35), 200 nM epoxomycin (+Epox), or 100 mM chloroquine and 100 mM leupeptin (+CL) for 18 hours. Blots were probed for SV2, VAMP2 and tubulin. F) Quantification of the fold change in degradation of SV2 and VAMP2 from each condition (n=3; **= $p < 0.01$).

of the average intensity in Rab3-expressing axons. We found that the steady-state levels of VAMP2 puncta were not significantly different between Rab3 and Rab35-expressing neurons (Figure 4.2A,B), indicating that this assay was not sensitive enough to detect subtle changes in VAMP2 steady-state levels. However, similar to our immunoblot experiments, we found that VAMP2 levels were significantly lower 24 hours after chx treatment in axons expressing Rab35 compared to those expressing Rab3 (Figure 4.2A,B). To further confirm these findings, we used the SNAP-tag system for quantitative fluorescence pulse-chase analysis (Bodor et al., 2012). The SNAP-tag is a self-labeling enzyme that allows for covalent attachment of an exogenously applied fluorescent compound to a protein of interest. We designed a dual SNAP- and Flag-tagged VAMP2, which was co-expressed in neurons with either mCh-Rab3 or mCh-Rab35. On 13 DIV, neurons were incubated for 30 minutes with the SNAP-tag substrate benzylguanine-Oregon Green (BG-OG, New England Biolabs), washed, and then returned to normal media. Neurons were subsequently fixed at two time points after labeling (15 and 48 hrs) and immunostained with anti-Flag antibody, allowing us to measure both the “pulsed” fraction of VAMP2-SNAP (via BG-OG intensity) and the total pool of VAMP2-SNAP (via Flag intensity) present at each time. After 15 hours, we saw no significant differences in the intensity of BG-OG labeling, the intensity of Flag immunostaining, or the colocalization of BG-OG with Flag immunostaining in Rab3 versus Rab35-expressing neurons, though there was a trend towards decreased BG-OG/Flag colocalization in Rab35-expressing neurons (Figure 4.3C,D). These results indicate that Rab35 expression does not lead to lower levels of VAMP2-SNAP expression or initial BG-OG labeling. However, after 48 hours, both the intensity of BG-OG labeling and the colocalization of BG-OG with Flag immunostaining were significantly reduced in Rab35-expressing neurons compared to Rab3 controls, while total VAMP2-SNAP levels were not

altered (Figure 4.3C,E). These data confirm that Rab35 stimulates degradation of the synaptic pool of SV proteins.

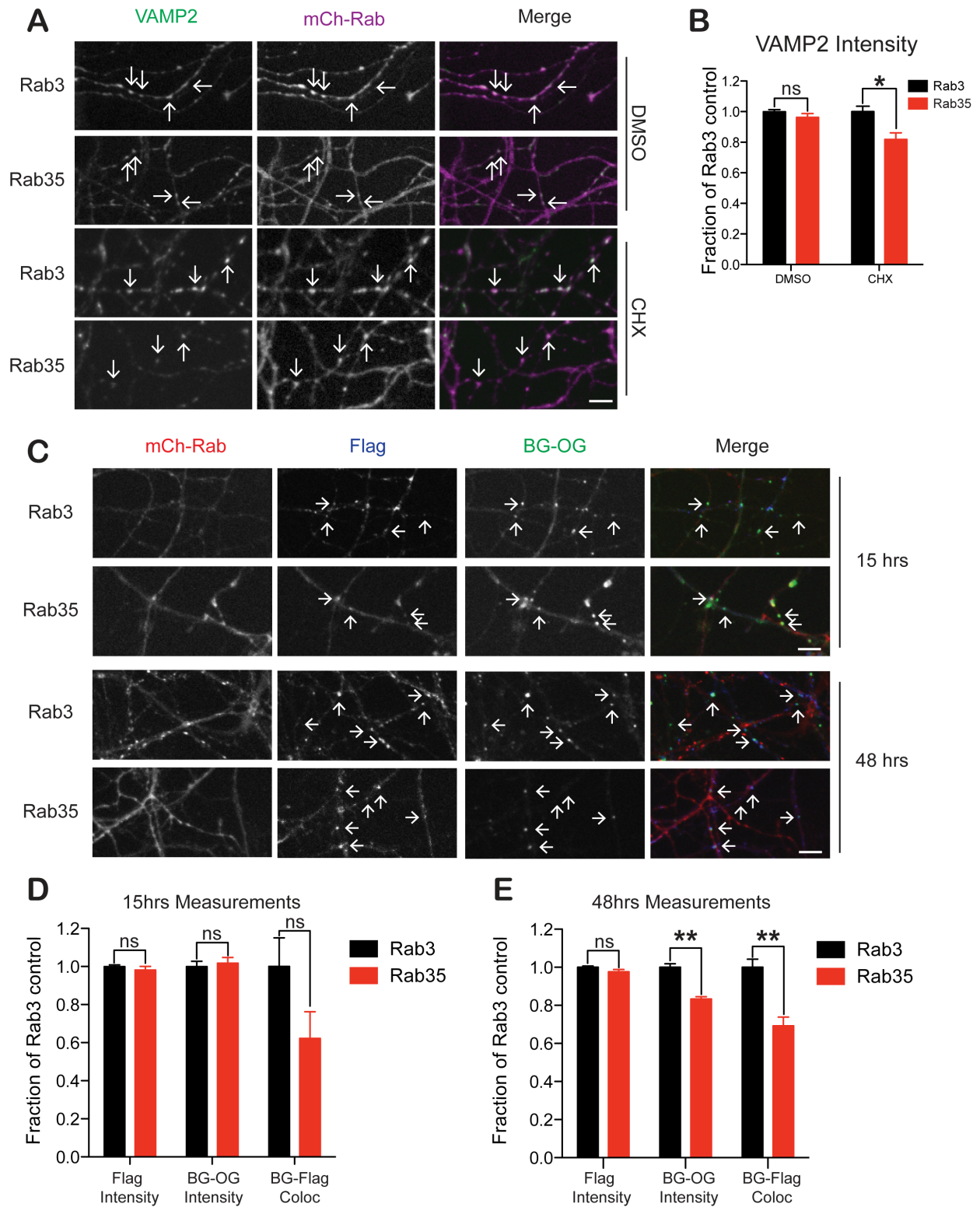


Figure 4.3 - Rab35 drives SV protein degradation at synapses.

A) Representative images from 14 DIV neurons transduced with either mCh-Rab3 or -Rab35, treated for 24 hours with DMSO or chx and immunostained with VAMP2 antibodies. Arrows represent VAMP2 puncta (green) in axons expressing mCh-Rab3 or mCh-Rab35 (purple). Scale bar=10 μ m. B) Quantification of the average fluorescence intensity of VAMP2 puncta, normalized to Rab3 (n=9 images/condition; 3 replicate weeks, each with 3 images/condition, ~100 puncta/image; *= p <0.05). C) Representative images from neurons expressing VAMP2-SNAP and either mCh-Rab3 or mCh-Rab35, fixed 15 or 48 hours after BG-Oregon Green (BG-OG) labeling and immunostained with Flag antibodies. Arrows represent VAMP2 puncta detected with Flag (blue) in axons expressing mCh-Rab3 or mCh-Rab35 (red). Scale bar=10 μ m. D) Quantification of the average fluorescence intensity of Flag staining (n=5; ~100 puncta/image), BG-OG labeling (n=10; ~100 puncta/image), and the fraction of BG-OG puncta that colocalize with Flag (n=6 for Rab3, n=5 for Rab35; ~75 puncta/image) in each condition normalized to Rab3 at the 15 hour time point. Student's two-tailed t-tests with a hypothetical value of 1.0 were performed. E) Quantification as in D for Flag staining (n=5; ~100 puncta/image), BG-OG labeling (n=7 images/condition; ~100 puncta/image; similar results obtained for 3 independent experiments; **= p <0.01), and BG-OG puncta colocalization (n=19 images/condition from 3 replicate weeks, ~75 puncta/image; **= p <0.01) for the 48 hour time point.

Rab35 is necessary for activity-dependent SV protein degradation upstream of the ESCRT pathway

Our data so far demonstrate that Rab35 overexpression is sufficient to drive SV2 and VAMP2 degradation via lysosomes. To determine if Rab35 is also necessary for the degradation of SV membrane proteins, we again utilized 24-hour cycloheximide treatment in conjunction with quantitative immunoblotting and immunofluorescence microscopy, this time in neurons expressing an shRNA against Rab35 (shRab35). This published shRNA (Allaire et al., 2010) efficiently reduced Rab35 protein levels by ~65% (Figure 4.4A). We first performed functional imaging studies in neurons co-expressing shRab35 and super-ecliptic pHluorin (SEP)-tagged synaptophysin, and found that knockdown of Rab35 between 3-14 DIV did not affect neuronal health, the ability of SVs to undergo exo/endocytosis, or the size of the total recycling pool of SVs (Figure 4.4B,C). Using the same time course as in previous experiments, we found that shRab35 significantly attenuated the degradation of SV2 and VAMP2 (by ~15%) compared to a scrambled control shRNA (scRNA), and did not alter the degradation of SNAP-25 or the active zone protein RIM1a (Figure 4.4D,E). Co-expression of shRNA-resistant Rab35 rescued this

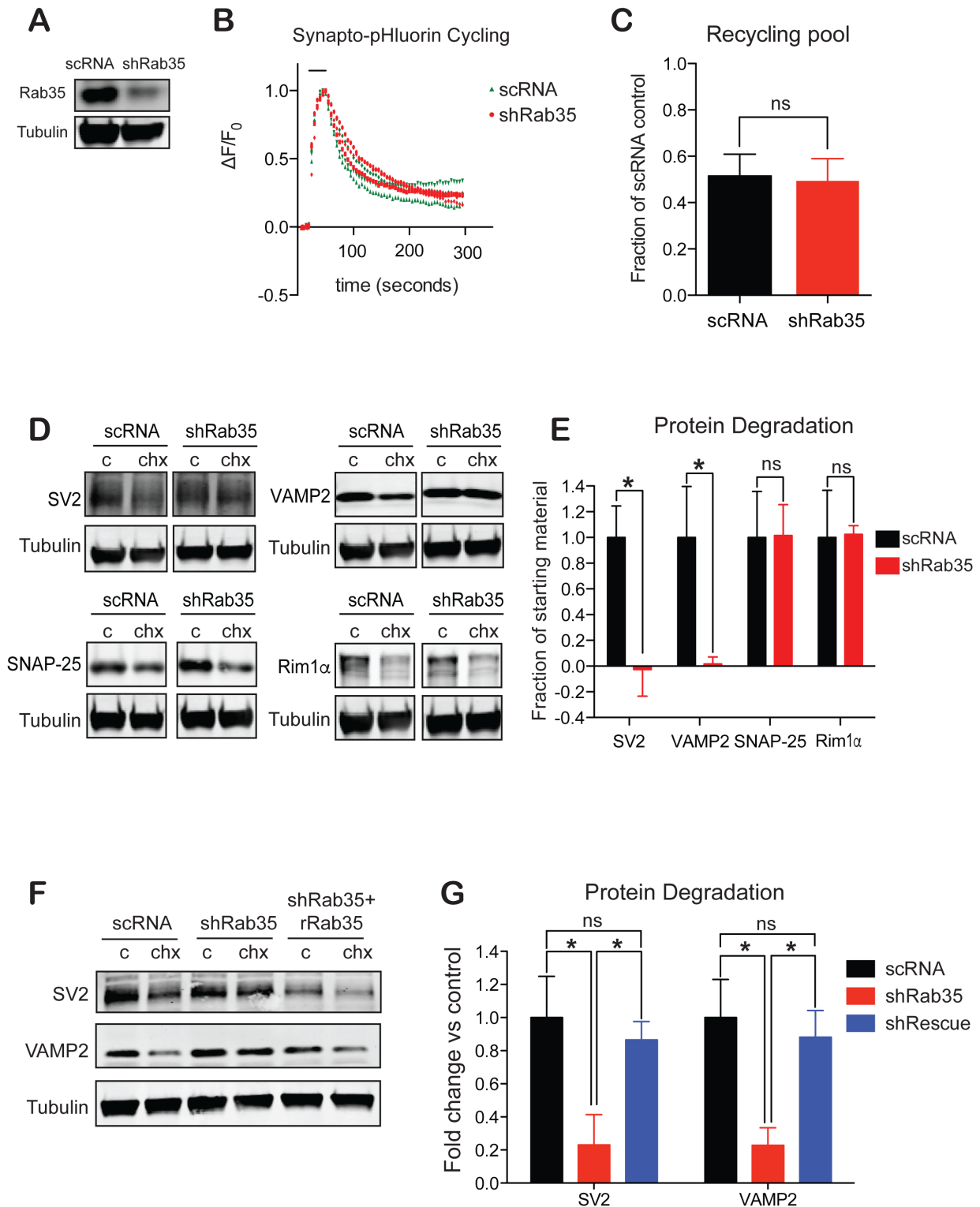


Figure 4.4 - Rab35 is necessary for SV membrane protein degradation

A) Immunoblot from 14 DIV neurons transfected with scRNA or shRab35 and probed for Rab35 and tubulin. Knockdown efficacy of Rab35 is 64.7±0.04% of scRNA control. B) Sample traces of synaptophysin-SEP fluorescence from 14 DIV neurons co-transfected with scRNA or shRab35 and synaptophysin-SEP, expressed as change in initial fluorescence over time. Images were acquired every 5 seconds before, during (black bar), and after

10 Hz, 30 seconds stimulation to elicit SV exo/endocytosis, as described in supplemental methods (n=3 experiments/condition). C) Quantification of the size of the recycling pool of synaptic vesicles in scRNA and shRab35-expressing neurons, measured as the fraction of peak fluorescence intensity of synaptophysin-SEP during stimulation (at $\sim t=50$ sec in B) versus its intensity following deacidification with NH_4Cl to visualize the entire SV pool. Values are normalized to scRNA control (n \geq 13). D) Immunoblots from 14 DIV neurons transduced with scRNA or shRab35, treated for 24 hours with DMSO (c) or chx and probed for SV2, VAMP2, SNAP-25, Rim1a and tubulin. Several immunoblots represent the same experiment and therefore have the same tubulin image. E) Quantification of the fold change in degradation of SV2, VAMP2, SNAP-25, and Rim1a for each condition (n=3-4, $*=p<0.05$). F) Immunoblots from 14 DIV neurons transduced with scRNA, shRab35, or shRab35+sh-resistant Rab35 (rRab35) treated for 24 hours with either DMSO (c) or cycloheximide (chx) and probed for SV2, VAMP2 and tubulin. G) Quantification of the fold change in degradation of SV2 and VAMP2 for shRab35 vs. scRNA control (n=4, $*=p<0.05$).

attenuation of SV protein degradation by shRab35 (Figure 4.4F,G). Together, these results demonstrate that Rab35 is both sufficient and necessary for the degradation of SV integral membrane proteins.

We subsequently examined whether Rab35 was necessary for activity-dependent SV protein degradation. As in the previous chapter, neurons expressing scRNA and shRab35 were treated with Bic/4AP to increase activity, and protein degradation was monitored after 24-hour chx treatment. Remarkably, we found that the ability of Bic/4AP to stimulate SV2 and VAMP2 degradation was nearly abolished in neurons expressing shRab35 (Figure 4.5A,B). Furthermore, Rab35 does not stimulate SV protein degradation by increasing neuronal activity, as blocking activity in Rab35-expressing neurons did not significantly alter the degradation of SV2 and VAMP2 compared to Rab35 overexpression alone (Figure 4.5C,D). These findings demonstrate that activity-dependent SV protein turnover is dependent on Rab35.

To determine if Rab35 acts upstream of the ESCRT pathway, we measured the degradation of SV2 and VAMP2 in neurons co-expressing scRNA or shHrs and mCh-Rab35. As anticipated, Rab35-mediated degradation of SV2 and VAMP2 was significantly attenuated in shHrs-expressing neurons (Figure 4.6A,B). Moreover, average VAMP2 immunofluorescence intensity was increased by 40% in the presence of shHrs/mCh-Rab35 vs. scRNA/mCh-Rab35 (Figure 4.6C,D). We also performed these experiments in neurons expressing mCh-Rab35 and

scRNA or shTSG101 and found similar results by immunoblotting and quantitative immunofluorescence (Figure 4.6E-H). Together, these data demonstrate that Rab35 acts upstream of the ESCRT pathway to mediate degradation of SV proteins.

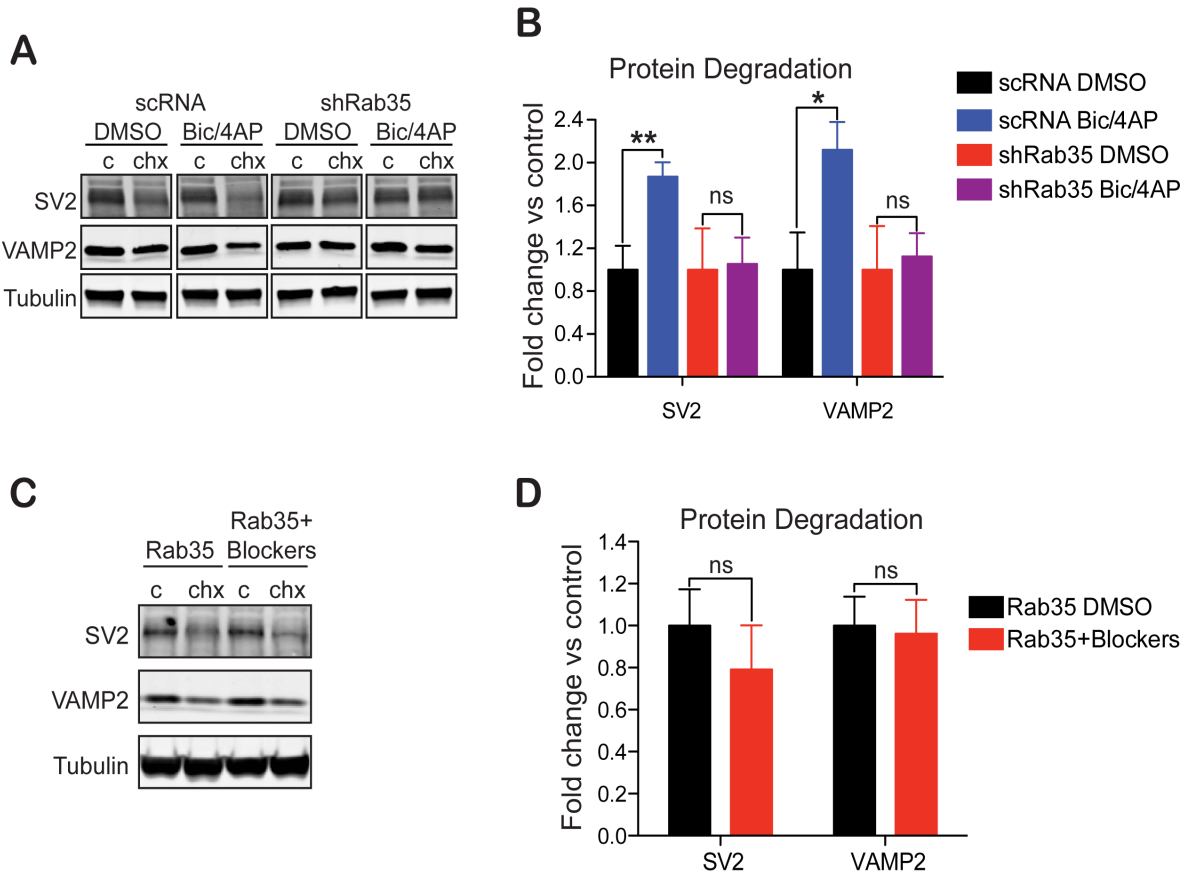


Figure 4.5 - Knockdown of Rab35 inhibits activity-dependent SV protein degradation.

A) Immunoblots from 14 DIV neurons transduced with scRNA or shRab35 and treated for 24 hours with DMSO (c) or chx in the presence of additional DMSO or bic/4AP, and probed for SV2, VAMP2 and tubulin. B) Quantification of fold change in degradation of SV2 and VAMP2 in the presence of scRNA or shRab35, +/- activity. As in Fig. 3.3, DMSO control is set to 1 for each condition (scRNA black bars, shRab35 red bars), and bic/4AP treatment is expressed as fold change vs. DMSO control for that condition (n=8; *p<0.05). C) Immunoblots from 14 DIV neurons transduced with mCh-Rab35 and treated for 24 hours with DMSO (c) or chx in the presence of additional DMSO or APV/CNQX/TTX to inhibit neuronal activity (blockers). Blots were probed for SV2, VAMP2 and tubulin. D) Quantification of the fold change in degradation of SV2 and VAMP2 for Rab35 + blockers vs. Rab35 DMSO control (n=3).

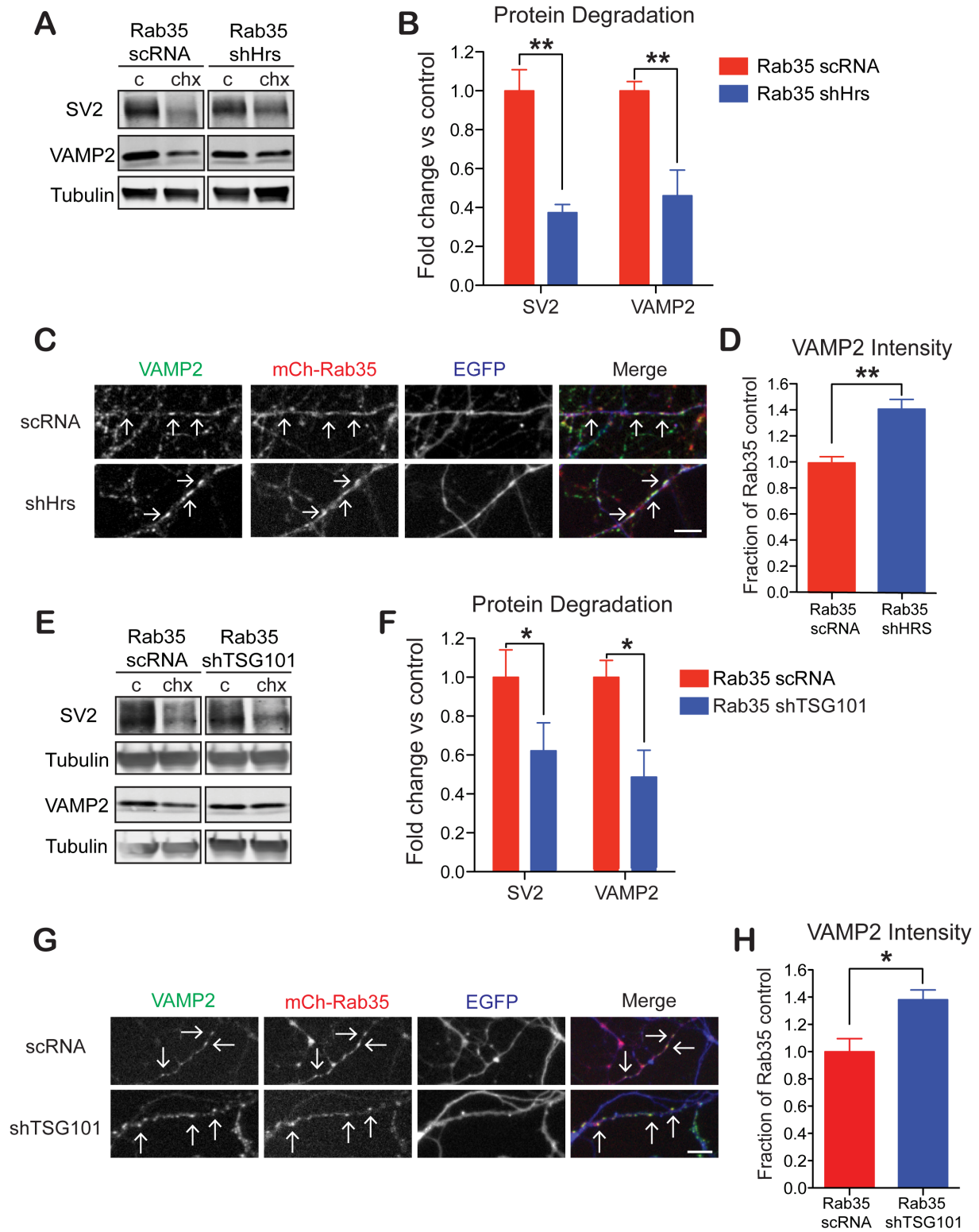


Figure 4.6 - The ESCRT pathway functions downstream of Rab35 to mediate SV protein degradation.

A) Immunoblots from 14 DIV neurons transduced with mCh-Rab35 and either scRNA or shHrs, treated for 24 hours with DMSO (c) or chx and probed for SV2, VAMP2 and tubulin. B) Quantification of the fold change in degradation of SV2 and VAMP2 for Rab35/shHrs vs. Rab35/scRNA control (n=3; **=p<0.01). C) Images from 14 DIV neurons transduced with mCh-Rab35 and either scRNA or shHrs, fixed 24 hours after chx treatment, and immunostained against VAMP2. Arrows represent VAMP2 puncta in axons expressing Rab35 and either scRNA or shHrs. Scale bar=10 μ m. D) Quantification of the average fluorescence intensity of VAMP2 puncta, normalized to Rab35 + scRNA control (n=6 images/condition from 2 replicate weeks, ~100 puncta/image; **=p<0.01). E) Immunoblots from 14 DIV neurons transduced with mCh-Rab35 and either scRNA or shTSG101, treated for 24 hours with DMSO (c) or chx and probed for SV2, VAMP2 and tubulin. F) Quantification of the fold change in degradation of SV2 and VAMP2 for Rab35/shTSG vs. Rab35/scRNA (n=3, *=p<0.05). G) Images from 14 DIV neurons transduced with mCh-Rab35 and either scRNA or shTSG101, fixed 24 hours after chx treatment and immunostained against VAMP2. Arrows represent VAMP2 puncta in axons expressing Rab35 and either scRNA or shTSG101. Scale bar=10 μ m. H) Quantification of the average fluorescence intensity of VAMP2 puncta, normalized to Rab35 + scRNA control (n=3 images/condition, ~100 puncta/image, similar results obtained for 2 independent experiments; *=p<0.05).

Hrs is an effector of Rab35

Our co-immunoprecipitation experiments demonstrated an interaction between Rab35 and Hrs (Figure 4.1A,B). To further characterize the specificity of this interaction, we co-expressed EGFP-Rab35 together with a series of mCh-tagged ESCRT proteins in HEK293T cells. We found that EGFP-Rab35 robustly co-localized with Hrs, but not with TSG101 or CHMP2B (Figure 4.7A). Next, we performed co-immunoprecipitation assays in HEK293T cells expressing HA-Rab35 together with a similar series of mCh-tagged ESCRT proteins. HA-Rab35 co-precipitated with Hrs, but not with STAM (another ESCRT-0 component), TSG101, or CHMP2B (Figure 4.7B). Given the specificity of the Rab35-Hrs interaction, we next investigated whether Hrs was a direct effector of Rab35. Effectors are recruited by active (GTP-bound) Rabs to carry out the relevant downstream vesicle sorting, uncoating, trafficking, tethering, or fusion steps (Stenmark, 2009) Here, we performed co-immunoprecipitation assays in HEK cell lysates expressing HA-Rab35 and Flag-Hrs, and subsequently incubated with either GDP or GTP γ S. We observed that significantly more HA-Rab35 was co-precipitated by Flag-Hrs in the presence of GTP γ S than GDP, as expected if Hrs is a Rab35 effector (Figure 4.7C,D). To confirm these findings, we performed pull-down experiments with GST-Rab loaded with GDP or GTP γ S,

coupled to glutathione-agarose beads, and incubated with HEK cell lysate expressing Flag-Hrs.

We again found that GST-Rab35-GTP pulled down significantly more Flag-Hrs (Figure 4.7E,F),

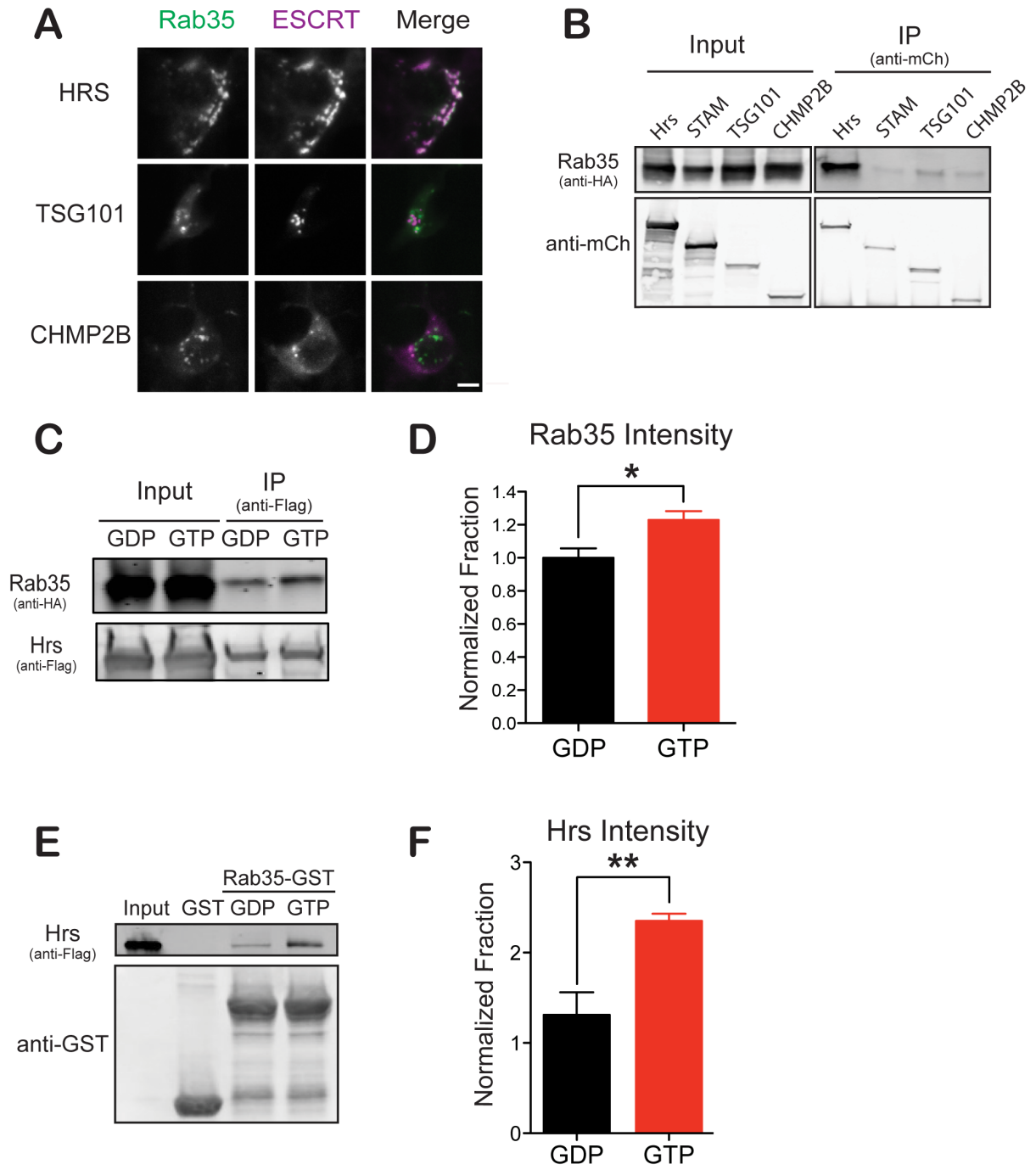


Figure 4.7 - ESCRT-0 component Hrs is an effector of Rab35.

A) Images of HEK293T cells co-expressing EGFP-Rab35 and the indicated mCh-tagged ESCRT proteins. Scale bar=10 μ m. B) Immunoblot of lysates from HEK293T cells expressing HA-Rab35 and either mCh-Hrs, -STAM, -TSG101, or -CHMP2B, immunoprecipitated (IP) with mCherry antibody and probed with HA or mCherry antibodies. C) Immunoblot of HEK cell lysates expressing HA-Rab35 and Flag-Hrs, incubated with either GDP or GTP γ s, subject to IP with Flag antibody, and probed with HA and Flag antibodies. D) Quantification of HA-Rab35 intensity normalized to Flag-Hrs intensity in the eluate and reported as a fraction of the amount in the GDP condition. Student's two-tailed t-tests with a hypothetical value of 1.0 were performed (n=5; *p<0.05). E) Immunoblot of HEK cell lysates expressing Flag-Hrs, subject to pull-down with GST, GST-Rab35-GDP or GST-Rab35-GTP γ s and probed with GST and Flag antibodies. F) Quantification of Flag-Hrs intensity, normalized to GST-Rab35 intensity in the eluate (n=4; **p<0.01).

consistent with the co-immunoprecipitation results. Thus, our data clearly show that Hrs is an effector of Rab35, providing a direct mechanistic link between Rab35 and the ESCRT pathway.

Based on this finding, we hypothesized that Rab35 would recruit Hrs to SV pools in order to initiate ESCRT complex formation. Since the available antibodies against Rab35 and Hrs are not suitable for immunofluorescence microscopy in neurons, we tested this prediction by co-transfecting neurons with mCh-Hrs and either soluble EGFP or EGFP-Rab35. Neurons were subsequently fixed and immunostained for VAMP2, and the percent colocalization of mCh-Hrs puncta with VAMP2 puncta was quantified and compared in the presence or absence of EGFP-Rab35. We found that while approximately 40% of mCh-Hrs puncta colocalized with VAMP2 at baseline, co-expression of EGFP-Rab35 increased this value to nearly 70% (Figure 4.8A,C), similar to neuronal activity (Figure 3.4A,C). These data confirm that Rab35 is able to effectively recruit Hrs to SV pools in axons. Similar results were seen with CHMP2B (Figure 4.8B,C), suggesting that Rab35 recruits Hrs to initiate formation of MVBs in axons.

To better visualize the spatial relationship between Rab35 and ESCRT pathway proteins in axons, we acquired super-resolution images of neurons co-transfected with EGFP-Rab35 and mCh-Hrs or CHMP2B-mCh. EGFP-Rab35 was observed along axons in small puncta and, more rarely, enlarged endosomal structures (Figure 4.8D,E), on which we focused in order to resolve the spatial distribution of Rab35 and the ESCRT proteins. EGFP-Rab35 and mCh-Hrs exhibited a high degree of colocalization on these enlarged endosomes (Figure 4.8D), indicating that they

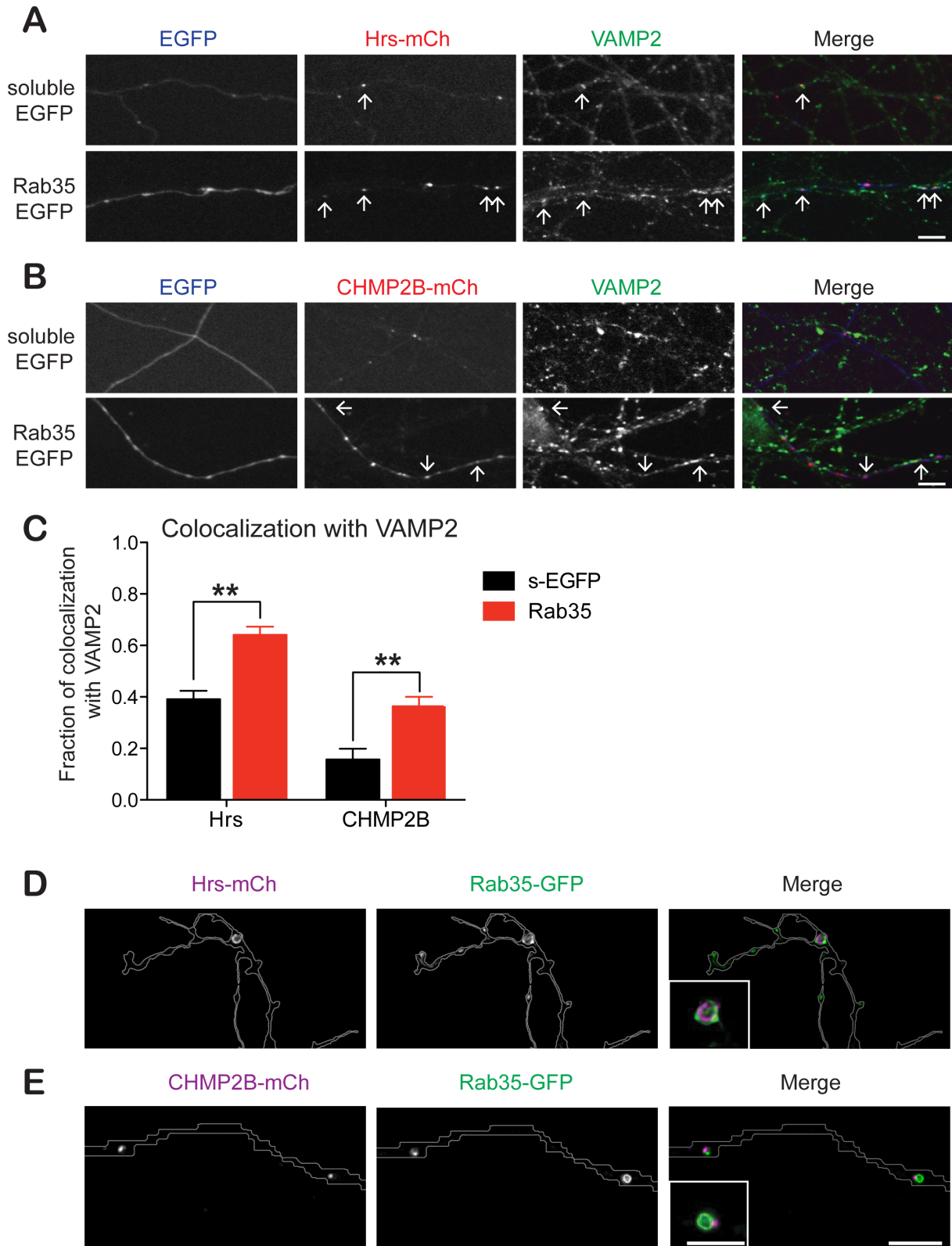


Figure 4.8 - Rab35 recruits ESCRT proteins to synaptic vesicle pools.

A) Images of neurons co-transfected with mCh-Hrs and either soluble EGFP or EGFP-Rab35, fixed and immunostained against VAMP2. Arrows represent mCh-Hrs puncta that colocalize with VAMP2 in axons expressing either soluble EGFP or EGFP-Rab35. Scale bar=10 μ m. B) Images of neurons co-transfected with

CHMP2B-mCh and either soluble EGFP or EGFP-Rab35, fixed and immunostained against VAMP2. Arrows represent CHMP2B-mCh puncta that colocalize with VAMP2 in axons expressing either soluble EGFP or EGFP-Rab35. Scale bar=10 μ m. C) Quantification of the fraction of Hrs and CHMP2B puncta that colocalize with VAMP2 in each condition (for Hrs: n=15 for control, n=19 for Rab35 from 3 replicate weeks, each with ~25 puncta/image. For CHMP2B: n=5 for control, n=8 for Rab35 from 2 replicate weeks, ~15 puncta/image; **=p<0.01). D) Super-resolution images of neurons co-transfected with EGFP-Rab35 and mCh-Hrs. Inset shows higher magnification view of Hrs/Rab35 colocalization on an enlarged endosome created by Rab35 overexpression. E) Super-resolution images of neurons co-transfected with Rab35 and CHMP2B-mCh. Outline of axon is shown. Inset shows higher magnification view of a Rab35-positive endosome and juxtaposed CHMP2B-mCh puncta. Scale bar=5 μ m, 2.5 μ m for inset.

interact on endosomal membranes. In contrast, CHMP2B-mCh puncta were typically smaller and immediately adjacent Rab35-positive endosomes (Figure 4.8D), potentially representing a later stage of MVB formation. Together with our findings in HEK cells, these results indicate that Rab35 colocalizes precisely with the ESCRT-0 component Hrs but much less with later ESCRT pathway components such as CHMP2B.

Neuronal activity stimulates Rab35 activation

The ability of Rab35 to initiate ESCRT protein recruitment suggests that neuronal activity serves as a signal to activate Rab35 itself. We tested this hypothesis with an antibody that specifically immunoprecipitates active, GTP-bound Rab35. To verify its specificity, we co-expressed HA-Rab35 in HEK293T cells together with soluble EGFP or EGFP-Connecdenn1, a GEF that activates Rab35 (Allaire et al., 2010; Marat and McPherson, 2010). Indeed, Rab35 was more robustly precipitated by the GTP-Rab35 antibody in lysates from cells expressing Connecdenn1 versus soluble EGFP (Figure 4.9A). To determine if Rab35 was activated by neuronal activity, we next compared the levels of GTP-Rab35 in neurons treated with DMSO or Bic/4AP. Remarkably, we found that the GTP-Rab35 antibody precipitated nearly two times more Rab35 from Bic/4AP-treated neurons than from control neurons (Figure 4.9B,C), suggesting that increased neuronal activity promotes Rab35 activation/GTP binding.

Since Rab35 and Hrs interact in a GTP-dependent manner, neuronal activity should also enhance their binding. To test this, we immunoprecipitated mCh-Hrs from neurons treated for 12 hours with Bic/4AP. Again, significantly more endogenous Rab35 was co-precipitated with Hrs following treatment with Bic/4AP versus DMSO (Figure 4.9D,E), indicating that neuronal activity increases the association between Rab35 and Hrs. This activity-dependent association likely catalyzes the recruitment of ESCRT proteins to SV pools, where they can initiate the formation of MVBs for SV protein degradation (Figure 4.9F).

Discussion

Our findings demonstrate that Rab35 mediates the use-dependent degradation of SV membrane proteins in mammalian neurons through the ESCRT pathway. Specifically, we find that activity induces the activation of Rab35, thereby promoting Hrs binding and recruitment to SV pools. These events in turn recruit the downstream ESCRT machinery, thereby initiating the formation of MVBs for delivery of specific SV proteins to lysosomes (Figure 4.9F). Together with our findings in chapter 3, we have identified a novel pathway that maintains SV integrity, by enabling neurons to replace proteins that become damaged or misfolded during SV recycling.

Rab GTPases as coordinators of SV protein turnover

In this chapter, we found that two Rab GTPases (Rabs 5 and 35) are capable of driving VAMP2 and SV2 degradation. While Rab35 interacts with Hrs and specifically mediates the degradation of SV integral membrane proteins, Rab5 does not interact with Hrs, and stimulates the turnover of multiple presynaptic proteins (plasma membrane and active zone-associated), suggesting that it activates a broader degradative program. One possibility, based on Rab5's link to the autophagic pathway (Dou et al., 2013; Ravikumar et al., 2008; Su et al., 2011), is that its overexpression in neurons activates macroautophagy. Indeed, previous studies have shown that

stimulating macroautophagy in neurons can induce the engulfment of SVs, cytoplasmic proteins, and other organelles by autophagosomes (Hernandez et al., 2012; Maday et al., 2014; Sanchez-Varo et al., 2011). Interestingly, a recent study has linked the SV-associated Rab26 to the autophagic pathway, showing that Rab26 overexpression induces SV clustering and engulfment by autophagosomes (Binotti et al., 2015). Although our findings indicate that basal and activity-dependent SV protein turnover occur through Rab35 and the ESCRT pathway, it is likely that specific stimuli and developmental programs (*e.g.* oxidative stress, protein aggregation, synapse elimination/pruning) can activate macroautophagy in order to degrade SVs and other synaptic components under certain conditions. Additional studies are needed to investigate the conditions under which the ESCRT pathway and macroautophagy are utilized for SV protein degradation.

Two other SV-associated Rab GTPases that we evaluated (Rabs 10 and 14) do not alter SV protein degradation, but do interact with Hrs. We hypothesize that these Rabs also participate in trafficking in the endolysosomal pathway, but target different classes of membrane-associated proteins. Gain and loss-of-function studies combined with stable isotope labeling with amino acids and mass spectrometry are likely to yield insights into the proteins targeted by these Rabs.

While many of the SV-associated Rabs have been implicated in endosomal recycling in other cell types (Babbey et al., 2006; Junutula et al., 2004), little is known about their roles in neurons. We hypothesize that these may participate in the sorting process that directs SV proteins for reuse/recycling versus degradation. Such sorting typically occurs in early or recycling endosomes of non-neuronal cells, and may occur within endosomes that form immediately upon SV endocytosis in presynaptic boutons (Watanabe et al., 2014). Gain and loss-of-function studies with these SV-associated Rabs, in combination with recently developed ‘flash-and-freeze’ fixation techniques (Watanabe et al., 2014), are likely to yield insights into

their roles in SV protein sorting, and may help identify signals that target SV proteins for recycling vs. degradation.

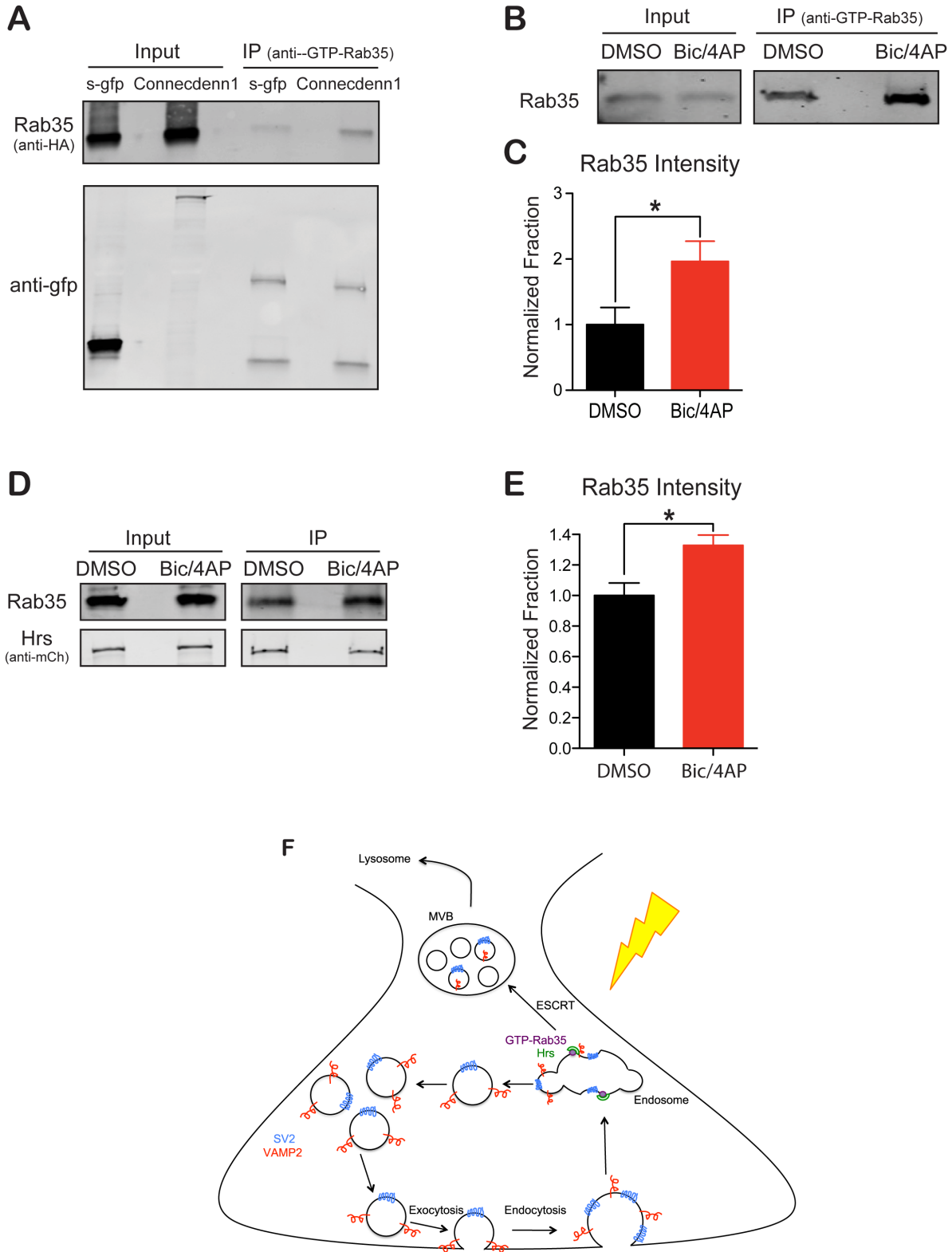


Figure 4.9 - Neuronal activity activates Rab35 and stimulates Rab35-Hrs binding.

A) Lysates from HEK293T cells co-transfected with HA-Rab35 and either soluble GFP or Connecdenn1-GFP, subject to IP with GTP-Rab35 specific antibody. Bound proteins and input were probed with HA antibody to detect Rab35. B) Immunoblots from 15 DIV neurons treated with DMSO or bic/4AP for 12 hours, then lysed and subject to IP with mouse GTP-Rab35 specific antibody and probed with rabbit Rab35 antibody. C) Quantification of Rab35 intensity in the eluate, normalized to input intensity and reported as a fraction of the DMSO control condition. Student's two-tailed t-tests with a hypothetical value of 1.0 were performed (n=7, * $p < 0.05$). D) Immunoblots from neurons transduced with mCh-Hrs and treated with DMSO or bic/4AP for 12 hours, then lysed and subject to IP with anti-mCherry antibody. Bound proteins and input were probed with Rab35 and mCherry antibodies. E) Quantification of Rab35 intensity in the eluate, normalized to input intensity and Hrs intensity in the eluate. Bic/4AP condition is reported as a fraction of the DMSO control condition. Student's two-tailed t-tests with a hypothetical value of 1.0 were performed (n=3, * $p < 0.05$). F) Putative pathway for activity-dependent SV protein degradation. Neuronal activity (lightning bolt) serves to activate Rab35, which then recruits its effector, Hrs, to presynaptic endosomes. This recruitment is hypothesized to initiate MVB formation, leading to retrograde transport and delivery of specific SV proteins (SV2 and VAMP2) to somatic lysosomes for degradation.

Rab35 links SV protein degradation to the ESCRT pathway through its effector Hrs

Previous studies identified Rab35 as an important regulator of the endosomal sorting and turnover of SV proteins (Fernandes et al., 2014; Uytterhoeven et al., 2011). Here, we provide mechanistic insight into how Rab35 mediates the degradation of SV proteins, by directly linking Rab35 to the ESCRT-0 component Hrs. The GTP-dependent Rab35/Hrs binding interaction implicates the ESCRT pathway as a critical mediator of SV protein degradation downstream of Rab35. Not only is the ESCRT pathway essential for recruiting ubiquitinated membrane proteins destined for degradation, but it also catalyzes the formation of MVBs to deliver this cargo to lysosomes. Previous work has shown that MVBs often appear in EM micrographs of presynaptic boutons following neuronal stimulation (Teichberg et al., 1975), suggestive of activity-dependent formation. Although our EM studies could not definitely show this, the concept is consistent with our data showing that neuronal activity stimulates protein turnover and the recruitment of ESCRT proteins to SV pools (Chapter 3).

Neuronal activity

We also provide the first example of neuronal activity as a signal for Rab GTPase activation. Though the GAPs and GEFs for many Rabs have been characterized (see (Barr and Lambright,

2010)), few studies have addressed the signals responsible for Rab activation/inactivation. A recent study found that CnrF, a Rab11a GAP protein, is activated by calcium release through vacuolar P2XA ion channels (Parkinson et al., 2014). This signal functions to inactivate Rab11a in response to P2XA channel activation. Similarly, neuronal activity may induce activation or inactivation of Rab35 GEF or GAP proteins, respectively, thereby stabilizing Rab35 in its GTP-bound conformation. Candidate GEFs and GAPs to regulate synaptic Rab35 activation include Connecdenn1, a presynaptically enriched GEF that interacts with clathrin to mediate SV recycling (Allaire et al., 2006), and TBC1D24/skywalker, a GAP shown to negatively regulate Rab35 activity in presynaptic terminals of *Drosophila* (Uytterhoeven et al., 2011). Whether and how these molecules regulate Rab35 activation in response to synaptic activity or other stimuli is an interesting topic for future studies.

Chapter 5 - Ubiquitination serves as a signal for VAMP2 degradation

Rationale

Entry of SV proteins into the degradative pathway is hypothesized to require a specific targeting signal. Ubiquitination is a post-translational modification that targets soluble proteins for degradation by the proteasome. However, its role in the degradation of integral membrane proteins, which are typically degraded by lysosomes, is less clear. Intriguingly, a recent study reported that SV membrane proteins are among the most highly ubiquitinated neuronal proteins (Na et al., 2012), suggesting that this modification may play an important role in their degradation. However, ubiquitination also regulates many non-degradative protein trafficking events (*i.e.* endocytosis, protein-protein interactions), and its role in SV protein trafficking/degradation is largely unexplored.

We have determined that specific SV proteins (VAMP2 and SV2) undergo activity-dependent degradation (Chapter 3). Given that neuronal activity has been shown to regulate ubiquitination (Ehlers, 2003) and to influence the protein composition of the postsynaptic density (Ehlers, 2003) and presynaptic active zone (Lazarevic et al., 2011), we examined whether ubiquitination acts as a signal for SV protein degradation. In this chapter, we demonstrate that ubiquitination is required for the basal and activity-dependent degradation of VAMP2. Further, we identify the E3 ligase, RNF167 as a major regulator of VAMP2 ubiquitination.

Results

Ubiquitination of VAMP2 is required for its basal and activity-dependent degradation

In previous experiments, we found that the SV integral membrane proteins SV2 and VAMP2 undergo activity-dependent degradation (Chapter 3). Here, we explore the function of ubiquitination in targeting VAMP2 to the degradative pathway. We created a ubiquitination-

resistant version of VAMP2 by replacing its seven lysine residues with arginine (KR VAMP2; Figure 5.1A). We verified that KR VAMP2 localized properly to synapses, recycled with normal kinetics, and exhibited dramatically reduced ubiquitin immunoreactivity compared to wild-type VAMP2 (WT VAMP2; Figure 5.1B-D).

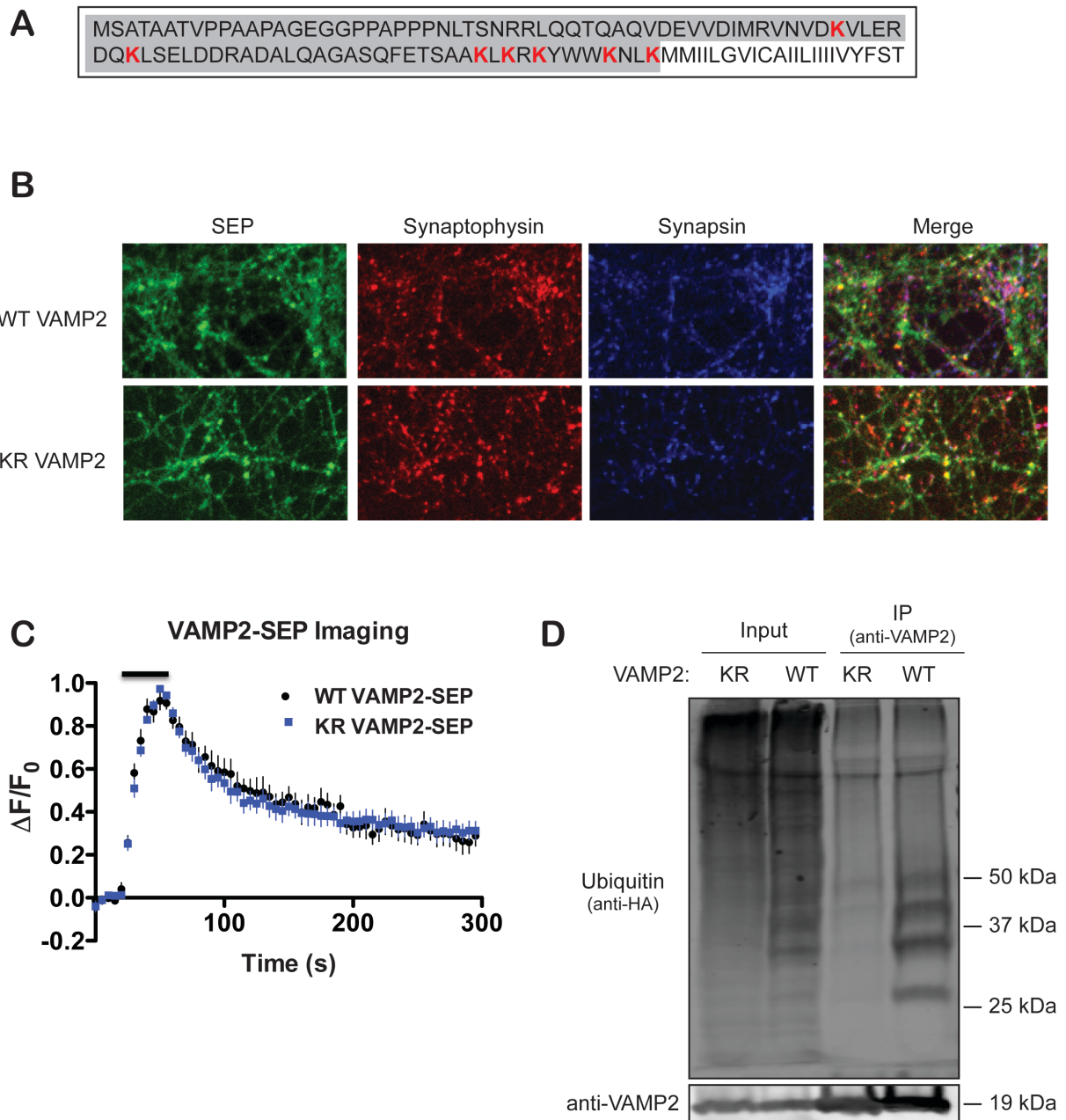


Figure 5.1 - KR VAMP2 localizes to synapses and exhibits normal recycling kinetics but reduced ubiquitination. A) Amino acid sequence of VAMP2 from *Rattus norvegicus*, showing the cytoplasmic N-terminal domain (shaded) and lysines (red) mutated to arginines in the KR VAMP2 construct. B) Representative images from

14 DIV neurons transduced with either WT VAMP2-SEP or KR VAMP2-SEP (green), and immunostained with synaptophysin (red) and synapsin (blue) antibodies to label SV pools. C) Sample traces of VAMP-SEP fluorescence from neurons transfected with WT VAMP2-SEP or KR VAMP2-SEP. D) Immunoblots of lysates from HEK293T cells co-expressing HA-ubiquitin and untagged WT VAMP2 or KR VAMP2, incubated for 4 hours with de-ubiquitinating enzyme inhibitors and subject to immunoprecipitation (IP) with VAMP2 antibody followed by probing with HA or VAMP2 antibodies.

To determine whether ubiquitination is necessary for the degradation of VAMP2, we transduced 7 DIV hippocampal neurons with either WT or KR VAMP2-SEP and assessed VAMP2 degradation using our cycloheximide-chase assay as previously described (Chapter 3). Interestingly, we observed a significant decrease in the degradation of KR VAMP2 compared to WT VAMP2 over the 24-hour time course (Figure 5.2A,B). Since we previously found VAMP2 to undergo activity-dependent degradation (Chapter 3), we asked whether KR VAMP2 degradation could be similarly sped with bicuculline/4AP (Bic/4AP) treatment (Chapter 3). Intriguingly, we found that while Bic/4AP significantly increased the degradation of WT VAMP2 compared to DMSO control, this treatment did not alter the degradation of KR VAMP2 (Figure 5.2C,D), suggesting that ubiquitination of VAMP2 is necessary for both its basal and activity-dependent degradation. Moreover, we noticed that the steady-state levels of KR VAMP2 were significantly higher than those of WT VAMP2 (Figure 5.2A,C), consistent with its lack of degradation and build-up over time. The functional effects of this KR VAMP2 build-up will be investigated in future experiments.

K63-linked poly-ubiquitination of VAMP2 is required for its degradation

We next tested which type of ubiquitination was required for VAMP2 degradation. While K48 poly-ubiquitination serves as a signal for proteasomal degradation, multi-mono-ubiquitination and/or K63 linkages serve as the signal for ESCRT-mediated degradation. Since we found the ESCRT pathway to be necessary for activity-dependent VAMP2 degradation (Chapters 3 & 4),

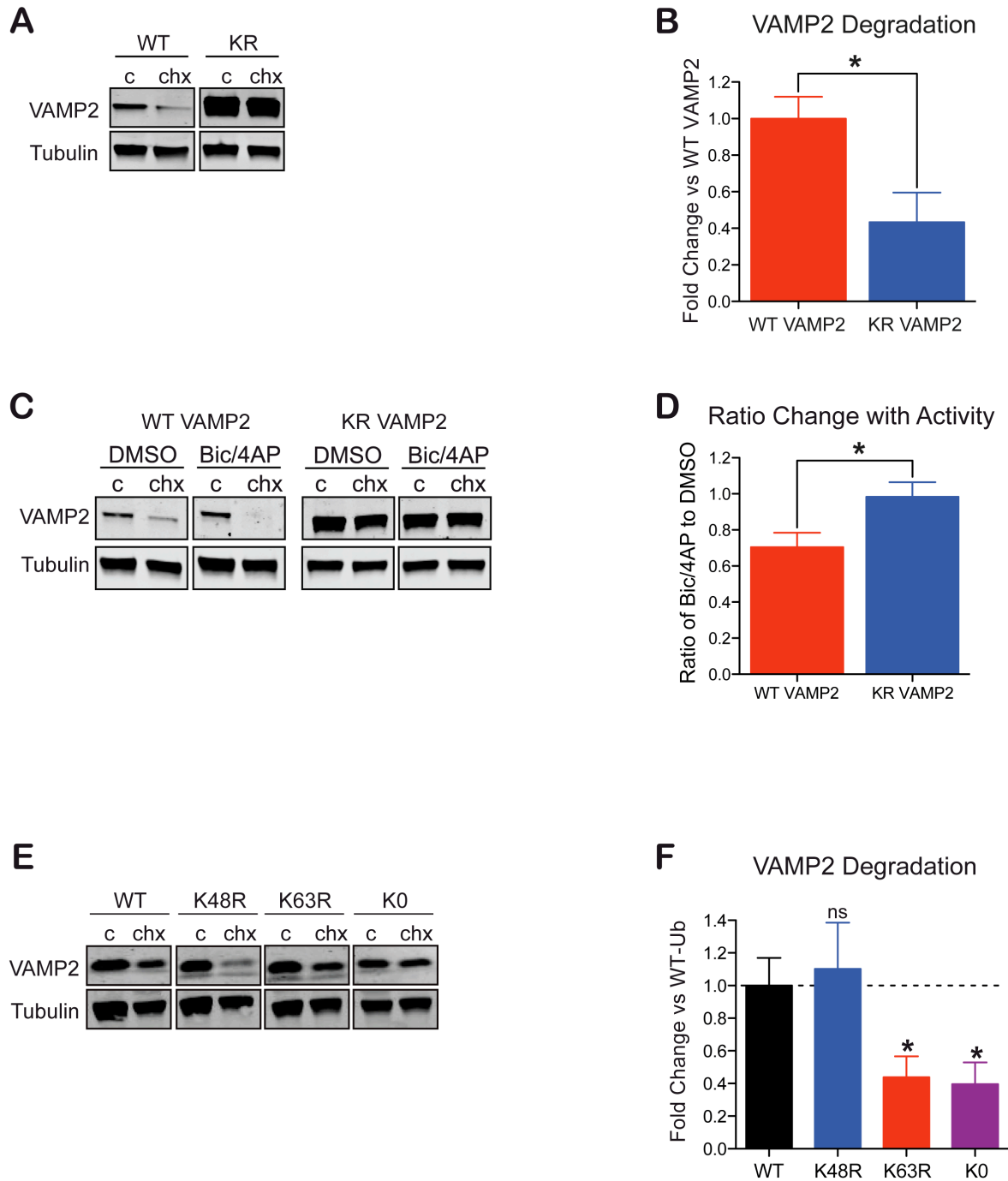


Figure 5.2 - Ubiquitination is required for basal and activity-driven degradation of VAMP2.

A) Immunoblots from 14 DIV neurons transduced with either WT or KR VAMP2-SEP, treated for 24 hours with DMSO (c) or chx and probed for VAMP2 and tubulin. B) Quantification of the fold change in degradation of VAMP2 for each condition (n=4, * $p < 0.05$). C) Representative immunoblots from 14 DIV neurons expressing WT or KR VAMP2-SEP, treated for 24 hours with DMSO (c) or chx in the presence of additional DMSO or Bic/4AP to stimulate neuronal activity, and probed for the same proteins as in A. D) Quantification of protein degradation in each condition, expressed as the fold change versus DMSO control (n=6, * $p < 0.05$). E) Representative immunoblots from 14 DIV neurons transduced with mCh-WT, K48R, K63R, or K0 ubiquitin treated for 24 hours with DMSO (c) or chx and probed for VAMP2 and tubulin. F) Quantification of the fold change in degradation of VAMP2 for each condition (n=7-14, * $p < 0.05$).

we hypothesized that multi-mono- or K63-ubiquitination would be required for VAMP2 degradation. To test this prediction, we transduced neurons with ubiquitin constructs containing K to R mutations that render them incapable of forming specific ubiquitin linkages. We compared the degradation of VAMP2 in the presence of wild-type ubiquitin (Ub-WT) vs. K48R, K63R, and K0 (in which all lysines are mutated to arginine such that only mono or multi-mono-ubiquitin linkages can form) ubiquitin mutants. Specifically, 10 DIV neurons were transduced with Ub-WT, Ub-K48R, Ub-K63R, or Ub-K0. On 14 DIV, neurons were treated with cycloheximide for 24 hours, then collected and subjected to immunoblotting against VAMP2. The expression of Ub-K48R did not significantly alter VAMP2 degradation compared to Ub-WT, while that of Ub-K63R and Ub-K0 significantly impaired VAMP2 degradation, suggesting the VAMP2 requires lysine-63 linked poly-ubiquitination for its degradation (Figure 5.2E,F).

Ubiquitination of VAMP2 is required for its degradation by Rab35

Our findings show that Rab35 is sufficient to drive VAMP2 degradation, and necessary for the basal and activity-dependent degradation of VAMP2. Therefore, we next asked if ubiquitination of VAMP2 is an important signal in the Rab35 pathway. For these experiments, neurons were co-transduced with mCh-Rab35 and either WT or KR VAMP2-SEP. As before, 24-hour cycloheximide treatment was used to measure the degradation of these proteins by both quantitative immunoblotting and immunofluorescence microscopy. Consistent with the role of ubiquitination as a degradative signal, we found that KR VAMP2 was resistant to Rab35-mediated degradation, exhibiting significantly less degradation than WT VAMP2 based on quantitative immunoblotting, and significantly greater intensity in axons by quantitative immunofluorescence (Figure 5.3A-D). These data suggest that ubiquitination is an important signal for SV protein degradation via the Rab35 pathway.

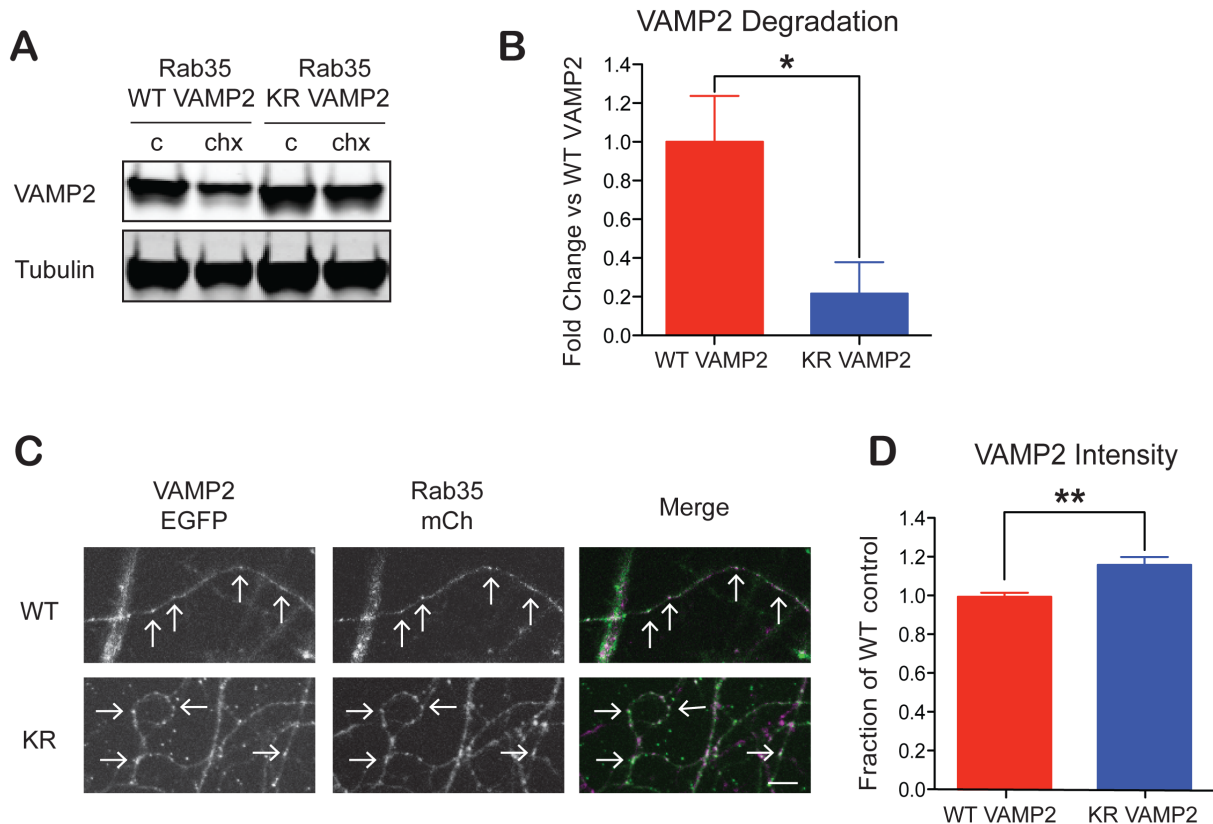


Figure 5.3 - Ubiquitination of VAMP2 is required for its Rab35-mediated degradation.

A) Immunoblots from 14 DIV neurons transduced with mCh-Rab35 and either SEP-WT or KR VAMP2, treated for 24 hours with DMSO (c) or chx and probed for VAMP2 and tubulin. B) Quantification of VAMP2 intensity in each condition, expressed as the fold change versus DMSO control (n=5, $*=p<0.05$). C) Images from 14 DIV neurons transduced with mCh-Rab35 and either SEP-WT or KR VAMP2, then fixed 24 hours after chx treatment. Arrows represent VAMP2 puncta (green) in axons expressing Rab35 (purple), scale bar=10 μ m. D) Quantification of the average fluorescence intensity of VAMP2 puncta, normalized to WT condition (2 replicate weeks, each with 3 images/condition, ~75 puncta/image, n=6, $**=p<0.01$).

RNF167 ubiquitinates VAMP2

Given the importance of ubiquitination for VAMP2 degradation, we next wanted to identify the specific enzymes responsible for ubiquitinating VAMP2. A series of E1, E2, and E3 enzymes are required to carry out the ubiquitination of target proteins. It was previously shown that another VAMP, VAMP3, was ubiquitinated by the RING domain ligase Goliath/RNF167 in *Drosophila* (Yamazaki et al., 2013). The lysine residues of VAMP3 are highly homologous to those of VAMP2 (Figure 5.4A), suggesting that RNF167 may also function in the ubiquitination of VAMP2. To test if RNF167 is capable of ubiquitinating VAMP2, we performed ubiquitination

assays in HEK293T cells expressing soluble-mCh or mCh-RNF167 along with HA-Ubiquitin and VAMP2. Significantly more HA-ubiquitin immunoreactivity was detected in VAMP2 immunoprecipitated from cells expressing RNF167 compared to soluble-mCh (Figure 5.4B,C), demonstrating that RNF167 can function as an E3 ligase for VAMP2.

RNF167 is necessary for the degradation of VAMP2

We next sought to determine if RNF167 is necessary for the ubiquitination and degradation of VAMP2 in neurons. To do so, we designed an shRNA against RNF167 (shRNF167) that led to an 80% reduction in RNF167 mRNA levels when expressed between 3-14 DIV (Figure 5.4 D). We subsequently used quantitative immunofluorescence microscopy to examine the degradation of VAMP2 in neurons expressing shRNF167. Specifically, 14 DIV neurons expressing soluble-EGFP or shRNF167 were treated with DMSO or cycloheximide for 24 hours, fixed, and immunostained for VAMP2. Average fluorescence intensities of VAMP2 puncta in axons expressing soluble-EGFP or shRNF167 were quantified and presented as a fraction of the average intensity in DMSO treated controls. We found that VAMP2 levels were increased by 25% in axons expressing shRNF167 compared to those expressing soluble-EGFP (Figure 5.4E,F), indicating that RNF167 is necessary for VAMP2 degradation.

Discussion

In this chapter, we show that ubiquitination of VAMP2 is necessary for its basal and activity-dependent degradation. Further, we identify the E3 ligase RNF167 as a ubiquitinating enzyme necessary for the degradation of VAMP2. These studies suggest that activity-dependent ubiquitination of VAMP2 is required for its degradation, though more work is needed to clarify whether and how RNF167 mediates this activity-dependent turnover.

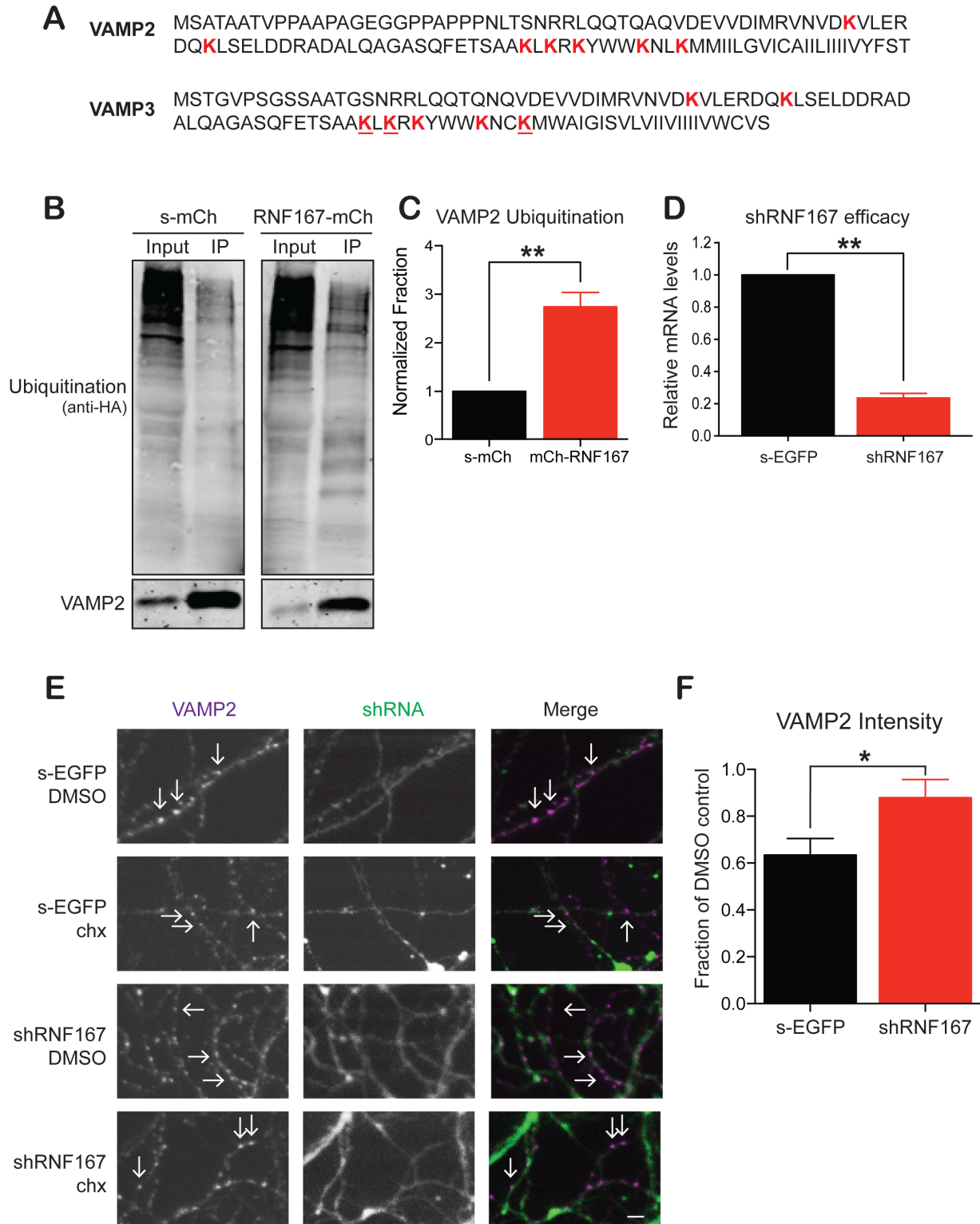


Figure 5.4 - RNF167 ubiquitinates VAMP2 and is necessary for its degradation.

A) Amino acid sequences of VAMP2 and VAMP3 from *Rattus norvegicus*. Lysine residues are shown in red with those demonstrated to be ubiquitinated by RNF167 underlined. B) Immunoblot of HEK cell lysates expressing either soluble-mCh or mCh-RNF167, HA-ubiquitin and untagged VAMP2, subject to IP with VAMP2 antibody and probed with HA or VAMP2 antibodies. C) Quantification of HA-ubiquitin intensity in the eluate, normalized to

VAMP2 intensity in the eluate (n=3, **p<0.01). D) Quantification of mRNA levels from 14 DIV neurons expressing soluble-EGFP or EGFP-shRNF167 determined by qPCR with primers to RNF167, GAPDH, and actin (n=3, **p<0.01). E) Images from 14 DIV neurons transduced with either soluble-EGFP or EGFP/shRNF167, fixed 24 hours after chx treatment, and immunostained against VAMP2. Arrows represent VAMP2 puncta (purple) in axons expressing EGFP +/- shRNA (green). Scale bar=10 μ m. F) Quantification of the fluorescence intensity of VAMP2 puncta, normalized to soluble-EGFP control condition (6 replicate weeks, each with 2-3 images/condition, ~250 puncta/image, n=6, *p<0.05).

Ubiquitination as a signal for SV protein degradation

SV membrane proteins are reported to be highly ubiquitinated (Na et al., 2012), although the role of ubiquitination in their trafficking and turnover has not been explored. Our study is the first to demonstrate that ubiquitination serves as a signal for SV membrane protein degradation, as ubiquitin-resistant KR VAMP2 cannot be efficiently degraded (Figure 5.2A,B). Previous studies have shown that artificially ubiquitinated VAMP2 (Ub-VAMP2) binds to Hrs and is a substrate for ESCRT-dependent degradation (Takahashi et al., 2015; Uytterhoeven et al., 2011). Since our previous data (Chapter 3) also demonstrate that SV protein degradation is ESCRT-dependent, we hypothesize that ubiquitination is a signal for the recognition of SV membrane proteins by ubiquitin-binding components of the ESCRT pathway. Most studies indicate that multi-mono-ubiquitination and/or K63 linkages serve as the signal for ESCRT-mediated degradation, but this is an ongoing area of investigation (see (Shields and Piper, 2011)). Our results show that lysine-63 linked poly-ubiquitination is necessary for VAMP2 degradation (Figure 5.2E-F). Given the high prevalence of ubiquitinated SV proteins in neurons, it is conceivable that different ubiquitin linkages mediate different protein trafficking events, in addition to protein degradation. Indeed, more work is needed to determine the potential roles of other ubiquitin linkages in SV protein trafficking.

RNF167 is an E3 ligase for VAMP2

Although we find that RNF167 is necessary for the degradation of VAMP2, more work is needed to determine if RNF167-mediated ubiquitination of VAMP2 lies upstream of the Rab35/ESCRT

pathway for degradation. Future studies will examine whether RNF167 is necessary for the activity-dependent degradation of VAMP2 using methods analogous to those used in Chapters 3 & 4. Briefly, we will treat shRNF167-transduced neurons with Bic/4AP to increase neuronal activity, and examine whether activity-dependent VAMP2 degradation is attenuated. Further, we will examine whether VAMP2 ubiquitination levels increase following neuronal activity. An intriguing possibility is that VAMP2 accumulates ubiquitin moieties through cycles of exo- and endocytosis, and that these cumulative linkages target VAMP2 and other heavily-used SV proteins for degradation. This mechanism could function to counteract any misfolding or damage accrued by proteins during rounds of SV cycling. Indeed, we have observed that long-term expression of KR VAMP2 leads to neuronal toxicity, suggesting that KR VAMP2 accumulates over time and potentially become damaged/misfolded in a way that compromises neuronal health. Additionally, this finding suggests that the build-up of excess protein and subsequent disruption of protein homeostasis is deleterious to neuronal health. These topics will be explored in future studies to more thoroughly understand the mechanisms behind VAMP2 ubiquitination and the consequences of its accumulation.

Chapter 6 - General Discussion and Future Directions

Our findings demonstrate that Rab35 and the ESCRT machinery are essential components of the pathway for use-dependent turnover of SV2 and VAMP2 in mammalian neurons. Additionally, we find that RNF167-mediated ubiquitination is essential for the degradation of VAMP2. While previous studies have linked Rab35 and the ESCRT pathway to SV protein recycling and turnover in *Drosophila* (Fernandes et al., 2014; Uytterhoeven et al., 2011), our study is the first to demonstrate a direct mechanistic link between Rab35 and the ESCRT pathway through Hrs, and the first to show that turnover of specific SV proteins is regulated by neuronal activity in a Rab35- and ESCRT-dependent manner. Specifically, we find that activity induces the activation of Rab35, thereby promoting its binding to Hrs and the localization of Hrs to SV pools. These events in turn recruit the downstream ESCRT machinery to presynaptic boutons, and are hypothesized to catalyze the formation of MVBs for delivery of ubiquitinated SV proteins to lysosomes. Furthermore, our study is the first to establish a role for RNF167-mediated ubiquitination in the degradation of VAMP2. Together, our studies identify a novel pathway that maintains SV integrity and presynaptic fitness, by enabling neurons to replace proteins that become damaged or misfolded during repeated cycles of SV exo/endocytosis.

Mechanisms of SV protein turnover

Although several studies have examined the mechanisms of SV protein degradation, many outstanding questions remain regarding this process. For instance, it is currently not known whether SV protein turnover is stochastic, with some constant number of proteins being degraded at any given moment, or specific, with particular proteins singled out for degradation based upon their age or conformational state. A previous study in *Drosophila* examined this question by investigating the turnover of young versus old VAMP2 using fluorescent timer

proteins that change from blue to red emission over time (Fernandes et al., 2014; Subach et al., 2009). In this study, older VAMP2 proteins were found to be preferentially degraded. Together with our findings that ubiquitination of VAMP2 is necessary for its degradation, these data support the idea that SV turnover is not stochastic, but rather that specific proteins are sorted out of the SV cycle and sent for degradation.

Use-dependent turnover of SV proteins

One of the most intriguing aspects of the Rab35/ESCRT degradative pathway is its regulation by neuronal activity. Not only are our studies the first to directly link neuronal activity to SV protein turnover, but they are also the first to link it to activation of a Rab GTPase. While we find that SV2 and VAMP2 undergo activity-dependent degradation, the degradation of Syt1 is unaffected by changes in activity levels (Chapter 3). Though we currently do not understand the mechanisms controlling this differential degradation, an interesting possibility is that different regulatory proteins (i.e. E3 ligases, Rab GTPases and/or chaperones) respond to certain stimuli and affect the stability of specific proteins. Indeed, we find that multiple Rab GTPases bind to Hrs, but do not affect SV2 and VAMP2 degradation (Chapter 4). These data suggest that while Rab35 is activated by neuronal activity to drive SV2 and VAMP2 degradation, other Rabs may be activated by different cues to regulate the degradation of other SV proteins. Indeed, it will be interesting to examine the degradation of other SV proteins in the presence of these Rabs to form a more comprehensive picture of the Rab-mediated regulation of SV protein degradation. Additionally, with the increasing development of GTP-bound, conformation specific Rab antibodies, it will be possible to test how different stimuli affect the activation of various Rab proteins.

Roles of ubiquitination at the synapse

We are just beginning to understand the mechanisms underlying SV protein ubiquitination. Several groups have shown that postsynaptic proteins are ubiquitinated and degraded in an activity-dependent manner (Ehlers, 2003; Lussier et al., 2011; Schwarz et al., 2010), and that ubiquitinating enzymes themselves are regulated by activity (Scudder et al., 2014), providing a mechanism for coupling neuronal activity with postsynaptic protein ubiquitination and degradation. In contrast, very few studies have explored the relationship between activity and presynaptic protein ubiquitination, although it has been reported that silencing neurons leads to the accumulation of SV and other presynaptic proteins (Lazarevic et al., 2011). One intriguing possibility is that ubiquitinating enzymes are activated or recruited to SV pools upon neuronal activity. We will examine this possibility in future studies assessing the role of RNF167 in the activity-dependent turnover of VAMP2. As we have shown that ubiquitination of VAMP2 is necessary for its activity-dependent degradation, we hypothesize that RNF167 is a critical component of this process. First, we will determine whether RNF167 is a necessary component of the activity-dependent turnover of VAMP2. As discussed in Chapter 5, we will use similar methods to our studies with Hrs and Rab35 in this process (Chapters 3 & 4). Further, we will examine whether RNF167 undergoes activity-dependent recruitment to synapses through live imaging and immunofluorescence microscopy. Specifically, we will examine whether the colocalization of RNF167 with VAMP2 is induced by increases in neuronal activity analogous to our studies with ESCRT proteins in Chapter 3. Additionally, it will be interesting to determine if RNF167 also functions as an E3 ligase for SV2 or other SV proteins, and if ubiquitination is a general mechanism for basal and activity-dependent degradation of SV membrane proteins.

Ubiquitin moieties can be attached to proteins singly or as poly-ubiquitin linkages built upon specific lysine residues (i.e. K6, K11, K29, K48, K63); thus, it is likely that synaptic

proteins can be modified by ubiquitination for a variety of reasons. Indeed, an assortment of ubiquitination events can be detected on the same protein (Bhat et al., 2014; Nonaka et al., 2005), suggesting that not only does the ubiquitination of these proteins affect their function but also that differential ubiquitination of the same protein may produce distinct functional outcomes. For example, studies have shown a role for dynamic ubiquitination in processes such as neurotransmission (Chen et al., 2003; Rinetti and Schweizer, 2010). Specifically, Rinetti & Schweizer found that application of the E1 activating enzyme inhibitor Ziram for as little as ten minutes led to an increase in the frequency of miniature excitatory postsynaptic currents. No protein accumulation was seen within this time frame, suggesting that the changes observed were not due to protein build-up, but instead to alterations in the dynamic ubiquitination state of presynaptic proteins. Since we are only just beginning to unravel the intricacies of the various roles of ubiquitination in presynaptic function, this will be an interesting and important subject for future investigations.

A role for endosomal sorting in SV protein degradation

Our findings contribute to the large body of evidence that SVs use synaptic endosomes as sorting stations to remove specific proteins from the SV cycle. We provide evidence that endosomes are important not only under high activity conditions, but also in the basal degradation of specific SV proteins (Chapter 3). Though we implicate the recruitment of both early and late components of the ESCRT pathway to SV pools, our findings cannot definitely conclude that MVB formation occurs within the presynaptic compartment. Future studies employing electron microscopy with more specific MVB labeling will be necessary to discern the exact localization of MVB formation in axons.

Additionally, we have begun to explore ESCRT protein dynamics in axons under both basal and high-activity conditions. Our preliminary studies show that the velocity of Hrs puncta increases dramatically in response to neuronal activity; however, much is left to explore regarding ESCRT protein and SV protein dynamics. For instance, it will be interesting to observe the dynamics of other ESCRT proteins and determine whether their dynamics also change in response to activity. Additionally, it will be interesting to determine the necessity of Rab35 in activity-dependent ESCRT protein trafficking. We have also begun to explore the dynamics of SV proteins in response to activity, and are interested in determining whether ubiquitination is required for the transport of VAMP2 out of synapses.

SV protein homeostasis and neurodegeneration

An inability to maintain SV protein homeostasis is implicated as a causative factor in neurodegenerative diseases. Indeed, the accumulation of damaged or misfolded SV-associated proteins can induce neurodegeneration in animal models and humans (Burgoyne and Morgan, 2015; Peng et al., 2013; Rozas et al., 2012; Sharma et al., 2012a; Sharma et al., 2012b; Williamson and Neale, 1998). Moreover, SV loss occurs in mouse models of neurodegenerative diseases, including Alzheimer's, Parkinson's, and lysosomal storage disorder, often prior to the emergence of other phenotypes (Esposito et al., 2012; Sanchez-Varo et al., 2011; Scott et al., 2010; Virmani et al., 2005). These findings suggest that maintaining functional SV pools is critical for synaptic and neuronal health, and that disruption of SV protein homeostasis mechanisms can trigger broader neurodegenerative processes. Interestingly, loss-of-function mutations in TBC1D24/skywalker and the ESCRT proteins Hrs and CHMP2b cause neurodegeneration in mice and *Drosophila* as well as humans (Fernandes et al., 2014; Guven and Tolun, 2013; Lee et al., 2007; Lee et al., 2009; Tamai et al., 2008), implicating this highly

conserved pathway in the etiology of neurodegenerative disease. While TBC1D24/skywalker mutations promote Rab35 over-activation and SV protein degradation, ESCRT mutations impair this process, leading to the accumulation of ubiquitinated proteins and degradative structures (Fernandes et al., 2014; Guven and Tolun, 2013; Lee et al., 2007; Lee et al., 2009; Tamai et al., 2008). Additionally, it was recently discovered that mice expressing artificially ubiquitinated VAMP2 (Ub-VAMP2) develop progressive degeneration of nerve terminals with obvious loss of SV density and the accumulation of tubulovesicular structures (Liu et al., 2015). Furthermore, in preliminary studies we observe toxicity with long-term expression of KR VAMP2. Our future work will characterize the nature of this toxicity to determine whether the lack of degradation of KR VAMP2 inhibits lysosomal function or interferes with the turnover of other SV proteins. All together, these intriguing findings suggest that both the exuberant, unregulated degradation of proteins and the accumulation of dysfunctional proteins are harmful to neurons. Thus, further study of SV protein ubiquitination and the Rab35/ESCRT pathway will not only provide insight into how SV protein turnover and homeostasis are regulated, but will also facilitate the identification of factors that promote or inhibit protein degradation, and could therefore serve as therapeutic targets for the treatment of neurodegenerative disease.

References

- Allaire, P.D., Marat, A.L., Dall'Armi, C., Di Paolo, G., McPherson, P.S., and Ritter, B. (2010). The Connecdenn DENN domain: a GEF for Rab35 mediating cargo-specific exit from early endosomes. *Molecular cell* *37*, 370-382.
- Allaire, P.D., Ritter, B., Thomas, S., Burman, J.L., Denisov, A.Y., Legendre-Guillemin, V., Harper, S.Q., Davidson, B.L., Gehring, K., and McPherson, P.S. (2006). Connecdenn, a novel DENN domain-containing protein of neuronal clathrin-coated vesicles functioning in synaptic vesicle endocytosis. *The Journal of neuroscience : the official journal of the Society for Neuroscience* *26*, 13202-13212.
- Altick, A.L., Baryshnikova, L.M., Vu, T.Q., and von Bartheld, C.S. (2009). Quantitative analysis of multivesicular bodies (MVBs) in the hypoglossal nerve: evidence that neurotrophic factors do not use MVBs for retrograde axonal transport. *The Journal of comparative neurology* *514*, 641-657.
- Alvarez-Castelao, B., and Schuman, E.M. (2015). The Regulation of Synaptic Protein Turnover. *The Journal of biological chemistry*.
- Ao, X., Zou, L., and Wu, Y. (2014). Regulation of autophagy by the Rab GTPase network. *Cell death and differentiation* *21*, 348-358.
- Babbey, C.M., Ahktar, N., Wang, E., Chen, C.C., Grant, B.D., and Dunn, K.W. (2006). Rab10 regulates membrane transport through early endosomes of polarized Madin-Darby canine kidney cells. *Molecular biology of the cell* *17*, 3156-3175.
- Banker, G., and Goslin, K. (1998). *Culturing Nerve Cells (Second Edition)* (Cambridge, MA: MIT Press).
- Barr, F., and Lambright, D.G. (2010). Rab GEFs and GAPs. *Current opinion in cell biology* *22*, 461-470.
- Bezprozvanny, I., and Hiesinger, P.R. (2013). The synaptic maintenance problem: membrane recycling, Ca²⁺ homeostasis and late onset degeneration. *Molecular Neurodegeneration* *8*.
- Bhat, K.P., Yan, S., Wang, C.E., Li, S., and Li, X.J. (2014). Differential ubiquitination and degradation of huntingtin fragments modulated by ubiquitin-protein ligase E3A. *Proc Natl Acad Sci U S A* *111*, 5706-5711.
- Binotti, B., Pavlos, N.J., Riedel, D., Wenzel, D., Vorbruggen, G., Schalk, A.M., Kuhnel, K., Boyken, J., Erck, C., Martens, H., *et al.* (2015). The GTPase Rab26 links synaptic vesicles to the autophagy pathway. *eLife* *4*, e05597.
- Bodor, D.L., Rodriguez, M.G., Moreno, N., and Jansen, L.E. (2012). Analysis of protein turnover by quantitative SNAP-based pulse-chase imaging. *Current protocols in cell biology* / editorial board, Juan S Bonifacino [et al] *Chapter 8*, Unit8 8.

- Brondyk, W.H., McKiernan, C.J., Burstein, E.S., and Macara, I.G. (1993). Mutants of Rab3A analogous to oncogenic Ras mutants. Sensitivity to Rab3A-GTPase activating protein and Rab3A-guanine nucleotide releasing factor. *The Journal of biological chemistry* 268, 9410-9415.
- Brose, N., Hofmann, K., Hata, Y., and Sudhof, T.C. (1995). Mammalian homologues of *Caenorhabditis elegans* unc-13 gene define novel family of C2-domain proteins. *The Journal of biological chemistry* 270, 25273-25280.
- Brymora, A., Valova, V.A., and Robinson, P.J. (2004). Protein-protein interactions identified by pull-down experiments and mass spectrometry. *Current protocols in cell biology / editorial board, Juan S Bonifacino [et al] Chapter 17, Unit 17 15.*
- Burgoyne, R.D., and Morgan, A. (2015). Cysteine string protein (CSP) and its role in preventing neurodegeneration. *Seminars in cell & developmental biology*.
- Burrone, J., Li, Z., and Murthy, V.N. (2006). Studying vesicle cycling in presynaptic terminals using the genetically encoded probe synaptopHluorin. *Nature protocols* 1, 2970-2978.
- Ceccarelli, B., Hurlbut, W.P., and Mauro, A. (1973). Turnover of transmitter and synaptic vesicles at the frog neuromuscular junction. *The Journal of cell biology* 57, 499-524.
- Chau, V., Tobias, J.W., Bachmair, A., Marriott, D., Ecker, D.J., Gonda, D.K., and Varshavsky, A. (1989). A multiubiquitin chain is confined to specific lysine in a targeted short-lived protein. *Science* 243, 1576-1583.
- Chen, H., Polo, S., Di Fiore, P.P., and De Camilli, P.V. (2003). Rapid Ca²⁺-dependent decrease of protein ubiquitination at synapses. *Proc Natl Acad Sci U S A* 100, 14908-14913.
- Clague, M.J., and Urbe, S. (2010). Ubiquitin: same molecule, different degradation pathways. *Cell* 143, 682-685.
- Clayton, E.L., and Cousin, M.A. (2008). Differential labelling of bulk endocytosis in nerve terminals by FM dyes. *Neurochem Int* 53, 51-55.
- Cohen, L.D., Zuchman, R., Sorokina, O., Muller, A., Dieterich, D.C., Armstrong, J.D., Ziv, T., and Ziv, N.E. (2013). Metabolic turnover of synaptic proteins: kinetics, interdependencies and implications for synaptic maintenance. *PLoS One* 8, e63191.
- Dou, Z., Pan, J.A., Dbouk, H.A., Ballou, L.M., DeLeon, J.L., Fan, Y., Chen, J.S., Liang, Z., Li, G., Backer, J.M., *et al.* (2013). Class IA PI3K p110beta subunit promotes autophagy through Rab5 small GTPase in response to growth factor limitation. *Molecular cell* 50, 29-42.
- Dulubova, I., Sugita, S., Hill, S., Hosaka, M., Fernandez, I., Sudhof, T.C., and Rizo, J. (1999). A conformational switch in syntaxin during exocytosis: role of munc18. *The EMBO journal* 18, 4372-4382.
- Ehlers, M.D. (2003). Activity level controls postsynaptic composition and signaling via the ubiquitin-proteasome system. *Nat Neurosci* 6, 231-242.

- Esposito, G., Ana Clara, F., and Verstreken, P. (2012). Synaptic vesicle trafficking and Parkinson's disease. *Developmental neurobiology* 72, 134-144.
- Fader, C.M., and Colombo, M.I. (2009). Autophagy and multivesicular bodies: two closely related partners. *Cell death and differentiation* 16, 70-78.
- Feng, Y., He, D., Yao, Z., and Klionsky, D.J. (2014). The machinery of macroautophagy. *Cell research* 24, 24-41.
- Fernandes, A.C., Uytterhoeven, V., Kuenen, S., Wang, Y.C., Slabbaert, J.R., Swerts, J., Kasprowicz, J., Aerts, S., and Verstreken, P. (2014). Reduced synaptic vesicle protein degradation at lysosomes curbs TBC1D24/sky-induced neurodegeneration. *The Journal of cell biology* 207, 453-462.
- Fesce, R., Grohovaz, F., Valtorta, F., and Meldolesi, J. (1994). Neurotransmitter release: fusion or 'kiss-and-run'? *Trends Cell Biol* 4, 1-4.
- Fischer von Mollard, G., Stahl, B., Walch-Solimena, C., Takei, K., Daniels, L., Khoklatchev, A., De Camilli, P., Sudhof, T.C., and Jahn, R. (1994). Localization of Rab5 to synaptic vesicles identifies endosomal intermediate in synaptic vesicle recycling pathway. *Eur J Cell Biol* 65, 319-326.
- Garden, G.A., and La Spada, A.R. (2008). Molecular pathogenesis and cellular pathology of spinocerebellar ataxia type 7 neurodegeneration. *Cerebellum* 7, 138-149.
- Geppert, M., Bolshakov, V.Y., Siegelbaum, S.A., Takei, K., De Camilli, P., Hammer, R.E., and Sudhof, T.C. (1994). The role of Rab3A in neurotransmitter release. *Nature* 369, 493-497.
- Gowrishankar, S., Yuan, P., Wu, Y., Schrag, M., Paradise, S., Grutzendler, J., De Camilli, P., and Ferguson, S.M. (2015). Massive accumulation of luminal protease-deficient axonal lysosomes at Alzheimer's disease amyloid plaques. *Proc Natl Acad Sci U S A* 112, E3699-3708.
- Grillo, F.W., Song, S., Teles-Grilo Ruivo, L.M., Huang, L., Gao, G., Knott, G.W., Maco, B., Ferretti, V., Thompson, D., Little, G.E., *et al.* (2013). Increased axonal bouton dynamics in the aging mouse cortex. *Proc Natl Acad Sci U S A* 110, E1514-1523.
- Guvan, A., and Tolun, A. (2013). TBC1D24 truncating mutation resulting in severe neurodegeneration. *Journal of medical genetics* 50, 199-202.
- Haas, A.L., Warms, J.V., Hershko, A., and Rose, I.A. (1982). Ubiquitin-activating enzyme. Mechanism and role in protein-ubiquitin conjugation. *The Journal of biological chemistry* 257, 2543-2548.
- Haberman, A., Williamson, W.R., Epstein, D., Wang, D., Rina, S., Meinertzhagen, I.A., and Hiesinger, P.R. (2012). The synaptic vesicle SNARE neuronal Synaptobrevin promotes endolysosomal degradation and prevents neurodegeneration. *The Journal of cell biology* 196, 261-276.

- Helton, T.D. and Ehlers, M.D. (2008). "Ubiquitin and Protein Degradation in Synapse Function". *Structural and Functional Organization of the Synapse*. Hell, J.W. and Ehlers, M.D. (eds). Springer Science and Business Media, 2008. 553-600. Print.
- Hata, Y., Slaughter, C.A., and Sudhof, T.C. (1993). Synaptic vesicle fusion complex contains unc-18 homologue bound to syntaxin. *Nature* *366*, 347-351.
- Hernandez, D., Torres, C.A., Setlik, W., Cebrian, C., Mosharov, E.V., Tang, G., Cheng, H.C., Kholodilov, N., Yarygina, O., Burke, R.E., *et al.* (2012). Regulation of presynaptic neurotransmission by macroautophagy. *Neuron* *74*, 277-284.
- Hershko, A., Heller, H., Elias, S., and Ciechanover, A. (1983). Components of ubiquitin-protein ligase system. Resolution, affinity purification, and role in protein breakdown. *The Journal of biological chemistry* *258*, 8206-8214.
- Heuser, J.E., and Reese, T.S. (1973). Evidence for recycling of synaptic vesicle membrane during transmitter release at the frog neuromuscular junction. *The Journal of cell biology* *57*, 315-344.
- Hicke, L., and Dunn, R. (2003). Regulation of membrane protein transport by ubiquitin and ubiquitin-binding proteins. *Annual review of cell and developmental biology* *19*, 141-172.
- Hollenbeck, P.J. (1993). Products of endocytosis and autophagy are retrieved from axons by regulated retrograde organelle transport. *The Journal of cell biology* *121*, 305-315.
- Hoopmann, P., Punge, A., Barysch, S.V., Westphal, V., Buckers, J., Opazo, F., Bethani, I., Lauterbach, M.A., Hell, S.W., and Rizzoli, S.O. (2010). Endosomal sorting of readily releasable synaptic vesicles. *Proceedings of the National Academy of Sciences of the United States of America* *107*, 19055-19060.
- Junutula, J.R., De Maziere, A.M., Peden, A.A., Ervin, K.E., Advani, R.J., van Dijk, S.M., Klumperman, J., and Scheller, R.H. (2004). Rab14 is involved in membrane trafficking between the Golgi complex and endosomes. *Molecular biology of the cell* *15*, 2218-2229.
- Kadota, T., Mizote, M., and Kadota, K. (1994). Dynamics of presynaptic endosomes produced during transmitter release. *J Electron Microsc (Tokyo)* *43*, 62-71.
- Katz, B., and Miledi, R. (1967). Ionic requirements of synaptic transmitter release. *Nature* *215*, 651.
- Kish-Trier, E., and Hill, C.P. (2013). Structural biology of the proteasome. *Annu Rev Biophys* *42*, 29-49.
- Komada, M., and Soriano, P. (1999). Hrs, a FYVE finger protein localized to early endosomes, is implicated in vesicular traffic and required for ventral folding morphogenesis. *Genes & development* *13*, 1475-1485.

- Lam, Y.A., Lawson, T.G., Velayutham, M., Zweier, J.L., and Pickart, C.M. (2002). A proteasomal ATPase subunit recognizes the polyubiquitin degradation signal. *Nature* *416*, 763-767.
- Langemeyer, L., Nunes Bastos, R., Cai, Y., Itzen, A., Reinisch, K.M., and Barr, F.A. (2014). Diversity and plasticity in Rab GTPase nucleotide release mechanism has consequences for Rab activation and inactivation. *eLife* *3*, e01623.
- LaVail, M.M., and LaVail, J.H. (1975). Retrograde intraaxonal transport of horseradish peroxidase in retinal ganglion cells of the chick. *Brain research* *85*, 273-280.
- Lazarevic, V., Schone, C., Heine, M., Gundelfinger, E.D., and Fejtova, A. (2011). Extensive remodeling of the presynaptic cytomatrix upon homeostatic adaptation to network activity silencing. *The Journal of neuroscience : the official journal of the Society for Neuroscience* *31*, 10189-10200.
- Leal-Ortiz, S., Waites, C.L., Terry-Lorenzo, R., Zamorano, P., Gundelfinger, E.D., and Garner, C.C. (2008). Piccolo modulation of Synapsin1a dynamics regulates synaptic vesicle exocytosis. *The Journal of cell biology* *181*, 831-846.
- Lee, J.A., Beigneux, A., Ahmad, S.T., Young, S.G., and Gao, F.B. (2007). ESCRT-III dysfunction causes autophagosome accumulation and neurodegeneration. *Current biology : CB* *17*, 1561-1567.
- Lee, J.A., Liu, L., and Gao, F.B. (2009). Autophagy defects contribute to neurodegeneration induced by dysfunctional ESCRT-III. *Autophagy* *5*, 1070-1072.
- Lees, G.J., Geffen, L.B., and Rush, R.A. (1981). Phentolamine increases neuronal binding and retrograde transport of dopamine beta-hydroxylase antibodies. *Neurosci Lett* *22*, 115-118.
- Li, G., and Stahl, P.D. (1993). Structure-function relationship of the small GTPase rab5. *The Journal of biological chemistry* *268*, 24475-24480.
- Li, L., and Chin, L.S. (2003). The molecular machinery of synaptic vesicle exocytosis. *Cellular and molecular life sciences : CMLS* *60*, 942-960.
- Liu, Y., Li, H., Sugiura, Y., Han, W., Gallardo, G., Khvotchev, M., Zhang, Y., Kavalali, E.T., Sudhof, T.C., and Lin, W. (2015). Ubiquitin-Synaptobrevin Fusion Protein Causes Degeneration of Presynaptic Motor Terminals in Mice. *The Journal of neuroscience : the official journal of the Society for Neuroscience* *35*, 11514-11531.
- Livak, K.J., and Schmittgen, T.D. (2001). Analysis of relative gene expression data using real-time quantitative PCR and the 2(-Delta Delta C(T)) Method. *Methods* *25*, 402-408.
- Lois, C., Hong, E.J., Pease, S., Brown, E.J., and Baltimore, D. (2002). Germline transmission and tissue-specific expression of transgenes delivered by lentiviral vectors. *Science* *295*, 868-872.

Lussier, M.P., Nasu-Nishimura, Y., and Roche, K.W. (2011). Activity-dependent ubiquitination of the AMPA receptor subunit GluA2. *The Journal of neuroscience : the official journal of the Society for Neuroscience* *31*, 3077-3081.

Maday, S., Twelvetrees, A.E., Moughamian, A.J., and Holzbaur, E.L. (2014). Axonal transport: cargo-specific mechanisms of motility and regulation. *Neuron* *84*, 292-309.

Maday, S., Wallace, K.E., and Holzbaur, E.L. (2012). Autophagosomes initiate distally and mature during transport toward the cell soma in primary neurons. *The Journal of cell biology* *196*, 407-417.

Mahoney, T.R., Liu, Q., Itoh, T., Luo, S., Hadwiger, G., Vincent, R., Wang, Z.W., Fukuda, M., and Nonet, M.L. (2006). Regulation of synaptic transmission by RAB-3 and RAB-27 in *Caenorhabditis elegans*. *Molecular biology of the cell* *17*, 2617-2625.

Marat, A.L., and McPherson, P.S. (2010). The connecdenn family, Rab35 guanine nucleotide exchange factors interfacing with the clathrin machinery. *The Journal of biological chemistry* *285*, 10627-10637.

McCaffrey, M.W., Bielli, A., Cantalupo, G., Mora, S., Roberti, V., Santillo, M., Drummond, F., and Bucci, C. (2001). Rab4 affects both recycling and degradative endosomal trafficking. *FEBS letters* *495*, 21-30.

Miller, T.M., and Heuser, J.E. (1984). Endocytosis of synaptic vesicle membrane at the frog neuromuscular junction. *J Cell Biol* *98*, 685-698.

Morris, S.J., Ralston, H.J., 3rd, and Shooter, E.M. (1971). Studies on the turnover of mouse brain synaptosomal proteins. *Journal of neurochemistry* *18*, 2279-2290.

Murthy, V.N., and Stevens, C.F. (1998). Synaptic vesicles retain their identity through the endocytic cycle. *Nature* *392*, 497-501.

Na, C.H., Jones, D.R., Yang, Y., Wang, X., Xu, Y., and Peng, J. (2012). Synaptic protein ubiquitination in rat brain revealed by antibody-based ubiquitome analysis. *Journal of proteome research* *11*, 4722-4732.

Nonaka, T., Iwatsubo, T., and Hasegawa, M. (2005). Ubiquitination of alpha-synuclein. *Biochemistry* *44*, 361-368.

Overly, C.C., and Hollenbeck, P.J. (1996). Dynamic organization of endocytic pathways in axons of cultured sympathetic neurons. *The Journal of neuroscience : the official journal of the Society for Neuroscience* *16*, 6056-6064.

Park, J.W., Vahidi, B., Taylor, A.M., Rhee, S.W., and Jeon, N.L. (2006). Microfluidic culture platform for neuroscience research. *Nat Protoc* *1*, 2128-2136.

- Parkinson, K., Baines, A.E., Keller, T., Gruenheit, N., Bragg, L., North, R.A., and Thompson, C.R. (2014). Calcium-dependent regulation of Rab activation and vesicle fusion by an intracellular P2X ion channel. *Nature cell biology* 16, 87-98.
- Pavlos, N.J., Gronborg, M., Riedel, D., Chua, J.J., Boyken, J., Kloepper, T.H., Urlaub, H., Rizzoli, S.O., and Jahn, R. (2010). Quantitative analysis of synaptic vesicle Rabs uncovers distinct yet overlapping roles for Rab3a and Rab27b in Ca²⁺-triggered exocytosis. *The Journal of neuroscience : the official journal of the Society for Neuroscience* 30, 13441-13453.
- Pavlos, N.J., and Jahn, R. (2011). Distinct yet overlapping roles of Rab GTPases on synaptic vesicles. *Small GTPases* 2, 77-81.
- Peng, L., Liu, H., Ruan, H., Tepp, W.H., Stoothoff, W.H., Brown, R.H., Johnson, E.A., Yao, W.D., Zhang, S.C., and Dong, M. (2013). Cytotoxicity of botulinum neurotoxins reveals a direct role of syntaxin 1 and SNAP-25 in neuron survival. *Nature communications* 4, 1472.
- Raiborg, C., and Stenmark, H. (2009). The ESCRT machinery in endosomal sorting of ubiquitylated membrane proteins. *Nature* 458, 445-452.
- Regazzi, R. (2007). "Rab GTPases and Their Role in the Control of Exocytosis". *Molecular Mechanisms of Exocytosis*. Regazzi R. (ed). Landes Bioscience and Springer Science and Business Media, 2007. 28-41. Print.
- Ravikumar, B., Imarisio, S., Sarkar, S., O'Kane, C.J., and Rubinsztein, D.C. (2008). Rab5 modulates aggregation and toxicity of mutant huntingtin through macroautophagy in cell and fly models of Huntington disease. *Journal of cell science* 121, 1649-1660.
- Rinetti, G.V., and Schweizer, F.E. (2010). Ubiquitination acutely regulates presynaptic neurotransmitter release in mammalian neurons. *The Journal of neuroscience : the official journal of the Society for Neuroscience* 30, 3157-3166.
- Rizzoli, S.O., Bethani, I., Zwilling, D., Wenzel, D., Siddiqui, T.J., Brandhorst, D., and Jahn, R. (2006). Evidence for early endosome-like fusion of recently endocytosed synaptic vesicles. *Traffic* 7, 1163-1176.
- Rizzoli, S.O., and Betz, W.J. (2005). Synaptic vesicle pools. *Nat Rev Neurosci* 6, 57-69.
- Rozas, J.L., Gomez-Sanchez, L., Mircheski, J., Linares-Clemente, P., Nieto-Gonzalez, J.L., Vazquez, M.E., Lujan, R., and Fernandez-Chacon, R. (2012). Motoneurons require cysteine string protein-alpha to maintain the readily releasable vesicular pool and synaptic vesicle recycling. *Neuron* 74, 151-165.
- Russell, R.C., Yuan, H.X., and Guan, K.L. (2014). Autophagy regulation by nutrient signaling. *Cell research* 24, 42-57.
- Sanchez-Varo, R., Trujillo-Estrada, L., Sanchez-Mejias, E., Torres, M., Baglietto-Vargas, D., Moreno-Gonzalez, I., De Castro, V., Jimenez, S., Ruano, D., Vizuete, M., *et al.* (2011).

Abnormal accumulation of autophagic vesicles correlates with axonal and synaptic pathology in young Alzheimer's mice hippocampus. *Acta neuropathologica*.

Sato, M., Sato, K., Liou, W., Pant, S., Harada, A., and Grant, B.D. (2008). Regulation of endocytic recycling by *C. elegans* Rab35 and its regulator RME-4, a coated-pit protein. *The EMBO journal* *27*, 1183-1196.

Schluter, O.M., Schmitz, F., Jahn, R., Rosenmund, C., and Sudhof, T.C. (2004). A complete genetic analysis of neuronal Rab3 function. *The Journal of neuroscience : the official journal of the Society for Neuroscience* *24*, 6629-6637.

Schluter, O.M., Schnell, E., Verhage, M., Tzonopoulos, T., Nicoll, R.A., Janz, R., Malenka, R.C., Geppert, M., and Sudhof, T.C. (1999). Rabphilin knock-out mice reveal that rabphilin is not required for rab3 function in regulating neurotransmitter release. *The Journal of neuroscience : the official journal of the Society for Neuroscience* *19*, 5834-5846.

Schmidt, O., and Teis, D. (2012). The ESCRT machinery. *Current biology : CB* *22*, R116-120.

Schwarz, L.A., Hall, B.J., and Patrick, G.N. (2010). Activity-dependent ubiquitination of GluA1 mediates a distinct AMPA receptor endocytosis and sorting pathway. *The Journal of neuroscience : the official journal of the Society for Neuroscience* *30*, 16718-16729.

Scita, G., and Di Fiore, P.P. (2010). The endocytic matrix. *Nature* *463*, 464-473.

Scott, D.A., Tabarean, I., Tang, Y., Cartier, A., Masliah, E., and Roy, S. (2010). A pathologic cascade leading to synaptic dysfunction in alpha-synuclein-induced neurodegeneration. *The Journal of neuroscience : the official journal of the Society for Neuroscience* *30*, 8083-8095.

Scudder, S.L., Goo, M.S., Cartier, A.E., Molteni, A., Schwarz, L.A., Wright, R., and Patrick, G.N. (2014). Synaptic strength is bidirectionally controlled by opposing activity-dependent regulation of Nedd4-1 and USP8. *The Journal of neuroscience : the official journal of the Society for Neuroscience* *34*, 16637-16649.

Shao, X., Fernandez, I., Sudhof, T.C., and Rizo, J. (1998). Solution structures of the Ca²⁺-free and Ca²⁺-bound C2A domain of synaptotagmin I: does Ca²⁺ induce a conformational change? *Biochemistry* *37*, 16106-16115.

Sharma, M., Burre, J., Bronk, P., Zhang, Y., Xu, W., and Sudhof, T.C. (2012a). CSPalpha knockout causes neurodegeneration by impairing SNAP-25 function. *The EMBO journal* *31*, 829-841.

Sharma, M., Burre, J., and Sudhof, T.C. (2011). CSPalpha promotes SNARE-complex assembly by chaperoning SNAP-25 during synaptic activity. *Nature cell biology* *13*, 30-39.

Sharma, M., Burre, J., and Sudhof, T.C. (2012b). Proteasome inhibition alleviates SNARE-dependent neurodegeneration. *Science translational medicine* *4*, 147ra113.

- Shi, L., Fu, A.K., and Ip, N.Y. (2012). Molecular mechanisms underlying maturation and maintenance of the vertebrate neuromuscular junction. *Trends Neurosci* 35, 441-453.
- Shields, S.B., and Piper, R.C. (2011). How ubiquitin functions with ESCRTs. *Traffic* 12, 1306-1317.
- Shimizu, H., Kawamura, S., and Ozaki, K. (2003). An essential role of Rab5 in uniformity of synaptic vesicle size. *Journal of cell science* 116, 3583-3590.
- Sollner, T., Bennett, M.K., Whiteheart, S.W., Scheller, R.H., and Rothman, J.E. (1993). A protein assembly-disassembly pathway in vitro that may correspond to sequential steps of synaptic vesicle docking, activation, and fusion. *Cell* 75, 409-418.
- Star, E.N., Newton, A.J., and Murthy, V.N. (2005). Real-time imaging of Rab3a and Rab5a reveals differential roles in presynaptic function. *The Journal of physiology* 569, 103-117.
- Stenmark, H. (2009). Rab GTPases as coordinators of vesicle traffic. *Nature reviews Molecular cell biology* 10, 513-525.
- Su, W.C., Chao, T.C., Huang, Y.L., Weng, S.C., Jeng, K.S., and Lai, M.M. (2011). Rab5 and class III phosphoinositide 3-kinase Vps34 are involved in hepatitis C virus NS4B-induced autophagy. *Journal of virology* 85, 10561-10571.
- Subach, F.V., Subach, O.M., Gundorov, I.S., Morozova, K.S., Piatkevich, K.D., Cuervo, A.M., and Verkhusha, V.V. (2009). Monomeric fluorescent timers that change color from blue to red report on cellular trafficking. *Nat Chem Biol* 5, 118-126.
- Sudhof, T.C. (2004). The synaptic vesicle cycle. *Annu Rev Neurosci* 27, 509-547.
- Takahashi, H., Mayers, J.R., Wang, L., Edwardson, J.M., and Audhya, A. (2015). Hrs and STAM function synergistically to bind ubiquitin-modified cargoes in vitro. *Biophysical journal* 108, 76-84.
- Takamori, S., Holt, M., Stenius, K., Lemke, E.A., Gronborg, M., Riedel, D., Urlaub, H., Schenck, S., Brugger, B., Ringler, P., *et al.* (2006). Molecular anatomy of a trafficking organelle. *Cell* 127, 831-846.
- Tamai, K., Toyoshima, M., Tanaka, N., Yamamoto, N., Owada, Y., Kiyonari, H., Murata, K., Ueno, Y., Ono, M., Shimosegawa, T., *et al.* (2008). Loss of hrs in the central nervous system causes accumulation of ubiquitinated proteins and neurodegeneration. *The American journal of pathology* 173, 1806-1817.
- Tanaka, K. (2009). The proteasome: overview of structure and functions. *Proceedings of the Japan Academy Series B, Physical and biological sciences* 85, 12-36.
- Tauskela, J.S., Fang, H., Hewitt, M., Brunette, E., Ahuja, T., Thivierge, J.P., Comas, T., and Mealing, G.A. (2008). Elevated synaptic activity preconditions neurons against an in vitro model of ischemia. *The Journal of biological chemistry* 283, 34667-34676.

Teichberg, S., Holtzman, E., Crain, S.M., and Peterson, E.R. (1975). Circulation and turnover of synaptic vesicle membrane in cultured fetal mammalian spinal cord neurons. *The Journal of cell biology* 67, 215-230.

Tian, X., Gala, U., Zhang, Y., Shang, W., Nagarkar Jaiswal, S., di Ronza, A., Jaiswal, M., Yamamoto, S., Sandoval, H., Duraine, L., *et al.* (2015). A voltage-gated calcium channel regulates lysosomal fusion with endosomes and autophagosomes and is required for neuronal homeostasis. *PLoS biology* 13, e1002103.

Uytterhoeven, V., Kuenen, S., Kasprovicz, J., Miskiewicz, K., and Verstreken, P. (2011). Loss of skywalker reveals synaptic endosomes as sorting stations for synaptic vesicle proteins. *Cell* 145, 117-132.

Virmani, T., Gupta, P., Liu, X., Kavalali, E.T., and Hofmann, S.L. (2005). Progressively reduced synaptic vesicle pool size in cultured neurons derived from neuronal ceroid lipofuscinosis-1 knockout mice. *Neurobiol Dis* 20, 314-323.

Vitalis, T., Laine, J., Simon, A., Roland, A., Leterrier, C., and Lenkei, Z. (2008). The type 1 cannabinoid receptor is highly expressed in embryonic cortical projection neurons and negatively regulates neurite growth in vitro. *Eur J Neurosci* 28, 1705-1718.

Voglmaier, S.M., Kam, K., Yang, H., Fortin, D.L., Hua, Z., Nicoll, R.A., and Edwards, R.H. (2006). Distinct endocytic pathways control the rate and extent of synaptic vesicle protein recycling. *Neuron* 51, 71-84.

Von Bartheld, C.S., and Altick, A.L. (2011). Multivesicular bodies in neurons: distribution, protein content, and trafficking functions. *Prog Neurobiol* 93, 313-340.

Waites, C.L., Leal-Ortiz, S.A., Andlauer, T.F., Sigrist, S.J., and Garner, C.C. (2011). Piccolo regulates the dynamic assembly of presynaptic F-actin. *The Journal of neuroscience : the official journal of the Society for Neuroscience* 31, 14250-14263.

Waites, C.L., Specht, C.G., Hartel, K., Leal-Ortiz, S., Genoux, D., Li, D., Drisdell, R.C., Jeyifous, O., Cheyne, J.E., Green, W.N., *et al.* (2009). Synaptic SAP97 isoforms regulate AMPA receptor dynamics and access to presynaptic glutamate. *The Journal of neuroscience : the official journal of the Society for Neuroscience* 29, 4332-4345.

Wang, D., Chan, C.C., Cherry, S., and Hiesinger, P.R. (2013). Membrane trafficking in neuronal maintenance and degeneration. *Cellular and molecular life sciences : CMLS* 70, 2919-2934.

Wang, Y., Okamoto, M., Schmitz, F., Hofmann, K., and Sudhof, T.C. (1997). Rim is a putative Rab3 effector in regulating synaptic-vesicle fusion. *Nature* 388, 593-598.

Wang, Y., Sugita, S., and Sudhof, T.C. (2000). The RIM/NIM family of neuronal C2 domain proteins. Interactions with Rab3 and a new class of Src homology 3 domain proteins. *The Journal of biological chemistry* 275, 20033-20044.

Watanabe, S., Trimbuch, T., Camacho-Perez, M., Rost, B.R., Brokowski, B., Sohl-Kielczynski, B., Felies, A., Davis, M.W., Rosenmund, C., and Jorgensen, E.M. (2014). Clathrin regenerates synaptic vesicles from endosomes. *Nature* *515*, 228-233.

Wijayatunge, R., Chen, L.F., Cha, Y.M., Zannas, A.S., Frank, C.L., and West, A.E. (2014). The histone lysine demethylase Kdm6b is required for activity-dependent preconditioning of hippocampal neuronal survival. *Molecular and cellular neurosciences* *61*, 187-200.

Williamson, L.C., and Neale, E.A. (1998). Syntaxin and 25-kDa synaptosomal-associated protein: differential effects of botulinum neurotoxins C1 and A on neuronal survival. *Journal of neuroscience research* *52*, 569-583.

Wucherpennig, T., Wilsch-Brauninger, M., and Gonzalez-Gaitan, M. (2003). Role of *Drosophila* Rab5 during endosomal trafficking at the synapse and evoked neurotransmitter release. *The Journal of cell biology* *161*, 609-624.

Yamazaki, Y., Schonherr, C., Varshney, G.K., Dogru, M., Hallberg, B., and Palmer, R.H. (2013). Goliath family E3 ligases regulate the recycling endosome pathway via VAMP3 ubiquitylation. *The EMBO journal* *32*, 524-537.

Yu, E., Kanno, E., Choi, S., Sugimori, M., Moreira, J.E., Llinas, R.R., and Fukuda, M. (2008). Role of Rab27 in synaptic transmission at the squid giant synapse. *Proceedings of the National Academy of Sciences of the United States of America* *105*, 16003-16008.

Zhang, N., Gordon, S.L., Fritsch, M.J., Esoof, N., Campbell, D.G., Gourlay, R., Velupillai, S., Macartney, T., Pegg, M., van Aalten, D.M., *et al.* (2015). Phosphorylation of synaptic vesicle protein 2A at Thr84 by casein kinase 1 family kinases controls the specific retrieval of synaptotagmin-1. *The Journal of neuroscience : the official journal of the Society for Neuroscience* *35*, 2492-2507.

Zuo, Y., Yang, G., Kwon, E., and Gan, W.B. (2005). Long-term sensory deprivation prevents dendritic spine loss in primary somatosensory cortex. *Nature* *436*, 261-265.